COO-2520-7
Distribution Category UC-94cb

LOW TEMPERATURE ALKALI METAL-SULFUR BATTERIES

FINAL REPORT

for Period December 1, 1974 - November 30, 1978

S. B. Brummer
R. D. Rauh
K. M. Abraham
F. W. Dampier
V. Subrahmanyam
G. F. Pearson
J. K. Surprenant
J. M. Buzby

EIC Corporation
55 Chapel Street
Newton, Massachusetts 02158

March, 1980

Prepared for

U.S. DEPARTMENT OF ENERGY
UNDER CONTRACT NO. DE-AC02-76ET25003
(Old No. EY-76-C-02-2520)

DISCLAIMER

ABSTRACT

This report describes work carried out on the development of rechargeable, ambient temperature Li/sulfur and Li/metal sulfide batteries. The Li/S system has the cathode material dissolved in the electrolyte, as Li_2S_n. Tetrahydrofuran, 1M $LiAsF_6$, is one of the more attractive electrolytes discovered for this cell, since it can dissolve up to ~10M S as Li_2S_n. Despite the oxidative nature of the electrolyte, Li is stable in it and can be electrodeposited from it on battery charge. Passivation of the Li due to insoluble Li^+-permeable films is thought to be responsible for this stability.

Cells of the configuration Li 5M S(as Li_2S_n), THF, 1M $LiAsF_6$/carbon can be discharged at 50°C with a utilization of nearly $1.5e^-/S$ at the C/3 rate. This corresponds to our rate-capacity goal for this battery (>50% utilization at C/3) in its proposed vehicular or load-leveling applications. Further improvements in rate are possible with Lewis acidic catalysts such as ϕ_3B or Ba^{+2}.

Rechargeability of 135 cycles of $0.1e^-/S$ and ~45 cycles of $0.5e^-/S$ have been demonstrated for this cell. The self-discharge reaction keeps the Li electrode free of electrically isolated dendrites. Ultimate failure on cycling is due to cathode depletion via precipitation of Li_2S on the anode in a form which is insoluble in the electrolyte. To date, attempts to solubilize the Li_2S by the internal generation of an oxidizing "scavenger" (e.g., Br_2) or by addition of Lewis acids have met only with limited success.

Cells of configuration Li/THF, 1M $LiAsF_6$/insoluble metal sulfide were investigated, using the following cathodes: CuS, NiS, SiS_2, MnS_2, FeS and Bi_2S_3. Of these, the most promising new material in terms of energy density and rechargeability is CuS. Well over 100 cycles for Li/CuS cells with moderate cathode loadings have been demonstrated, giving cathode efficiencies of >0.8 eq/mole. CuS compares favorably with TiS_2 in terms of energy density and rechargeability and is superior in terms of economics.

TABLE OF CONTENTS

LIST OF FIGURES

LIST OF FIGURES
(Continued)

LIST OF FIGURES
(Continued)

LIST OF TABLES

LIST OF TABLES
(Continued)

I. INTRODUCTION

Since the inception of this program in December 1974, we have been exploring the feasibility of novel, ambient or slightly elevated temperature secondary batteries based on an alkali metal anode (Na or Li), an organic electrolyte, and a sulfur or metal sulfide cathode. Such systems are directed at high energy density (∿200 Whr/kg), high rate (C/3-C/6) applications such as electric vehicles. Within this general category, three kinds of batteries have been investigated.

• Li/Sulfur. Primary Li/S batteries have traditionally suffered from poor cathode utilization due to the insulating nature of both S and its reduction product, Li_2S. As a result of observations of Li stability in highly oxidizing solvents (e.g., $SOCl_2$, SO_2), a Li/dissolved S battery was selected for investigation. The liquid catholyte is comprised of a Li-compatible aprotic organic solvent containing dissolved Li polysulfide, Li_2S_n. The polysulfide is necessary since neutral S is insoluble in polar media. The general configuration of the battery is

	Organic Solvent	Carbon
Li	LiX Supporting Electrolyte	Current
	Dissolved Li_2S_n	Collector

Unlike solid S, the dissolved S_n^{-2} maintains good contact with the current collector during all phases of discharge and charge.

As described in Section II, the development of the Li/Li_2S_n cell has progressed in several phases. First, electrolytes had to be found in which 5-6M S (as Li_2S_n) could be dissolved in order to achieve the requisite energy densities. Based on the results of studies of polysulfide formation, chemistry and electrochemistry in aprotic solvents, tetrahydrofuran, 1M $LiAsF_6$ was chosen as a favorable battery electrolyte. Up to 10M S can be dissolved in this medium as polysulfide by the in situ reaction of stoichiometric quantities of Li_2S and S_8. Furthermore, S_n^{-2} showed reversible redox behavior in these solutions, being reducible to Li_2S and oxidizable not to insoluble S_8, but to very long chain polysulfides.

The second phase of development, the capacity and rate characteristics of these cells was demonstrated. Cell structures similar to those for Li/$SOCl_2$ were produced in which the Li_2S_n could be discharged with nearly complete efficiency at up to the C/4 rate. The discharge plateau is mostly flat at ∿2V. Best rates and capacities are obtained at slightly elevated temperatures (∿50°C), as would be obtained in normal resistive heating of cells operating at moderate to high rates. Rates are improved somewhat by the addition of some Lewis acids which complex S_n^{-2}.

The third phase of development dealt with the rechargeability of the system. The most unusual aspect of the Li/Li_2S_n battery is that it is rechargeable at all, since charging necessitates the electrodeposition of Li from the highly reactive electrolyte. Yet, despite the oxidizing nature of the electrolyte, Li is relatively stable in it. For example, at 50°C Li foil reacts with 5M S as $\sim Li_2S_{10}$ in THF at a rate of only $\sim$10 $\mu A/cm^2$ ($\sim$1% per day self-discharge in our cell design). Only Li_2S and low order polysulfides can be detected as products. This stability is reflected in half-cell cycling studies of the Li electrode which show that the polysulfide actually <u>improves</u> the cycling efficiency. Similar results have been obtained with full cells. To date, positive limited cells have been cycled >120 times at 0.1 e^-/S utilization with an average Li electrode efficiency of $\sim$95%, while >85% efficiency has been obtained with cells cycled at $\geq$0.4 e^-/S for up to 50 consecutive cycles.

In nonoxidizing-electrolyte systems, such as those containing solid cathodes (e.g., Li/TiS_2), the inefficiency of the anode is a result of the formation of electrically isolated Li dendrites. This active material is lost from the system, resulting in the necessity of using large excesses of Li in constructing the cells unless the Li electrode is highly efficient. One of the most attractive features of the Li/dissolved Li_2S_n battery is that this kind of loss phenomenon does not occur. We have demonstrated that the cycling efficiency of the anode is the same as that of the whole cell. This means that Li that would have been isolated as dendrites in the Li/TiS_2-type of cell reacts directly with the catholyte via the relatively slow self-discharge reaction.

The failure mode on cycling Li/Li_2S_n cells appears to be connected with irreversibilities in the self-discharge reaction. All evidence indicates that eventually Li_2S becomes isolated on the anode in a form that cannot be resolubilized by ambient Li_2S_n, and the cathode capacity is gradually diminished. Several approaches to the solubilization of this Li_2S have been investigated, e.g., addition of Lewis acids and <u>in situ</u> generation of oxidizing agents like Br_2. None have been completely effective in extending the cell's cycle life. It is in this area that further developmental effort is required.

- <u>Li/Metal Sulfide</u>. The configuration of this cell is

Li	Organic Solvent LiX Supporting Electrolyte	Transition Metal Sulfide

As mentioned previously, secondary Li batteries of this type must have very efficient Li electrodes due to the phenomenon of Li dendrite isolation. However, recent progress on parallel research programs at EIC make such systems increasingly attractive. It is now possible to cycle a Li electrode at practical depths of discharge with an efficiency

exceeding 98%. Thus, a 100 cycle battery need contain only a twofold stoichiometric excess of Li. Improvements on even this performance are still being realized.

The aim of the limited research carried out on such batteries on this program has been to develop a cathode of high energy density consistent with the DOE economic goals for electric vehicles. A screening of simple, light transition metal sulfides indicates that TiS_2 and CuS can be cycled most reversibly over the long term and have acceptable and nearly equal practical energy densities. CuS has a history of use as a Li primary battery cathode, and considerable technology already exists regarding its fabrication, capacity and rate characteristics. The economy of CuS (relative to TiS_2, in particular) makes it an attractive choice for further development. Rechargeability of CuS has been demonstrated for loadings of 8.5 mAh/cm^2, with utilizations of over 0.8 e^-/mole maintained for at least 100 cycles.

• Na/Li_2S_n. Exploratory research was carried out on cells of configuration

Na Liquid	β-Al_2O_3	Organic Solvent LiX Supporting Electrolyte Dissolved Li_2S_n	Carbon Current Collector

This cell operates at a moderate temperature (~150°C), and avoids many of the materials problems associated with the higher temperature analog, which uses molten Na_2S_n as the cathode. Our preliminary results, obtained during the second year of this program, are summarized in reference (1), and will not be expanded here.

The remainder of this final report consists of three additional sections and three appendices. Section II describes the research on the Li/Li_2S_n cell, including the investigations of Li_2S_n catholyte formation as well as rate, capacity and rechargeability studies. In Section III, the work on Li/metal sulfide cells is discussed, with particular emphasis on the CuS cathode. Section IV presents a summary of the salient program results. A significant part of this work has been published in the open literature, and a list of these publications is provided in Appendix A. Appendix B describes the design of a practical Li/Li_2S_n battery. In Appendix C is reproduced a paper on the rechargeability of Li/Li_2S_n batteries which was presented at the annual IECEC meeting in 1977.

II. THE Li/Li_2S_n SECONDARY BATTERY

A. Background

Considerable development activity has been undertaken recently on liquid cathode primary Li batteries. Li is stable to catholytes such as $SOCl_2$ and SO_2 by virtue of a thin passivating film of reaction products which forms on the Li surface.

The goal of this part of the research program was to develop a Li secondary battery with a liquid cathode. A reversible cathode material soluble in a Li-compatible nonaqueous medium was required. An early observation that S_8 could be dissolved in dimethyl sulfoxide by electrochemical reduction to form deeply colored solutions allowed us to postulate sulfur as a dissolved cathode in a cell of configuration

$$\text{Li} \,\Big|\, \begin{matrix}\text{Organic Solvent} \\ \text{Soluble Sulfur}\end{matrix} \,\Big|\, \begin{matrix}\text{Carbon} \\ \text{Current Collector}\end{matrix}$$

The Li/S system is attractive not only because it uses inexpensive materials (i.e., Li, S, C - see Appendix B), but also because of its high theoretical energy density (~1300 Wh/lb). The latter allows that even with a significant dilution of the sulfur in the electrolyte a high energy density system can be obtained. In Figure 1, the calculated capacities of dissolved sulfur catholytes are plotted as a function of S solubility and efficiency of utilization on discharge. Volume capacities above ~0.15 Ah/cm^3 are required to yield practical systems of >100 Wh/kg. Thus, at least 4M S solubility is required which, on discharge, must accept considerably more than 1 e^-/S.

Using these considerations, the research and development program was divided into four stages:

- Obtaining the required S solubility in aprotic organic solvents.
- Evaluating S redox behavior in the same media, in order to determine potentials and reversibilities of reactions.
- Evaluating the capacity and rate characteristics of the dissolved sulfur cathode in prototype cells.
- Evaluating Li compatibility with the sulfur-containing electrolytes; determining rechargeability and failure modes on extended cycling of prototype cells.

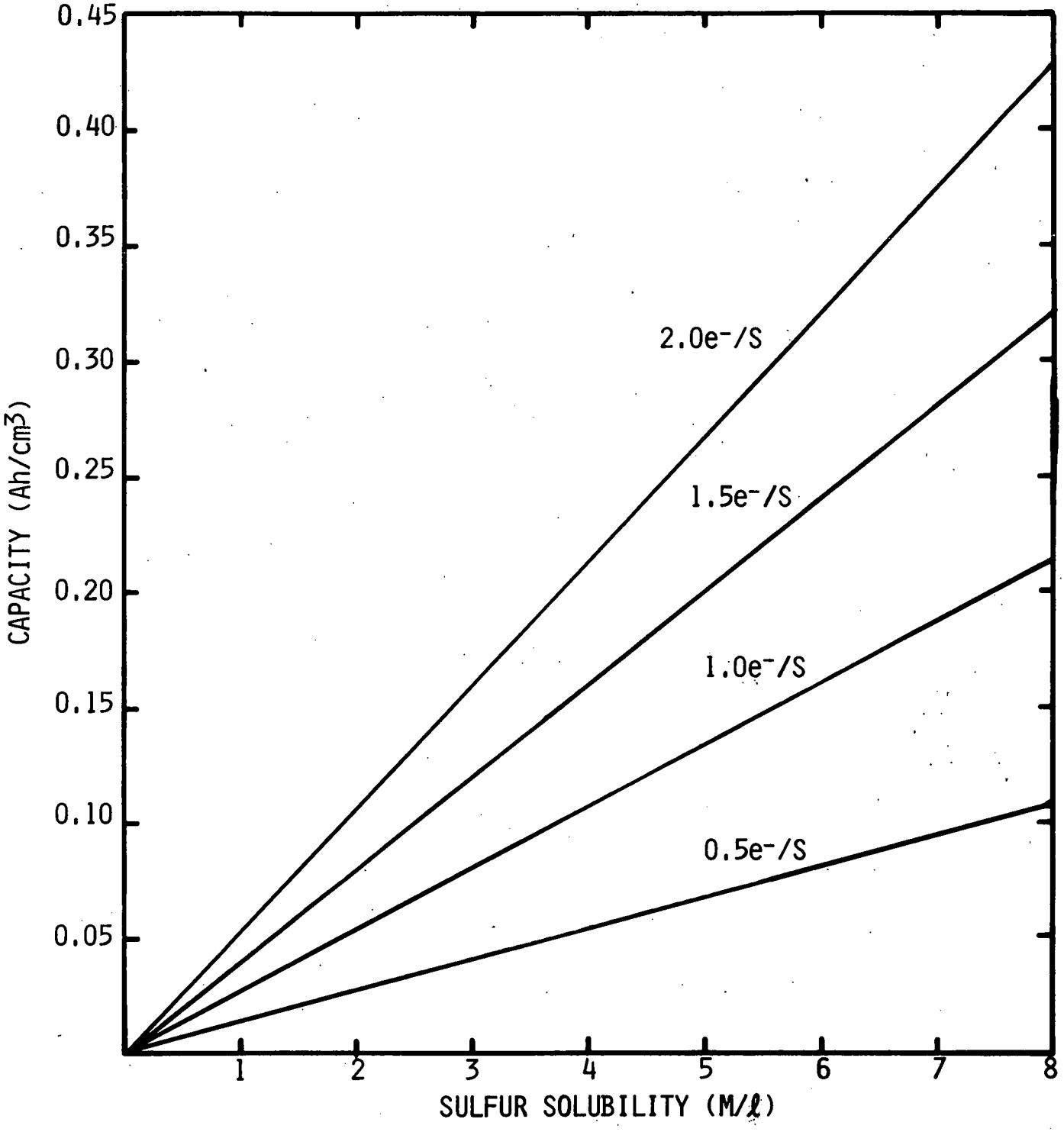

Fig. 1: Capacity of dissolved S_n^{-2} electrolytes as a function of sulfur solubility and cathodic utilization.

Each of these aspects of the Li/dissolved S battery development is described in turn in the following subsections.

B. Formation and Characterization of Li Polysulfides in Aprotic Solvents

1. Introduction

The formation of polysulfides in both aqueous (2-4) and nonaqueous (5-16) media has been frequently reported. In aqueous solution, the interconversion of polysulfide species is mediated by hydrolysis. In aprotic nonaqueous solvents, however, the polysulfide equilibria are determined solely by their first order interactions. Investigations of polysulfides in dimethylformamide (DMF), dimethyl sulfoxide (DMSO) and hexamethylphosphoramide have led to the assignment of visible absorption bands and extinction coefficients of several polysulfide species and at least one radical anion (S_3^-). These absorption characteristics are listed in Table 1 for DMSO solutions. In addition, some equilibrium constants have been evaluated for polysulfides in DMSO.

TABLE 1

ABSORPTION CHARACTERISTICS OF POLYSULFIDES IN DIMETHYL SULFOXIDE

Species	λ_{max}	ε_{max} (ℓ mol^{-1} cm^{-1}) (11)
S_8^{-2}	492	4.0×10^3
S_6^{-2}	475	3.8×10^3
S_4^{-2}	420	0.9×10^3
S_3^-	618	4.45×10^3

The assignments given in Table 1 have been a subject of debate in the literature. They represent, in our view, the most probably correct interpretation of published results. The peaks assigned to S_8^{-2}, S_6^{-2} and S_4^{-2} have been observed in DMSO solutions of the corresponding Na_2S_n crystalline solids. They have also been assigned on the basis of their appearance at appropriate stoichiometries during the electrochemical reduction of S_8 in DMSO or DMF, and during the titration of S_8 with S_4^{-2}. In addition, the spectral transitions in Table 1 follow an expected trend toward lower energy with increasing polysulfide chain length. There are some indications that these maxima are slightly red-shifted in DMF.

Perhaps the most controversy has surrounded the assignment of the peak at 618 nm. Early work had ascribed this transition to S_2^- (9), S_4 (16) or S_6^{-2} (12). However, Chivers and Drummond (15) pointed out that

this peak corresponds rather closely to the known solid state spectrum of S_3^-, and that vibrational spectra also support the assignment of S_3^- over S_2^-. The S_4 structure has been rejected because the absorbing species has been shown to be charged (17). When the electrochemical reduction of S_8 in DMSO or DMF is monitored spectrally, the 618 nm peak is at maximum intensity at an average reduction stoichiometry of 8/3, corresponding to S_6^{-2} (11,13). However, temperature and concentration effects on the 618 nm absorption in DMSO solutions of S_6^{-2} are indicative of a monomer-dimer equilibrium. These solutions display maxima at 618 nm and 475 nm, with a definite isosbestic point. High temperature and low concentration both favor the species absorbing at 618 nm. The S_6^{-2} assignment of the 618 nm peak has been recently reconsidered by the original authors (13).

Other radical anions have not been observed with certainty in non-aqueous solvents, indicating that S_3^- has a unique stability (perhaps in analogy to the allyl radical). However, S_2^- absorbs at ca. 400 nm (15), and its differentiation from S_4^{-2} is therefore difficult using electronic absorption spectroscopy. An anion radical indicated by esr to exist at high $S:S^{-2}$ ratios in DMF was tentatively assigned by Giggenbach (8) and later by Badoz-Lambling et al. (13) as S_4^-. Also at high $S:S^{-2}$ ratios, Seel and Guttler (7) attributed the absorption at 512 nm in DMF to S_4^-. However, they failed to differentiate between this species and S_8^{-2}, which also absorbs in the same spectral region.

In order to develop a catholyte of practically useful capacity for a Li/dissolved S battery, it is necessary to investigate the formation of concentrated solutions of Li_2S_n in aprotic solvents. In particular, we are concerned with finding the best methods for forming polysulfides in situ, as well as the factors which govern polysulfide solubility and equilibria. This, in turn, entails the identification of individual polysulfide species in a variety of media. Hence, the present study involves not only the synthesis of polysulfide solutions, but also their spectral and chemical analysis.

2. Experimental Procedures

Dimethylacetamide (DMAC), dimethylformamide (DMF), dimethyl sulfoxide (DMSO), propylene carbonate (PC) and tetrahydrofuran (THF) were obtained from Burdick and Jackson Laboratories and were of spectroscopic "distilled in glass" quality. Methyl formate (MF) and pyridine were Eastman spectro-quality.

γ-Butyrolactone (BL), sulfolane (SL), methyl acetate (MA) and dimethyl sulfite (DMSI) were obtained as reagent grade and were distilled before use on a Teflon spinning-band column (Perkin-Elmer 251 Auto Annular Still). DMSI, BL, and SL had to be distilled at reduced pressure to prevent thermal decomposition. Sulfur (99.9995%, Ventron Corp.) and Li_2S (97+%, Foote Mineral Company) were used as received.

All operations and storage of materials were carried out in an Ar-filled glove box (Vacuum-Atmospheres Corp.). Air-tight spectrophotometry cells were filled in the glove box. If the cells were not air-tight, oxidation of the polysulfide solutions occurred, resulting in spectral shifts and misleading results. Spectra were recorded on a Perkin-Elmer Coleman 124D double beam spectrophotometer.

Chemical analyses for polysulfides were performed using methods suggested by Schwarzenbach and Fisher (18). Total S was determined by oxidizing the polysulfide to SO_4^{-2}, then precipitating $BaSO_4$: to 0.5 ml of the nonaqueous S_n^{-2} solution (~1-5M in S) were added 5-15 ml of 7N NH_4OH and 5 to 10 ml of 30% H_2O_2. After the initial reaction had subsided, the solution was heated at ~80°C to expel the excess H_2O_2 and NH_3. The solution was then made up to 50 ml in a volumetric flask with H_2O and 5 drops of 6N HCl. Next, a measured 2-5 ml of the resulting SO_4^{-2} solution was diluted with 20 ml of methanol and the pH adjusted to between 2.5 and 4. The solution was titrated against 0.005M $Ba(ClO_4)_2$ in the presence of Thorin indicator. After all the $BaSO_4$ had precipitated, the end point appeared as a permanent pink color.

Standard iodimetry was employed for the S^{-2} analysis. To an aliquot of the nonaqueous sulfide solution a measured excess of 0.05N I_2 solution was added. After shaking the flask for ~10 sec, the unreacted I_2 was titrated against 0.05N $Na_2S_2O_3$ using a starch indicator. The overall reaction is

$$S_n^{-2} + I_2 \rightarrow 2I^- + nS$$

3. Preparation and Analysis of Li_2S_n Solutions

Although a series of Na and K polysulfides have been synthesized and characterized in the crystalline state, the only Li polysulfide to be reported is Li_2S_2 (19,20). However, nonaqueous solutions of Li polysulfides may be produced either chemically or electrochemically. Three such methods are investigated in the present work.

One method of polysulfide production is the direct reaction of elemental S with Li metal:

$$2Li + \frac{n}{8} S_8 \rightarrow Li_2S_n \qquad (1)$$

Here, enough elemental S was first added to the electrolyte to form a 0.6M solution, if all dissolved. An excess of Li metal dispersion (70 μ) was then added. The solutions became somewhat colored immediately, the amount of polysulfide formed varying with solvent. In general, the reaction proceeded slowly at room temperature, with extensive reactions taking place only in DMSO, γ-butyrolactone (BL) and tetrahydrofuran (THF). DMSO,

sulfolane, and BL were blue-green at the onset of the reaction, when the polysulfide concentration was low. As more polysulfide formed in DMSO and BL, the solutions became dark red. In THF, the blue color was not produced, even at high dilution.

The second method to be investigated for Li polysulfide formation was the electrochemical reduction of S_8. In DMSO, DMF and dimethylacetamide (DMAC) the reduction:

$$2e^- + S_8 \rightarrow S_8^{-2} \qquad (2)$$

occurs at 2.7V vs. Li^+/Li. In the other solvents investigated, the first reduction wave of S_8 occurs at ∿2.2V, and overlaps polysulfide reductions. The formation of S_8^{-2} was carried out potentiostatically. The cell contained a carbon cloth working electrode, 10 cm^2 per side. The Li counter electrode, in a separate compartment, was changed frequently during the electrolysis. A Luggin capillary Li^+/Li reference electrode was employed. The working electrode compartment contained enough solid S to yield a 5M solution. The solubility of S_8 was only ∿5 mM, but this was sufficient to maintain the reduction current. The formation and dissolution of polysulfide went smoothly in DMAC, DMF, DMSO, methyl acetate (MA) and THF, while little dissolution and low currents were obtained in BL and propylene carbonate (PC).

The production of polysulfides in DMSO via reduction of S_8 at constant potential was monitored using cyclic voltammetry on a vitreous carbon electrode. The principal change during the reduction was in the magnitude of the polysulfide oxidation peak. Before electrolysis, scanning the saturated S_8 solution initially positive from open circuit led to no oxidation on the first sweep, as expected. As S_8 became reduced to polysulfide and dissolved, an oxidation peak at 3.2V developed. After some dissolution, this peak was always present on the first (anodic) sweep, starting at open circuit.

In DMSO and in THF, the electrolysis was carried out long enough to ensure at least a 5M S solution, if all the S were dissolved in Li_2S_8. Chemical analysis of these solutions showed between 1 and 2M total S, and a ratio of total S to S^{-2} of 15 to 25, depending on the running time of the electrolysis. The stoichiometry of the reaction was not investigated in detail. It seems probable, however, that some of the reduced S was lost through disproportionation reactions leading to the precipitation of Li_2S, viz.

$$nS_8^{-2} \rightleftarrows S_{7n+1}^{-2} + (n-1)\ S^{-2} \qquad (3)$$

The most thorough investigation of Li polysulfide formation in solution was made of the reaction

$$Li_2S + \frac{(n-1)}{8} S_8 \rightarrow Li_2S_n \qquad (4)$$

This method is faster and more easily controlled than the previous two methods. The extent of reaction (4) was compared for several solvents. Solutions were prepared by adding appropriate amounts of Li_2S and S_8 to the solvent to yield a 0.5M S solution with a $S°:S^{-2}$ ratio of 3, if all dissolved. At least 0.1M S could be dissolved as polysulfides in seven of the twelve solvents tested.

The relative success of the three methods of polysulfide formation is summarized in Table 2. The best solvents of polysulfide appear to be DMAC, DMF, DMSO, and THF. Dimethyl sulfite, methyl formate, nitromethane and PC are notably poor solvents for polysulfides. Reaction with Li is the least successful method, probably due to the ease with which the metal is passivated. The reason for the lack of electrochemical polysulfide formation in BL is not yet understood.

The production of Li polysulfides by the reaction of Li_2S with S_8 was investigated in more detail. In particular, the effect of polysulfide chain length (order) on S solubility was evaluated in THF, DMSO and MA. The following experiment was carried out: Enough Li_2S was first added to the solvent to bring the S^{-2} concentration to 1.0 M/l, although very little of the salt actually dissolved. Sulfur was then added in 1.0 M/l aliquots. After each addition, the solution was stirred for 24 hours at 25°C in an Ar atmosphere. Samples were withdrawn for chemical and spectral analysis before adding the next aliquot. The S^{-2} and total S concentrations were determined as a function of added S°. In addition, visible absorption spectra were recorded of the diluted samples.

Greater than 10M S could be dissolved as Li_2S_n in both THF and DMSO, while little more than 1M S was obtained in MA. A graph of log n, the logarithm of the average chain length of the polysulfides in solution, as a function of added S° in all three solvents, is given in Figure 2. The dissolution of the Li_2S in THF and in DMSO was incomplete until greater than 3 M/l S° had been added. At these low $S°:S^{-2}$ ratios, the actual polysulfides formed in solution had an average order of 3-4 in DMSO and 5-6 in THF. Polysulfides of lesser chain length must have low stability or solubility in these solvents. It was further determined that in THF, Na_2S_4 has a solubility of $\sim$0.01M, while in DMSO the solubility is >1M. If excess Na_2S_4 is allowed to stir with THF, solutions are eventually formed of polysulfide order >10 due to disproportionation.

For $S°:S^{-2}$ ratios of 4 to 7, nearly all the Li_2S and S° went into solution in both DMSO and THF, so that the analyzed dissolved total S was close to that added. At higher ratios, the S° was in excess; the analyzed polysulfide orders were nevertheless greater than 8, albeit less than the theoretical maximum. An excess of S° led to the formation of S_{10-11}^{-2} in THF and S_{8-9}^{-2} in DMSO after the 24-hour reaction period.

TABLE 2

ABILITY OF APROTIC ORGANIC SOLVENTS TO DISSOLVE
>0.1M/ℓ as Li_2S_n at 25°C

METHOD A: $2Li + \frac{n}{8} S_8 \rightarrow Li_2S_n$

METHOD B: $S_8 + 2e^- \rightarrow S_8^{-2}$

METHOD C: $Li_2S + \frac{(n-1)}{8} S_8 \rightarrow Li_2S_n$

Solvent	Method A	Method B	Method C
γ-Butyrolactone (BL)	+	-	+
Dimethylacetamide (DMAC)	*	+	+
Dimethylformamide (DMF)	*	+	+
Dimethyl sulfite	-	ND	-
Dimethyl sulfoxide (DMSO)	+	+	+
Methyl acetate (MA)	-	+	+
Methyl formate (MF)	ND	ND	-
Nitromethane (NM)	ND	ND	-
Propylene carbonate (PC	-	-	-
Pyridine	ND	ND	**
Sulfolane	-	ND	+
Tetrahydrofuran (THF)	+	+	+

+ = Dissolution of >0.1M as Li_2S_n
- = Dissolution of <0.1M as Li_2S_n
* = Solvent reacted with Li
** = Solvent reacted with polysulfides
ND = Not done

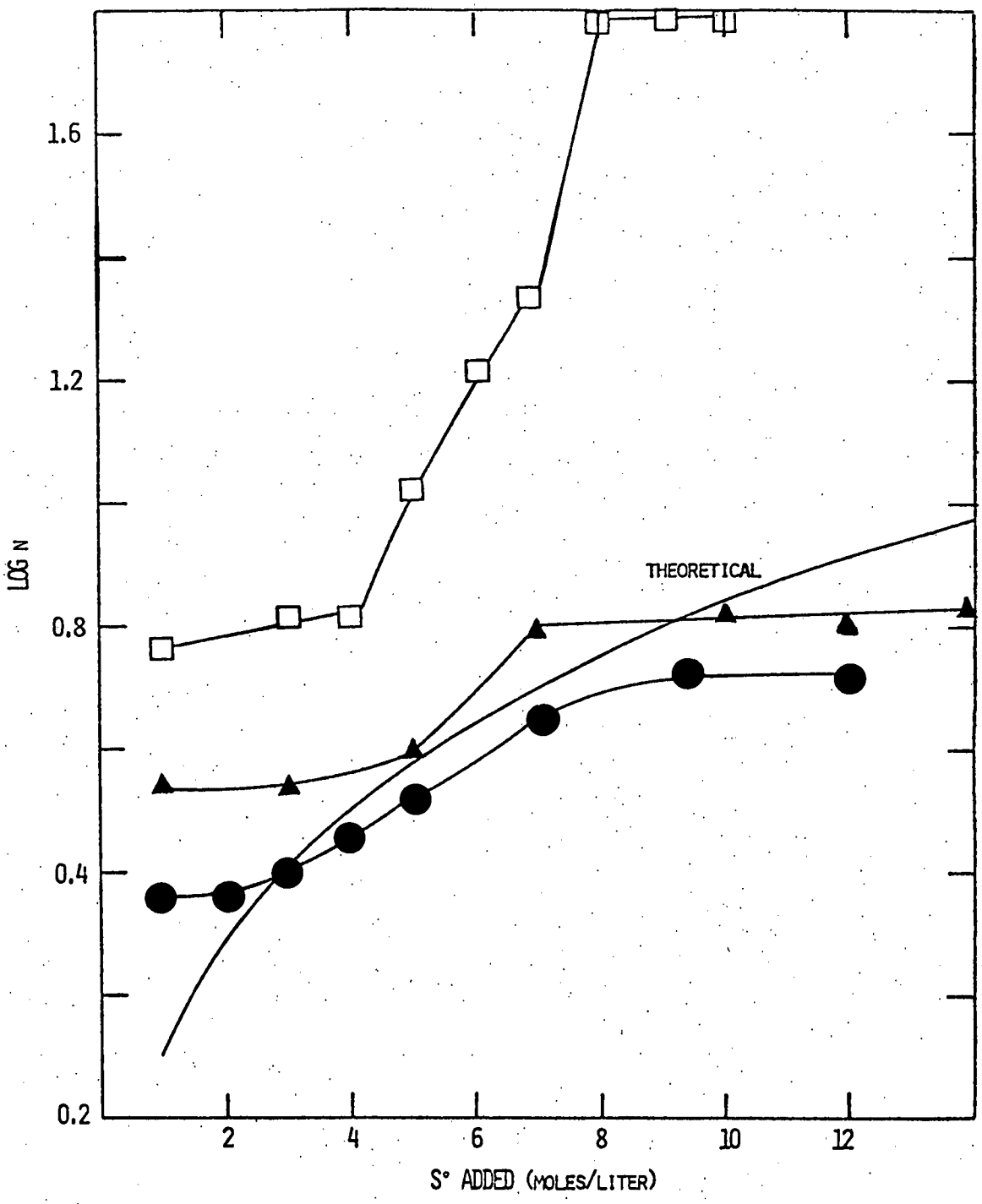

Fig. 2. Average orders of polysulfides in solution formed by adding aliquots of sulfur to 1M Li_2S. It is assumed that all the sulfur in solution is polysulfide. T = 25°C. ● DMSO; ▲ THF; □ MA. The theoretical curve is for total reaction of $Li_2S + S \rightarrow Li_2S_n$ (dissolved).

In DMSO, solutions of Li_2S_n may be concentrated by vacuum evaporation to a deep red glassy residue. In THF, solutions initially ∿10M in S could also be concentrated further by vacuum evaporation, but it was possible to remove all of the solvent, leaving behind a light brown mixture of solids. In MA, such concentration led readily to a very light precipitate. In each case, when rediluted, the residue or precipitate yielded the spectral properties of the original solution.

The instability of solid Li_2S_n (19,20) apparently prevents its precipitation. In DMSO, the glassy residue left after evaporation is most likely a solvate of Li_2S_n which prevents the disproportionation:

$$Li_2S_n \rightarrow Li_2S + \left(\frac{n-1}{8}\right)S_8 \qquad (5)$$

Reaction (5) is indicated in MA and perhaps in THF, where solvent-solute interactions are weaker.

Methyl acetate demonstrated low S solubility but very high polysulfide chain lengths. The limiting solubility of ∿1.0M S was attained after the addition of the first aliquot of S°, with an analyzed polysulfide order of 9.2. Thereafter, both Li_2S and S° were in excess, although the dissolved polysulfide order was observed to increase after each 24-hour period. By the tenth S° addition, the polysulfide order had increased to over 100.

4. Spectral Properties of Polysulfide Solutions

The solutions obtained in DMSO, THF and MA at the various $S°:S^{-2}$ ratios were diluted, and visible, near UV absorption spectra recorded. Care was taken to exclude O_2, as oxidation of S_n^{-2} yields higher order polysulfides and alters the spectrum.

The spectra of the DMSO-polysulfide solutions were similar to those already published (5,10,12,13). The peak between 400 and 500 nm, indicative of the polysulfide order (cf. Table 1), moved from 420 nm to 492 nm as the order was increased from 4 to 8. The peak at 618 nm, attributed to S_3^-, reached maximum intensity of n = 6, due to the monomer-dimer equilibrium

$$S_6^{-2} \rightleftarrows 2S_3^- \qquad (6)$$

The 618 nm peak predictably decreased relative to the peak between 400 and 500 nm as the polysulfide concentration was increased. Solutions having an average composition of Li_2S_8 showed no shift in the 492 nm maximum when the total S concentration was increased from 10^{-3}M to >2M, the spectra being obtained using an adjustable narrow path length cell.

Hence, no evidence for an equilibrium of the type

$$S_8^{-2} \not\rightleftharpoons 2S_4^- \qquad (7)$$

was observed.

In THF, spectra of polysulfides of a given average chain length differ markedly from those recorded in DMSO. As shown in Figure 3, spectra of low order polysulfides in THF are characterized by a shoulder at ∿400 nm which moves to a limit of ∿440 nm as n increases. The wide variety of colors exhibited by polysulfides in DMSO is absent in THF. This is due primarily to the lack of a 618 nm peak and the apparently similar absorption spectra of all S_n^{-2} species in THF.

This extraordinary difference in polysulfide spectra in THF and DMSO is illustrated in Figure 4. Here, a 4.5M solution in THF of S as $Li_2S_{9.7}$ was diluted 1:160 with THF. As in Figure 3, the spectrum shows only a shoulder at ∿400 nm. On further dilution of the solution by a factor of 3:5 with DMSO, the solution turns from yellow-orange to deep purple. The resulting spectrum has a peak at 618 nm, corresponding to S_3^-, and a second peak at ∿500 nm. This latter peak is red-shifted from the normal S_8^{-2} absorption (492 nm). It may correspond to n > 8 polysulfides, to S_4^- (λ_{max} = 513)(15) or to a mixture of such species.

To date, the only polysulfide radical anion identified with certainty in solution is S_3^-. Others (such as S_4^-) probably exist, and are indicated under certain conditions in THF and MA. For example, on aging in an inert atmosphere, a new peak at ∿500 nm appears in THF, Li_2S_n solutions. A likely candidate for this species is S_m^-, formed via the slow disproportionation of S_n^{-2}.

In MA, the lowest average polysulfide order observed is 9.2. The primary polysulfide peak in MA is similar to that in THF (400-440 nm) as a function of n. Also present is a shoulder at ∿465 nm, not observed in THF. On aging, MA/Li_2S_n solutions develop a peak at 529 nm. As with THF, these complex spectra are probably due to a slow equilibration of S_m^- and S_n^{-2} species.

To observe the effects of solvent on the spectra of long chain polysulfides, solutions of Li_2S_{100} in MA were diluted 10:1 with MA and with DMSO. The effects of such dilutions are shown in Figure 5. The primary peak in MA (433 nm) moves to 449 nm on adding DMSO. Also, the peak at 529 nm becomes a broad shoulder at 536 nm. Also in DMSO, the absorbances are about double those in MA, for the same sulfur concentrations.

The hyperchromic effects and red shifts generally observed for polysulfides in DMSO (or DMF) compared to THF or MA probably reflect

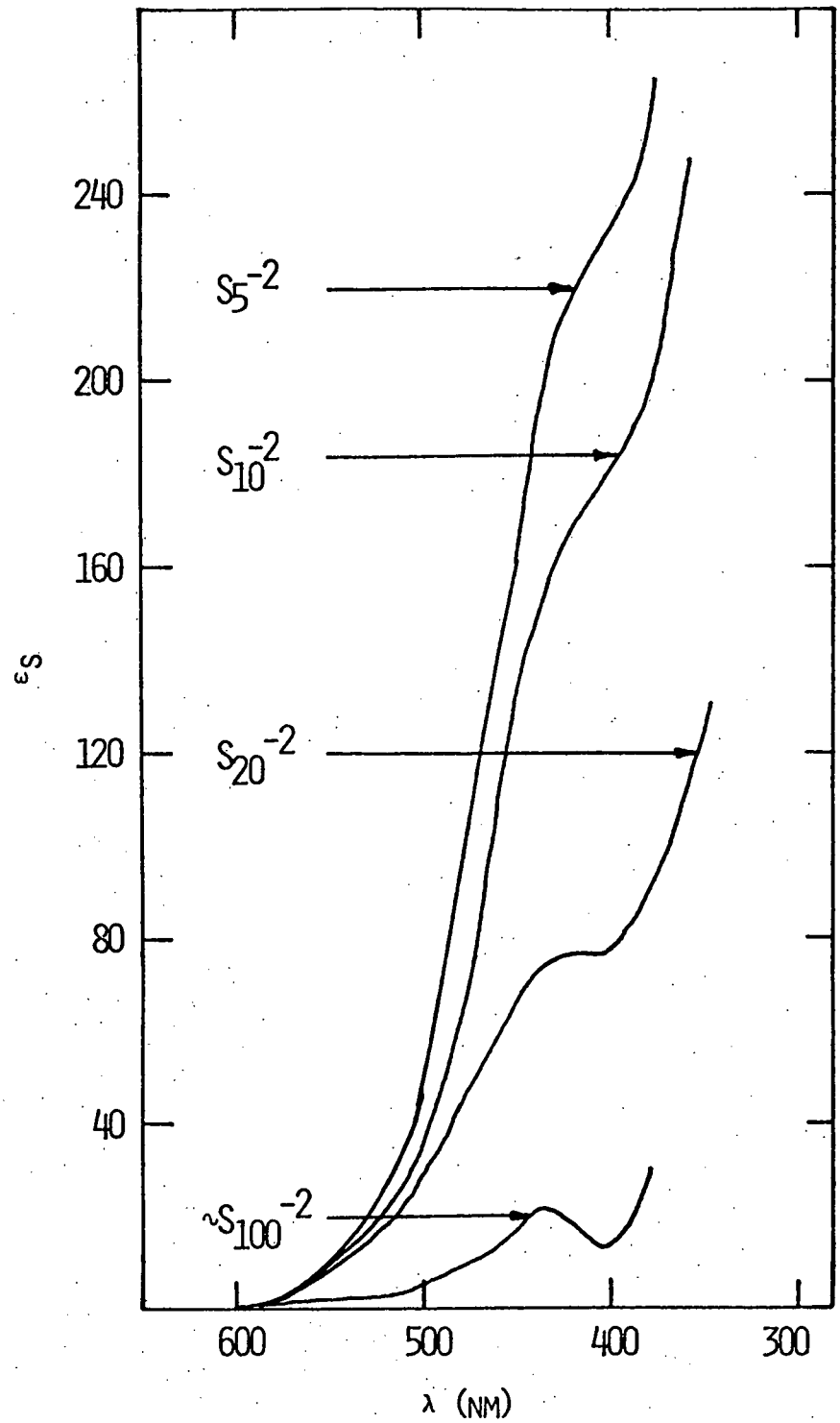

Fig. 3. Spectra of Li_2S_n in THF at 25°C, as a function of average polysulfide order. T = 25°C. ε_S is the extinction coefficient based on the total S concentration.

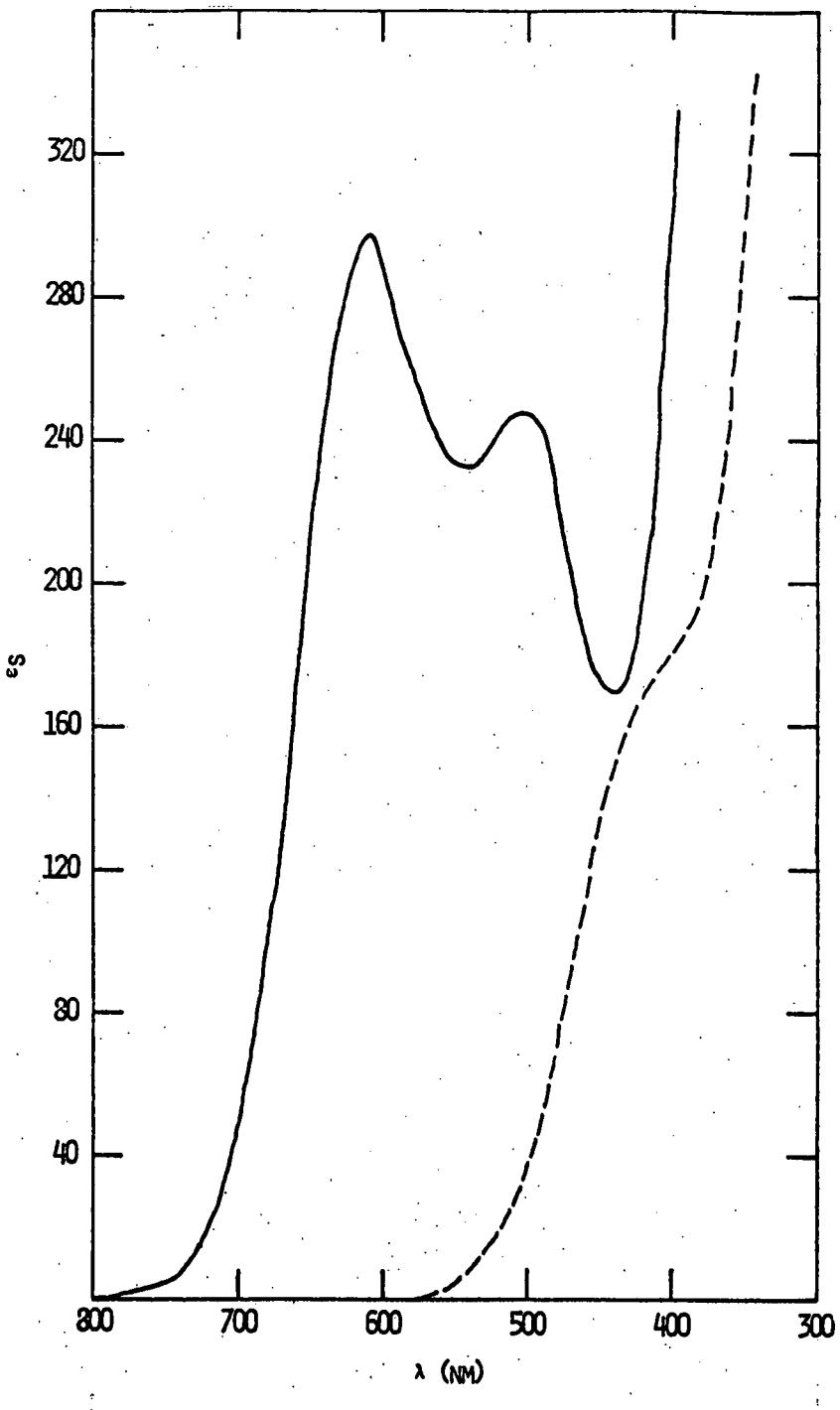

Fig. 4. Spectra of $Li_2S_{9.7}$ dissolved in (---) THF (0.027M S) and in (——) 3:2 THF/DMSO (0.016M S). T = 25°C.

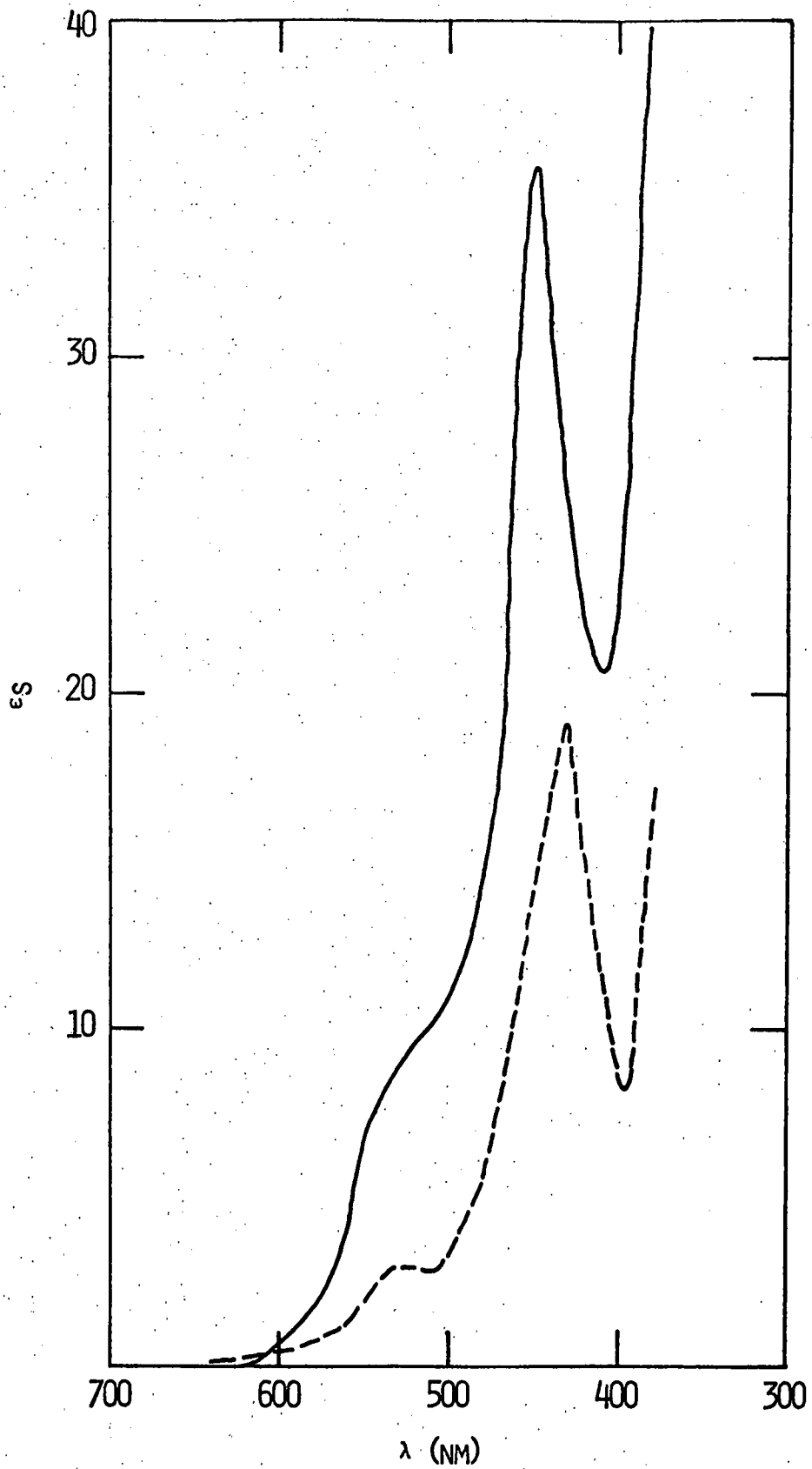

Fig. 5. Spectra of Li_2S_{100} dissolved in (---) MA (0.04M S) and in 1:10 MA/DMSO (0.04M S). T = 25°C.

differences in the ground state geometries of the solvates. It is also clear that the equilibration between S_m^- and S_n^{-2} species is affected by solvent, the former species giving rise to complications in the absorption spectra. In DMSO, S_3^- is readily produced, but in THF and MA, only absorbances which may correspond to longer chain anion radicals are observed, and these are often slow to evolve. Again, fundamental differences in the solvation and consequent electronic structure of polysulfides are indicated in different solvents.

5. Conclusions

Solubility limits of S as Li_2S_n, when produced by reaction (4), are given in Table 3 for several aprotic organic solvents of varying dielectric constant (D) and basicity. The latter is reflected by the Gutmann donor number DN_{SbCl5} (21,22). Also shown in Table 3 are the average polysulfide chain lengths needed to achieve the maximum S solubility in MA, THF and DMSO. The solubilities and average chain lengths were determined by chemical analysis of total S and S^{-2} in the experiment described above and summarized in Figure 2.

TABLE 3

RELATIONSHIP OF DIELECTRIC CONSTANT AND SOLVENT BASICITY TO POLYSULFIDE SOLUBILITY AND CHAIN LENGTH. n_{max} IS THE AVERAGE POLYSULFIDE ORDER OBTAINED IN A SATURATED SOLUTION WHEN EXCESS S° IS ADDED TO 1M Li_2S.

Solvent	Approx. [S] as Li_2S_n	Dielectric Constant	Donor Number (DN_{SbCl5})	n_{max}
Nitromethane	0.1M	35.9	2.7	-
Propylene carbonate	<0.1M	65.0	15.1	-
Sulfolane	0.1-1.0M	43.3	14.8	-
Methyl acetate	1.5M	6.68	17.0	>100.0
Tetrahydrofuran	10.0M	7.5	20.0	10.2
Dimethyl sulfoxide	10.0M	46.7	29.8	8.9

It may be concluded from Table 3 that polysulfide solubility relates less to dielectric constant (D) than to solvent basicity. High solvent basicity is apparently essential for high polysulfide solubility, while no significant correlation is found with D.

As also seen in Table 3, the favored polysulfide chain length is related to dielectric constant. Polysulfides of highest average order are formed in MA, followed by THF and DMSO. Solvents of high D can stabilize the more localized negative charge of the lower order polysulfides, while low D favors the formation of long chains.

It is possible, on the basis of the present results, to postulate a mechanism for the interaction of basic solvents with polysulfides, which explains the effect of such media on the visible spectra of S_n^{-2} species. Giggenbach (8) has suggested three electronic structures for S_4^{-2}:

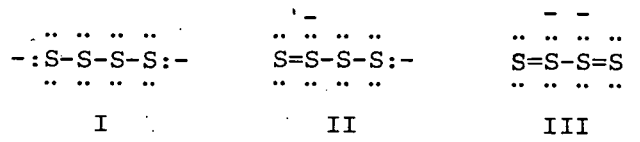

I II III

The double bond character of structures II and III is a result of $d\pi$-$d\pi$ interactions, due to the promotion of the electrons from nonbonding p orbitals on the terminal sulfur atoms to d orbitals on the central sulfur atoms. Longer chain polysulfides would exhibit similar structures, with more extensive electron delocalization obtainable from $d\pi$ bonding.

The conjugation in structures II and III would give rise to low energy electronic spectral transitions. The lowest energy electronic transitions for S_4^{-2} in H_2O, THF and DMSO occur at λ_{max} = 358 nm (3), 400 nm and 420 nm, respectively. It is therefore likely that I is stabilized in hydrogen bonding solvents (8), while II and III become more prevalent as the solvent basicity is increased. The vacant nonbonding orbitals in II and III constitute acidic sites which are subject to complexation by basic solvents, resulting in high polysulfide solubility.

Basic solvents which show substantial S_3^- formation have $R_2C{=}O$ or $R_2S{=}O$ structural units in common. This fact, coupled with the very large spectral shifts and spectral intensity increases observed in these solvents, is suggestive of a more specific solvent-solute interaction for both anion and radical anion species. Such complexes might contain planar conjugated sulfur moieties, explaining the extreme polysulfide spectral differences between THF and DMSO.

The results further indicate that the type of complexation giving rise to species absorbing at 490-500 nm for moderate chain length polysulfides in DMSO is replaced by another kind of interaction for very long chain polysulfides (as in MA and MA, DMSO solutions), resulting in a somewhat higher energy absorption (Figure 5). The exact structure of these polysulfide-solvent complexes has not yet been determined.

In summary, one can select a priori which aprotic solvents will dissolve polysulfides and make qualitative predictions concerning favored polysulfide order (and solution color). Solvents of high D and DN show high polysulfide solubility, and stabilize low order polysulfides and S_3^-. S_n^{-2} solutions are red at high concentration and blue or green at low concentration. Solvents of low D and high DN show high solubility of longer chain polysulfides. Solutions are yellow-red at all dilutions, turning red on standing. Solvents of low DN show poor affinity for polysulfides.

C. Electrochemistry of Polysulfides in Nonaqueous Solvents

Since polysulfide solubility, disproportionation equilibria, and spectra are highly solvent dependent, it is not surprising that electrochemical properties of these species should show a similar environmental sensitivity. As was reported in detail in the First Semiannual Report of this program (23), cyclic voltammograms of S_8 were recorded in over a dozen aprotic media. In DMSO, it has been well-documented by Sawyer and co-workers (9,10) that the most positive reduction reaction of neutral sulfur is

$$S_8 + 2e^- \rightarrow S_8^{-2} \qquad (8)$$

In our First Semiannual Report, it was shown that this reaction occurs at E_{max} = 2.7V-2.9V vs. Li^+/Li in DMSO, dimethylformamide (DMF) and dimethylacetamide (DMAC), but only at 2.0 to 2.2V in THF, butyrolactone (BL), sulfolane (SL), MA, PC and dimethyl sulfite (DMSI). This sharp difference is illustrated in Figure 6, where the cyclic voltammograms of S_8 in DMSO and THF are compared.

Since S_8 is nonpolar and only very slightly soluble in these solvents, it is assumed that the energy of solvent-solute complexation is also uniformly weak. Conversely, the charged reduction product in equation (8) is very strongly solvated in many polar media, as indicated in the previous subsection. Thus, the solvent-dependent potentials of S_8 reduction can be ascribed almost exclusively to the relative strengths of the solvent-solute complex.

It is interesting to note that no clear-cut correlation between redox potential of S_8 and S_8^{-2} (or other polysulfide) solubility can be made. For example, the S_8^{-2} solubility in DMSO and THF are about equally high, while it is practically zero in PC. This is probably because the Li_2S_n formation reactions of the type

$$Li_2S + S_8 \rightleftarrows 2Li^+ + S_9^{-2} \qquad (9)$$

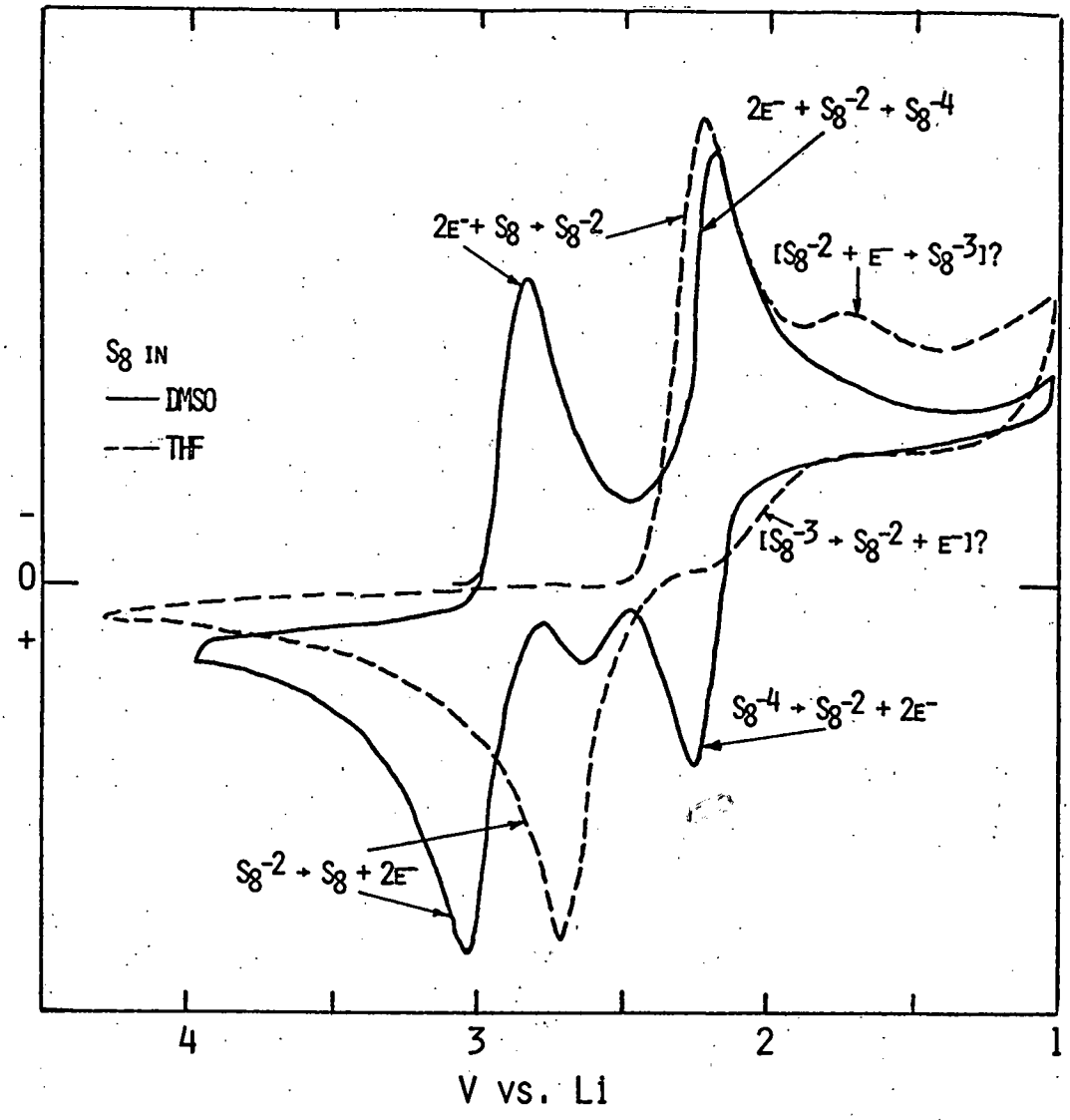

Fig. 6: Cyclic voltammograms of S_8 in DMSO and THF.

are shifted to the right by large specific S_n^{-2}-solvent interactions, but to the left by high dielectric constant.

In a Li/dissolved Li_2S_n battery, the reduction potential of S_8 is not as important as that of S_n^{-2}. Furthermore, the potential of the reduction

$$S_n^{-2} + 2e^- \rightarrow S_n^{-4} \qquad (10)$$

appears to be much less solvent dependent than that of S_8. As shown in Figure 6, the reduction of polysulfide occurs at 2.1-2.2V in both THF and DMSO. This similarity results from the highly polar nature of reactants and products in polysulfide reduction, so that differences in solvation energy are relatively solvent-insensitive.

The mechanisms of polysulfide redox reactions are quite complex. Yet, it is important to know the details of these reactions as they determine the charge-discharge potentials and capacities of the Li_2S_n electrode. Using spectroelectrochemical techniques coupled with potentiostatic coulometry, we have investigated the oxidation and/or reduction reactions of S_8, S_8^{-2}, S_6^{-2}, and S_4^{-2} and S^{-2} in DMSO. The results, which also incorporate published investigations in DMSO and DMF by Sawyer and co-workers (10,11) and by Delamar and co-workers (13,24), are presented in Table 4.

The reduction of S_4^{-2} is very slow in basic aprotic solvents. However, this reduction has been observed in aqueous base on Hg electrodes at a potential corresponding to 2.7V vs. Li (25). The following catalytic scheme was proposed:

$$Hg + S_4^{-2} \rightleftarrows Hg...S + S_3^{-2} \qquad (11)$$

$$2e^- + Hg...S \rightarrow Hg + S^{-2} \qquad (12)$$

We have found that the rate of reduction of S_4^{-2} is also enhanced on a Ag electrode, probably by a similar mechanism. We have also found that the reduction of S_4^{-2} is aided by homogeneous catalysts such as Ba^{+2}, which probably holds the S_4^{-2} in a rigid configuration by complexation,

$$S_4^{-2} + Ba^{+2} \rightleftarrows$$

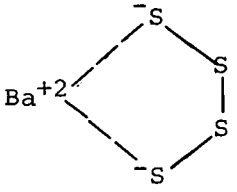

(13)

Reduction of S_4^{-2} in presence of Ba^{+2} (with a low surface area carbon electrode) leads to a product analyzed as S_2^{-2}.

TABLE 4

OBSERVED REDOX REACTIONS OF S_n^{-2} IN DMSO ON C

Polysulfide Species	Oxidized or Reduced	E_{max} (V vs. Li)	Reaction Mechanism
S_8, $S_n°$	Red.	2.7	$S_8 \rightarrow S^{-2}$
S_n^{-2} (n>4)	Red.	2.1	$S_n^{-2} \rightarrow [S_n^{-4}] \rightleftarrows 2S_{n/2}^{-2}$
S_n^{-2} (n<4)	Red.	2.1? Very Slow	$S_n^{-2} \rightarrow [S_n^{-4}] \rightleftarrows 2S_{n/2}^{-2}$
S^{-2}	Ox.	3.5	$S^{-2} \rightarrow [S°] \xrightarrow{S^{-2}} S_2^{-2}$
S_2^{-2}	Ox.	3.0-3.5	$S_2^{-2} \rightarrow [S_2°] \xrightarrow{S^{-2}} S_3^{-2}$
S_3^{-2}	Ox.	3.0	$S_3^{-2} \rightarrow S_3^{-} \rightleftarrows 1/2\ S_6^{-2}$
S_m^{-2}	Ox.	3.1	$S_m^{-2} \rightarrow S_m° \underset{}{\overset{S_n^{-2}}{\rightleftharpoons}} S_{n+m}^{-2}$
S_8^{-2}	Ox.	3.05	$S_8^{-2} \rightarrow S_8°(\text{linear}) \rightleftarrows S_8°(\text{octagonal})$

Unlike in DMSO, reduction of S_n^{2-} in THF can be carried out to nearly the Li_2S limit, albeit at decreasing rates with decreasing ambient chain length. In Figure 7, the potentiostatic reduction of S_n^{2-} in THF is followed by cyclic voltammetry. It is seen that reduction rates of short chain polysulfides are low but finite; in DMSO, reduction essentially ceases at S_4^{2-}.

The effects of acidic complexing agents on S_n^{-2} reduction kinetics in THF was investigated. The effect of the Lewis acid triphenyl boron (ϕ_3B) is particularly striking. As shown in Figure 8, the addition of ϕ_3B to a solution of S_{10}^{-2} in THF shifts the polysulfide absorption spectrum from λ_{max} = 420 nm to a limiting $\lambda_{max} \approx 390$ nm at a 2:1 complex stoichiometry. Chemical analysis has shown that addition of the ϕ_3B does not alter the S^{-2}/S ratio. The complex is probably represented by the structure

$$[\phi_3B\cdots{}^{-}S + S_8 + S^{-}\cdots B\phi_3]^{-2}\ 2Li^{+}$$

Similar spectral shifts are noted on the addition of protic solvents to THF.

The reduction in THF of S_{10}^{-2} and $S_{10}^{-2}\cdot\phi_3B$ are compared in Figure 9. The voltammograms show that ϕ_3B also enhances the S_n^{-2} reduction rate. (When <u>complete</u> complexation is approached, electrode passivation is observed on reduction, and the voltammograms become quite noisy.)

Spectra of S_n^{-2} show large shifts to higher energies in acidic solvents such as MeOH, compared to basic solvents, such as DMSO. Since such shifts are also observed when ϕ_3B is added to THF solutions, we hypothesize that acidic coordination favors the localization of the highest energy S_n^{-2} electrons on the terminal sulfur atoms, in nonbonding p-orbitals, e.g.,

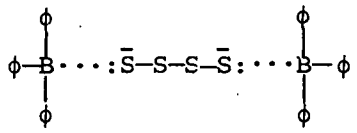

(I)

However, basic coordination favors their delocalization into the next highest d-orbitals:

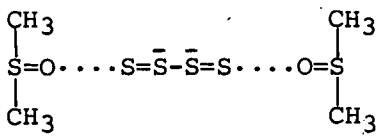

(II)

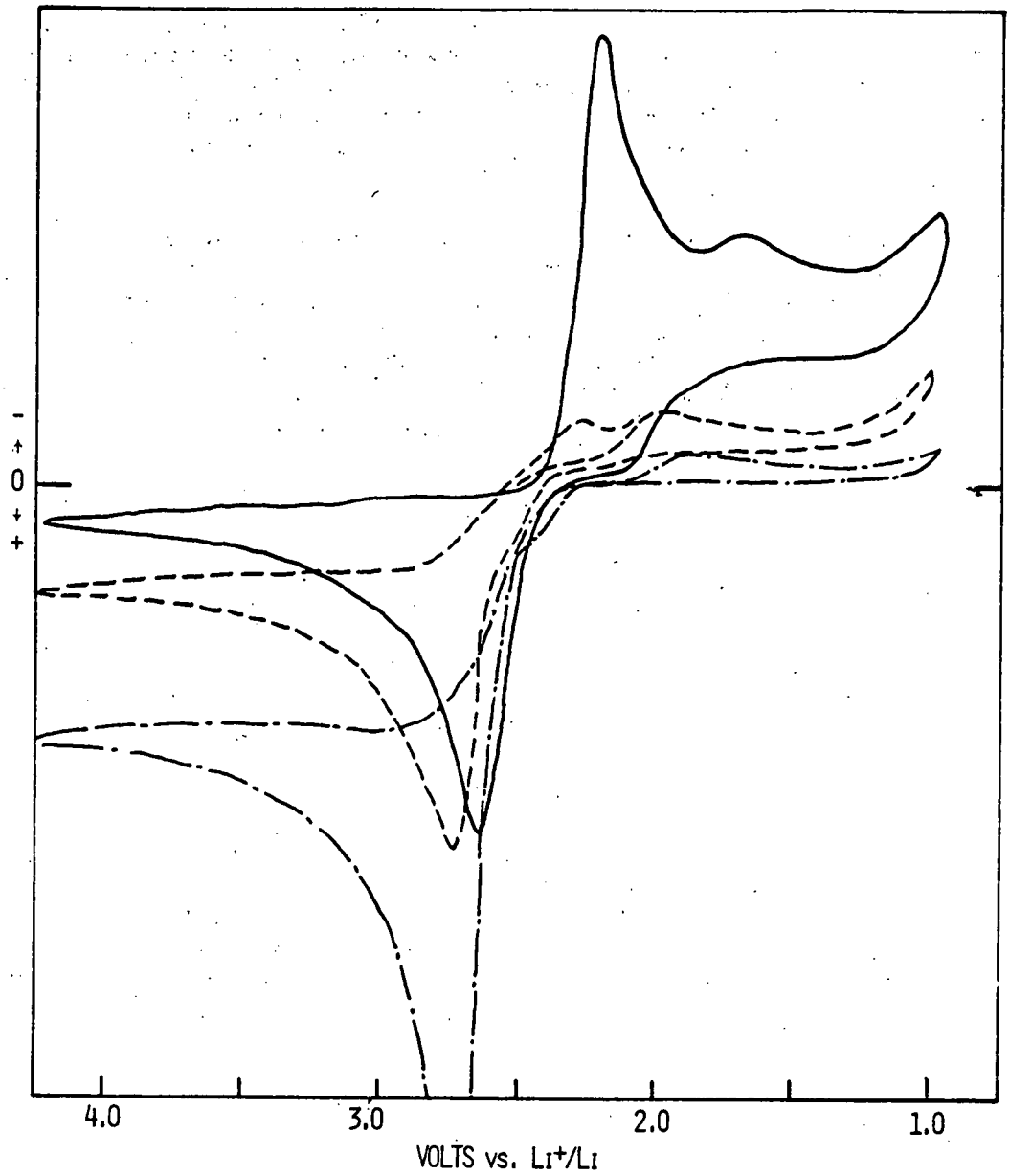

Fig. 7: S Reduction in THF, 1M $LiAsF_6$. Cyclic voltammograms on vitreous C. ——— 0.04M S as S_8
----- After reduction at 2.25V for 0.54 e^-/S
—·— After continuing reduction at 2.0V for 0.55 e^-/S
Sweep speed = 0.1 V/sec.

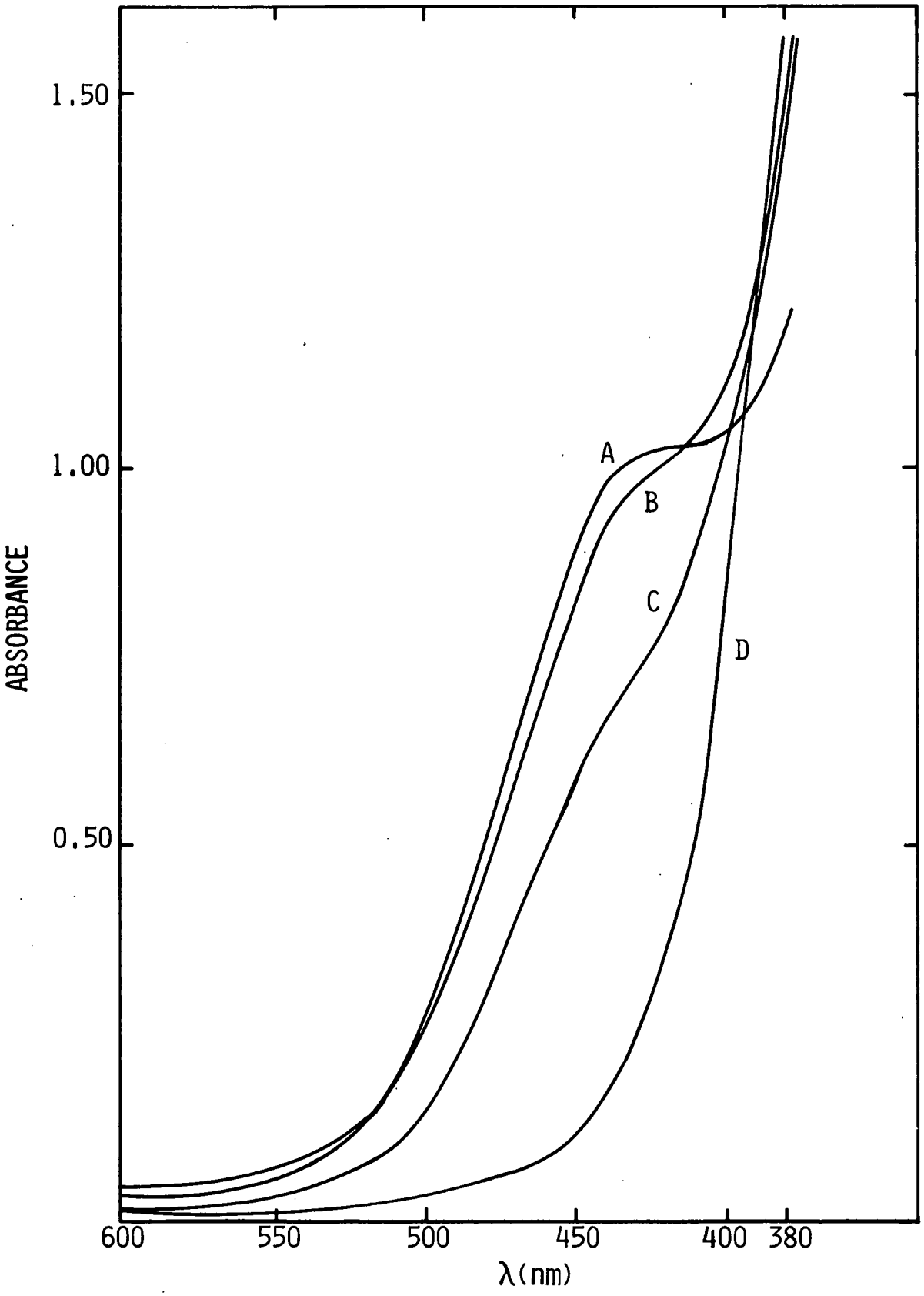

Fig. 8: Visible absorption spectra of Li_2S_{10} in THF (0.05M S) as a function of added amounts of $(C_6H_5)_3B$. A = no $(C_6H_5)_3B$; B = $[S_{10}^{-2}]/[(C_6H_5)_3B]$ = 1.66; C = $[S_{10}^{-2}]/[(C_6H_5)_3B]$ = 1; D = $[S_{10}^{-2}]/[(C_6H_5)_3B]$ = 0.5.

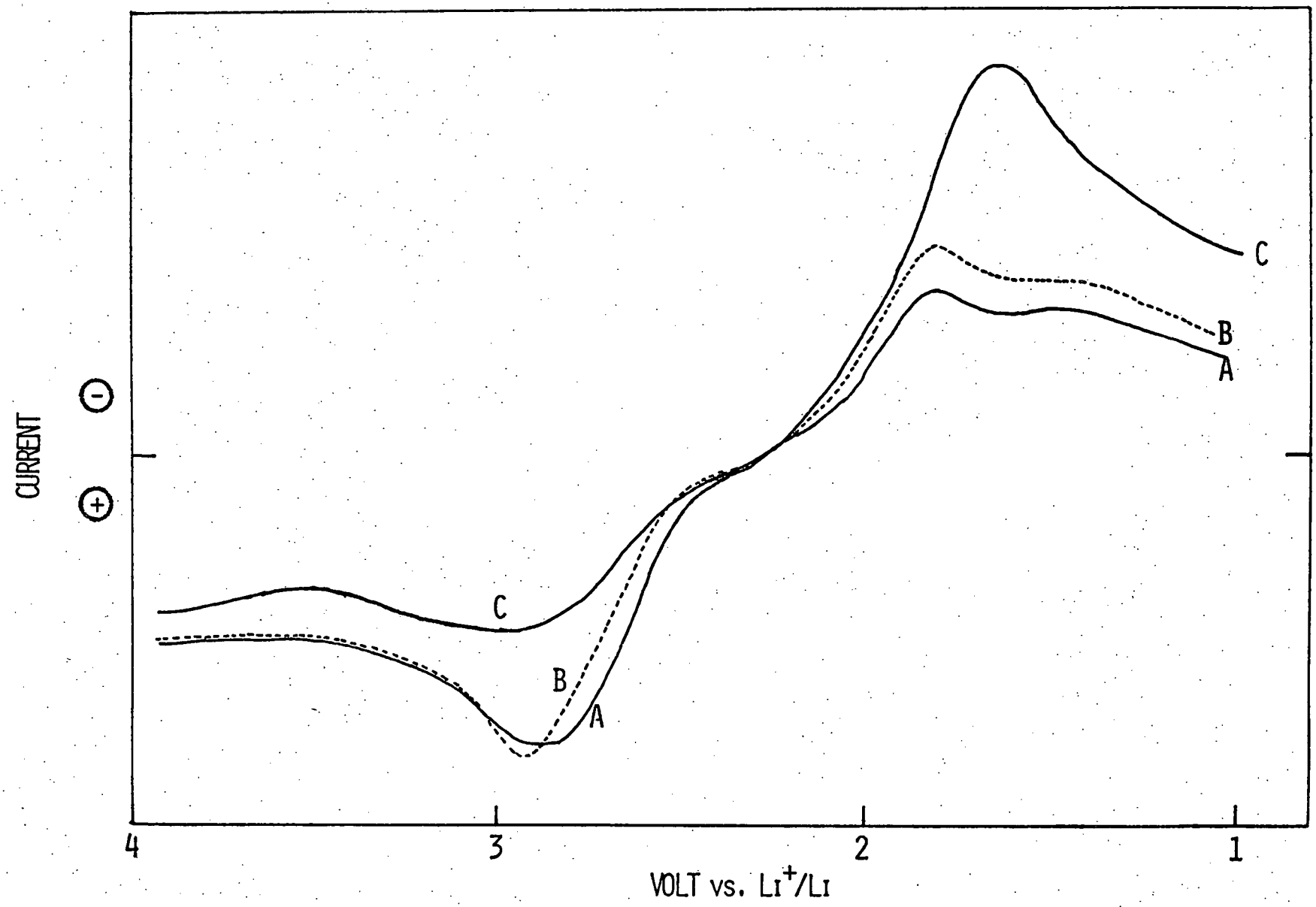

Fig. 9: Linear sweep voltammograms of Li_2S_{10} (0.2M S) in THF, 1M $LiAsF_6$. A, no $(C_6H_5)_3B$; C, $[S_{10}^{-2}]/[(C_6H_5)_3B] = 1$.

The d-orbital conjugation gives rise to lower order spectral transitions. More important, however, is that the transfer of electrons from an electrode to the vacant d-orbitals of I is likely to be easier than their transfer to the complexed nonbonding p-orbitals of II. This argument explains the catalytic effect of Lewis acids on the S_n^{-2} reduction rate. It also explains why THF, which appears to yield polysulfide structures intermediate between I and II, enables more complete polysulfide reduction than DMSO.

As a result of the studies of polysulfide solubility and electrochemistry, THF has become the solvent of choice for the Li/Li_2S_n battery. THF and its derivatives have also been shown to be compatible with the Li electrode. In the remainder of this section, we summarize the key results regarding rate, capacity, and rechargeability of this system.

D. A Lithium/Dissolved Sulfur Battery with an Organic Electrolyte - Rate and Capacity Studies

1. Background

As stated earlier, an ambient temperature Li/S battery utilizing an organic electrolyte has many attractive possibilities, among them high energy density, and the use of relatively low cost, relatively safe materials. Previous attempts to develop such a cell have involved the incorporation of insoluble S_8 directly into the current collector (26-28). In general, very poor discharge efficiencies were obtained. One explanation put forth for these results is that some of the S_8 was reduced to soluble polysulfide, S_n^{-2}, which "escaped" from the cathode current collector and self-discharged on the Li anode (29). One recent moderately successful approach to increasing the S utilization efficiency was to add a Lewis acid, BF_3, supposedly to suppress polysulfide formation (29,30).

The highest rate Li batteries, such as $Li/SOCl_2$ (31-33) and Li/SO_2 (34,35), have employed liquid cathodes. Here, very good electrical contact is maintained between the cathode material and the current collector through all phases of discharge. Both S_8 and its ultimate discharge product, Li_2S, are electrical insulators. Thus, it is likely that insulation of the cathode material, rather than S_n^{-2} formation, led to poor results of Li/S cells. In our experience, the reaction between Li and dissolved S_n^{-2} is very slow, and the formation of dissolved S_n^{-2} enhances cathode utilization. In this regard, the explanation of the effect of BF_3 on sulfur utilization is not very convincing.

In contrast to most previous work on Li/S batteries, we have chosen to investigate a system where the S is completely dissolved in the electrolyte, as Li_2S_n (36,37). Hence, the theoretical cell reaction becomes

$$\left(2\,\frac{n}{m}-1\right)\,Li + S_n^{-2} \rightleftarrows \left(\frac{n}{m}\right)S_m^{-2} + \left(2\,\frac{n}{m}-1\right)\,Li^+ \qquad (14)$$

Here, a penalty is paid in the theoretical energy density, since the S is initially partially reduced. However, the penalty is small if the value of n is large and m is close to 1. Certain basic, aprotic organic solvents which are compatible with Li have been shown to dissolve large amounts of Li_2S_n (38). Among the best of these is tetrahydrofuran, THF, where >10M S as $\sim Li_2S_9$ can be dissolved by the in situ reaction of Li_2S and S_8.

It is the purpose of this section of the report to present results on the capacity, rate capabilities, system stability of the Li/dissolved S battery in its current state of development.

2. Experimental

Tetrahydrofuran was obtained from Burdick and Jackson Laboratories and was spectroscopic, "distilled in glass" quality. Sulfur (99.9995%, Ventron Corp.) and Li_2S (97+%, Foote Mineral Company) were used as received. The supporting electrolyte, $LiAsF_6$, was obtained from U.S. Steel, Agri-Chemicals Division, and was certified to contain less than 70 ppm H_2O.

Solutions of $LiAsF_6$ in THF were prepared first, using procedures which have been reported elsewhere (39). To these solutions, stoichiometric amounts of sulfur and Li_2S were added to form Li_2S_n solutions of the required concentration and average polysulfide chain length (38). The reaction and dissolution were complete after stirring for 24 hours. Electrolyte containing 5M S, prepared this way, was dark red and of moderate viscosity. Concentrations of sulfur and "sulfidic" sulfur were determined for each preparation of electrolyte using standard analytical procedures (38).

All operations and storage of materials were carried out in an Ar-filled glove box (Vacuum-Atmospheres Corp.).

3. Results and Discussion

Cell Description. Cells were of the general configuration

$$Li \,\Big|\, \begin{matrix}5M\ S \\ \text{as } Li_2S_n\end{matrix},\ \begin{matrix}\text{Organic} \\ \text{Solvent}\end{matrix},\ 1M\ LiX \,\Big|\, \begin{matrix}\text{Teflon-Bonded} \\ C\ \text{Current Collector}\end{matrix}$$

The anodes were composed of 4.7 cm^2 of 0.015" thick Li foil pressed onto either side of stainless steel Exmet supports. Current collectors were Teflon-bonded carbon (40) of similar area, also on stainless steel Exmet supports. Microporous polypropylene (Celgard 2500, Celanese Corp.) was

used as a separator. Cells generally contained two anodes and three current collectors, arranged C/Li/C/Li/C and snugly fitted into rectangular glass vials. After the cells were checked for short circuits, the catholyte was pipetted in. The cells were mounted in an inert atmosphere housing beneath a glass dome for viewing. Leak-free electrical feedthroughs (Conax) were provided through the base of the housing. Assembly was conducted in an Ar-filled glove box (Vacuum-Atmospheres Corp.), after which the housing containing the cells could be removed for testing in an open atmosphere or an environmental chamber.

Fully assembled cells show open circuit potentials (OCP) of ∿2.35V when THF is used as a solvent. Cell resistances measured using a 1 kHz AC impedance bridge were 1-2Ω. Separate measurements on the catholyte revealed conductivities for 4.4M S as Li_2S_9 of 2.84 x 10^{-3} and 3.92 x $10^{-3}\Omega^{-1}$ cm^{-1} at 24.9°C and 53.7°C, respectively (41).

Discharge Capacities. Discharge capacities were measured galvanostatically at 0.5 mA/cm^2. In our prototype cells, for 75% cathode utilization, this corresponds roughly to the C/50 rate, but in a totally optimized design it is projected to be the C/24 rate (vide infra).

The first ∿10% of the discharge is sloping, from ∿2.3V to 2.0V. From studies of the electrochemistry of sulfur in THF (36,42-44), this portion is assigned to the reduction of residual S_8 suspended and/or dissolved in solution. The remainder of the discharge is flat, occurring at 2.0-2.1V, attributable to S_n^{2-} reduction. During this period, the OCP is 2.15V. At the end of discharge, the cell polarizes sharply. The usual cutoff potential in these experiments is 1.5V. Discharge curves at 25°C and 50°C are reproduced in Figure 10.

At room temperature, capacities were typically in the range of 1.5 e^-/S for 5.4M S as $Li_2S_{12.2}$ in THF, 1M $LiAsF_6$. Substantial increases in capacity are noted on increasing the temperature to 50°C. Under these conditions, capacities of up to 1.83 e^-/S are obtained on low rate discharge. The cathode stoichiometries are summarized as follows:

$$\text{Room temperature:} \quad S_{12.2}^{-2} + 18.3e^- \rightarrow 10.4S_{1.2}^{-2} \qquad (15)$$

$$50°C: \quad S_{12.2}^{-2} + 22.4e^- \rightarrow 12.2S^{-2} \qquad (16)$$

Thus, for the present configuration, optimal energy densities would be obtained at temperatures somewhat above ambient. Therefore, although room temperature operation is still important, many of our initial experiments characterizing the rate and rechargeability of this cell have been carried out at 50°C.

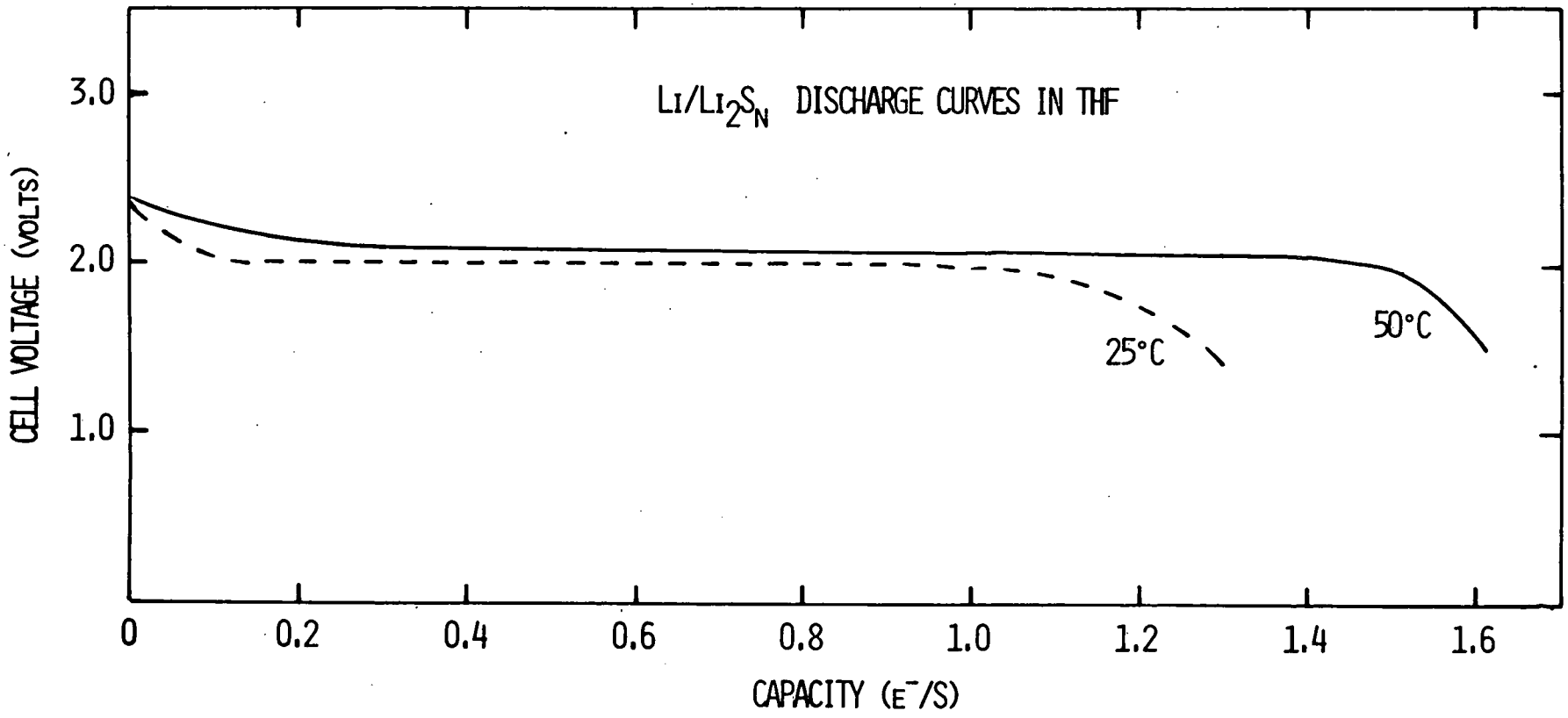

Fig. 10. Typical discharge curves of Li/Li_2S_n (5M S), THF cells at 25 and 50°C. Cell A/V = 7.5 cm^{-1}. Rate = 0.5 mA/cm^2.

Rate Capabilities. Initially, discharge rate capabilities were measured in "low rate" packages. In these cells the carbon electrodes were 1.75 ± 0.05 mm thick, and the ratio of Li area to solution volume was 7.5 cm^{-1}. At rates exceeding 0.5 mA/cm^2, the discharge capacities obtained at room temperature fall off sharply in this configuration. At 1 mA/cm^2, capacities ranging from 0.2 to 1.0 e^-/S have been observed, depending on the cell stack pressure, and filling procedures. Results under these conditions are quite irreproducible, as they lie on the steep slope of the capacity vs. rate curve. At these transitional rates, the discharge curves often show an erratic, "spiking" behavior, as if insoluble reduction products were alternately being formed, then dissolved away from the primary reduction sites.

Rates are improved somewhat at 50°C. The rate vs. capacity curve for cells discharged galvanostatically at this temperature in the "low rate" cell is reproduced in Figure 11. At 1 mA/cm^2, capacities exceeding 1.6 e^-/S are still possible, but the capacity drops sharply at higher rates. It was noted that the residual neutral sulfur in solution reduces at a higher rate than S_n^{-2}, and that this comprises much of the capacity above 4 mA/cm^2.

The discharge rates observed for Li/Li_2S_n cells are considerably below those predicted by elementary diffusional laws. In addition, charging of the cell can be carried out at substantially higher rates than discharging, without erratic or extreme polarization. These observations support the notion that factors other than simple mass transfer limit the discharge rate. The two most probable limitations are (1) blockage of the interior of the electrode by a surface layer of insoluble Li_2S and (2) the reduction kinetics of lower order polysulfides.

In order to explore the mechanism of rate limitation, capacity-rate curves were constructed for these cells as a function of S concentration. The results are shown in Figure 11. The rate capabilities increase considerably with decreasing Li_2S_n concentration. A further analysis of these curves shows that at any given intermediate rate, the specific charge passed is relatively independent of concentration. For example, at the 4 mA/cm^2 discharge rate, ∿24 $coul/cm^2$ are obtained in each instance. The conductivity of the electrolyte shows only a small variation with S concentration, i.e., 2.8×10^{-3} and $4.5 \times 10^{-3} \Omega^{-1} cm^{-1}$ with and without 4.3M S (as Li_2S_8)(41). Thus, a consistent model for capacity limitation at these rates is the formation of a passivating layer of discharge products at the current collector whose depth is determined by the iR drop within the pores, this drop being similar for the solutions studied.

The data in Figure 11 were used to design a new "high rate" cell package, in which a stoichiometry of ∿1 e^-/S could be obtained at 4 mA/cm^2 for the 4.3M S catholyte. This goal was reached by adjusting the A/V

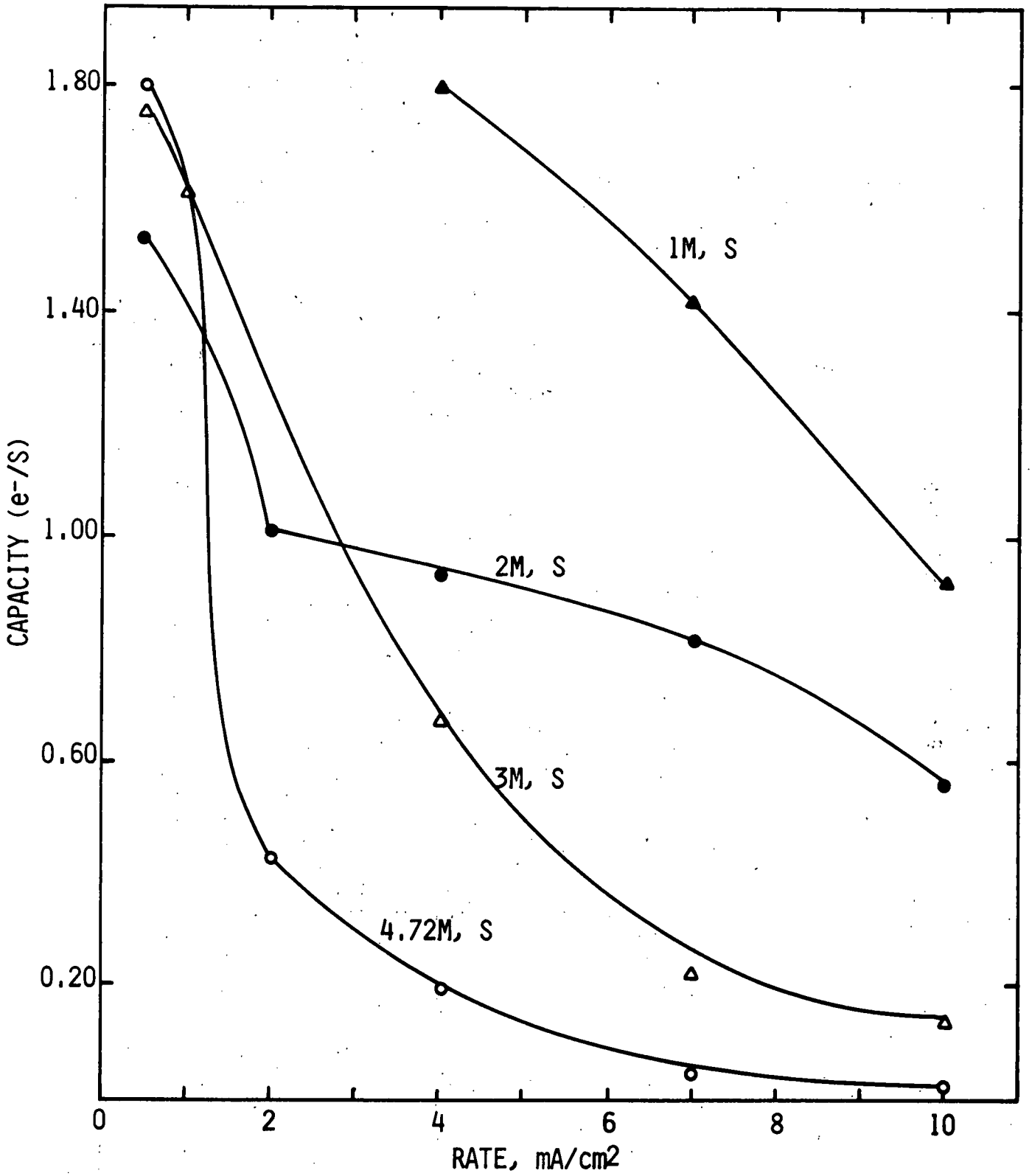

Fig. 11: Rate vs. capacity curves for Li/Li_2S_n, 1M $LiAsF_6$, THF cells at 50°C as a function of S concentration.

ratio in the cell package, so that 1 e^-/S was equivalent to ∿24 coul/cm^2. This thinner cell package utilized carbon electrodes 0.72 ± 0.05 mm thick and had an A/V ratio of 15.7 cm^{-1}, similar to that characterizing high rate Li/$SOCl_2$ D cells (45,46). Discharge curves obtained at 4 mA/cm^2 in "low" and "high rate" cells are compared in Figure 12. At 4 mA/cm^2, discharge stoichiometries of 0.97 to 1.12 e^-/S have been measured at 4 mA/cm^2 for the 4.3M S catholyte in the modified cells, while 0.2 e^-/S was typical of this rate in the initial configuration.

Catalysis of S_n^{-2} Reduction. Additional experiments were undertaken to determine whether the rate capabilities of Li/Li_2S_n cells could be improved further by using catalysis. Spectroscopic and electrochemical studies of sulfur and polysulfides in nonaqueous solvents suggest that the dynamic equilibria and redox chemistry of these species is strongly affected by solvent complexation. Cyclic voltammograms of S_8 in over a dozen nonaqueous, aprotic solvents have been recorded, and each has unique features (43). Spectra of solutions of S_n^{-2} reveal large differences between ethers, like THF, and basic C=O or S=O containing solvents like dimethylacetamide and dimethyl sulfoxide. The reduction rates of S_n^{-2} species are also affected by solvent. In dimethyl sulfoxide, for example, the reduction rate of S_n^{-2} at 2V vs. Li^+/Li is negligible when $n \leq 4$. However, with THF as a solvent, reduction is slow for short chain polysulfides, but rates in dilute solution are still significant for $n < 2$ (42). One possibility for heterogeneous catalysis is to employ an electrode which complexes with sulfur. For example, Kovacova and Zezula catalyzed the reduction of S_4^{-2} (25) and S_2^{-2} (47) in aqueous 2M NaOH using a Hg electrode. They suggest the intermediacy of a Hg-sulfur complex, viz.

$$S_4^{-2} \rightleftarrows S_3^{-2} + Hg\text{--}S \qquad (17a)$$

$$Hg\text{--}S + 2e^- \rightarrow Hg + S^{-2} \quad E_{1/2} = -0.8V \text{ vs. SCE} \approx 2.4V \text{ vs. } Li^+/Li \qquad (17b)$$

This concept has been explored for dilute solutions of Li_2S_n in DMSO. A polysulfide solution 0.05M in S in DMSO can be reduced only to S_4^{-2} at a constant potential of 2.0V vs. Li^+/Li. However, reduction on a Ag electrode could be extended down to $S_{1.8}^{-2}$, presumably via a mechanism similar to equation (17). Tests on cells containing Ag-impregnated current collectors have so far been inconclusive.

As indicated by the solvent effects on S_n^{-2} reduction, the mode of polysulfide complexation is the key to controlling the kinetics of reduction. The spectra of S_n^{-2} species in a variety of nonaqueous solvents demonstrate that acidic and basic complexation give rise to different electronic structures for the polysulfide chain. In general, lower solvent basicity results in enhanced S_n^{-2} reduction kinetics. Thus, acidic complexing agents can be added to Li_2S_n/THF solutions, to improve cell discharge rates.

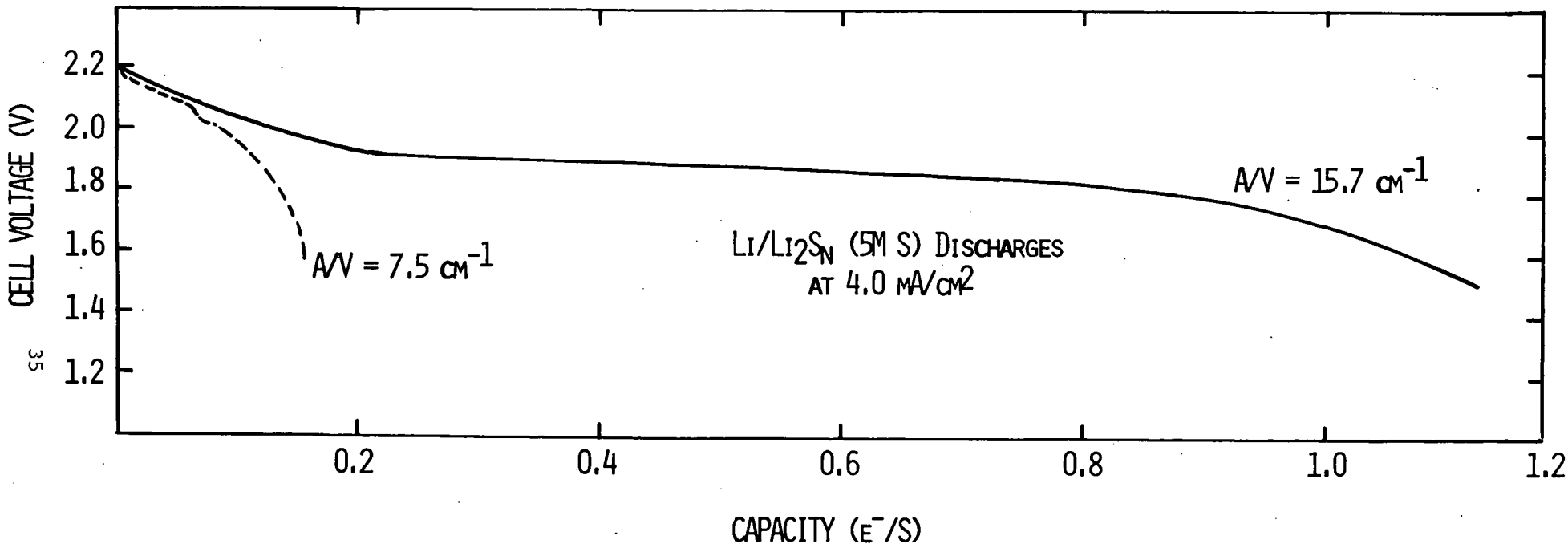

Fig. 12. Effect of cell geometry on the rate-capacity behavior of Li/Li_2S_n cells discharged at 50°C. A/V = Li electrode area/solution volume.

Results using Ba^{+2} and triphenyl boron (ϕ_3B) to complex S_n^{-2} have shown this to be a promising approach. In a dilute polysulfide solution in DMSO, added $Ba(ClO_4)_2$ allowed S_n^{-2} reduction to proceed down to $S_{2.8}^{-2}$ at 2.0V. In actual cell tests, Ba^{+2} also enhanced the discharge rates. Cells containing 0.1N $Ba(ClO_4)_2$ and an average of 4M S gave a capacity of 1.1 e^-/S when discharged at 2 mA/cm^2 and at 50°C. Above that rate, capacities were at least twice those obtained without Ba^{+2}.

Absorption spectral monitoring of a titration of S_{10}^{-2} in THF with ϕ_3B shows clearly a final complex of 2:1 stoichiometry (44), probably represented by the structure

$$[\phi_3B\text{-}S\text{-}S_8\text{-}S\text{-}\phi_3B]^{-2}\ 2Li^+$$

Voltammetric experiments on dilute polysulfide solutions have shown that ϕ_3B also enhances the S_n^{-2} reduction rate. However, when complete complexation of S_n^{-2} is approached, cathodic voltammetric scans on carbon give indications of electrode passivation. Apparently, the complex between low order polysulfides or S^{-2} and ϕ_3B is insoluble in THF, and is of high molar volume. This conclusion is supported by the observation that, when ϕ_3B and Li_2S are stirred in THF in a molar ratio of 2:1, a mild reaction occurs, with the formation of an insoluble white solid. Although no structural determination was carried out, this white solid is probably the sparingly soluble 2:1 complex.

Experiments using ϕ_3B in full cells confirm the effect. As illustrated in Figure 13, cells containing 1M S as Li_2S_{10}, and less than one ϕ_3B per S_{10}^{-2}, show 20-50% greater discharge capacities at 10 mA/cm^2, compared to a cell without ϕ_3B. At lower rates (4 mA/cm^2), however, when nearly full utilization of the cathode is realized in the baseline cell, the cells containing ϕ_3B do not do as well, in direct proportion to the amount of ϕ_3B present. Again, we must suspect premature passivation of the carbon current collector with bulky Li_2S- or Li_2S_2-ϕ_3B complexes.

The effect of ϕ_3B on cells containing 4.35M S is similar, in that there is some increase in capacity over the baseline cell above 4 mA/cm^2, but the baseline cell catches up with and eventually surpasses the ϕ_3B cells if the discharge is continued at 2 mA/cm^2. Another problem with these more concentrated solutions is that the addition of large amounts of ϕ_3B sharply increases their viscosity.

In summary, two mechanisms of rate limitation appear to be acting simultaneously: precipitation of the Li_2S in the cathode and a kinetic inhibition of S_n^{-2} reduction. Complexation of S_n^{-2} with ϕ_3B enhances its rate of reduction, but also appears to aggravate the passivation phenomenon. Additives to the electrolyte which solubilize Li_2S would certainly improve the latter. It is entirely possible that such Li_2S

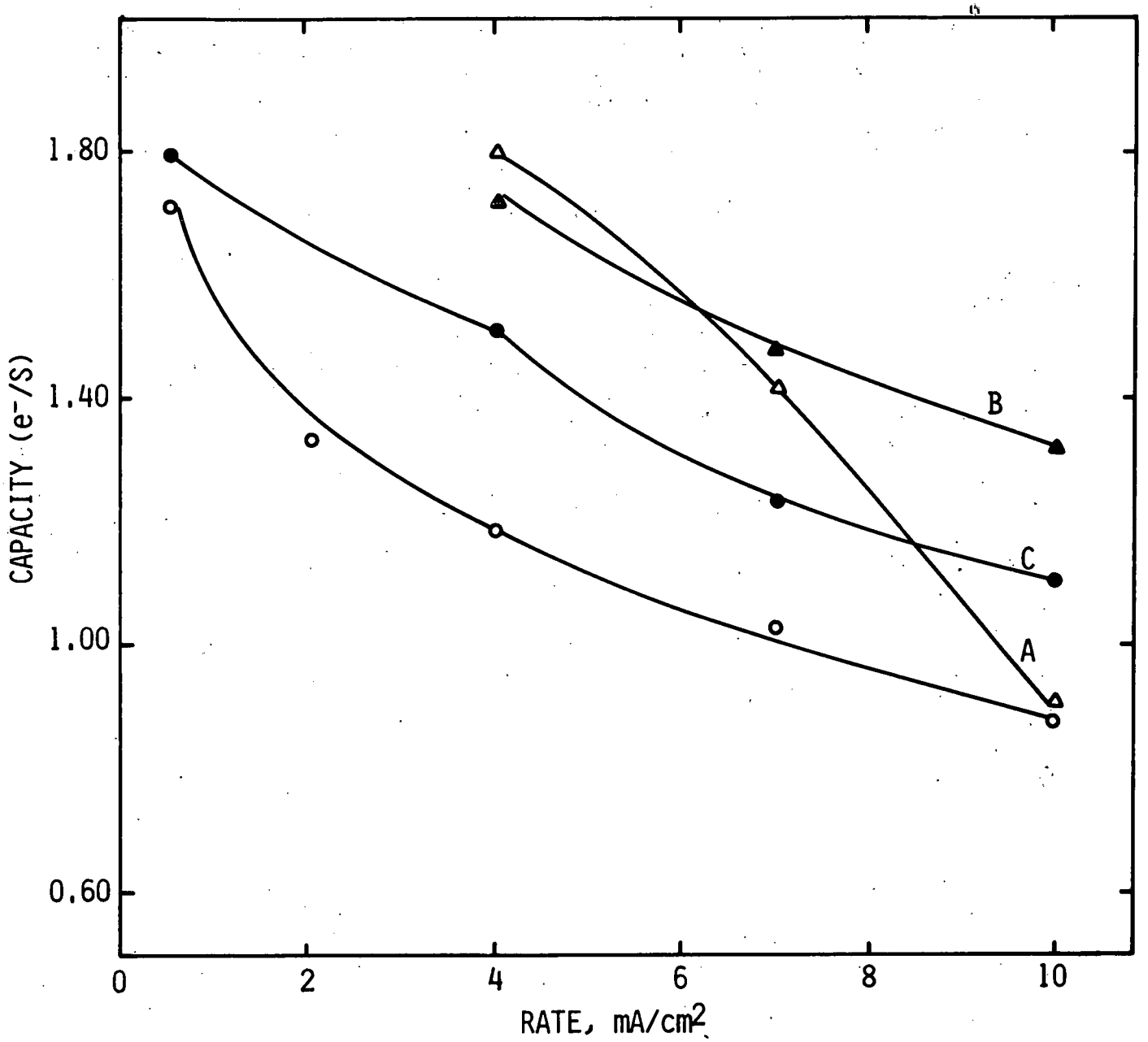

Fig. 13: Rate vs. capacity curves for Li/Li_2S_n (1M S), 1M $LiAsF_6$, THF cells at 50°C as a function of added amounts of $(C_6H_5)_3B$. A = Li_2S_{10} (1M S), no $(C_6H_5)_3B$; B = Li_2S_{10} (1M S), 0.06M $(C_6H_5)_3B$; C = Li_2S_{10} (1M S), 0.1M $(C_6H_5)_3B$; D = Li_2S_{10} (1M S), 0.2M $(C_6H_5)_3B$.

solubilizing agents would also be Lewis acids which catalyze S_n^{-2} reduction.

System Stability. The rate of reaction of Li_2S_n solutions with Li metal has been measured for foil contacting bulk solution and for assembled prototype cells. Tubes sealed under Ar were prepared containing 12 ml of 4.5M S as Li_2S_8 in THF or DMSO, 1M $LiAsF_6$. The tubes also contained 20 cm^2 of 0.015" thick Li foil, which was completely immersed in the solution. The tubes were stored at various temperatures. Periodically, aliquots of the solutions were removed and analyzed, using standard iodimetry, for total sulfidic sulfur, S^{-2}. In THF, the Li corrosion rate via reaction (14), over 30 days storage, was 13.8 $\mu A/cm^2$ at 47.5°C and 3.4 $\mu A/cm^2$ at room temperature. Other experiments (48) with storage at 71°C for 30 days gave a corrosion rate of 28 $\mu A/cm^2$. Finally, storage of complete cells at 71°C for 20 days resulted in a loss of capacity at the rate of 22 $\mu A/cm^2$, in fair agreement with the tube storage tests.

For a typical high rate, liquid cathode cell design, we calculate the C rate to be approximately 15.4 mA/cm^2.* Therefore, these self-discharge rates correspond to deactivation rates of 0.5%/day at room temperature, 2.1%/day at 47.5°C and 4.4%/day at 71°C. In DMSO, self-discharge rates are 20-50% of those in THF, but capacities, discharge rates and anode rechargeability are inferior. It is not unlikely, however, that the solvent for this battery would be determined by its application-primary or secondary, high or low rate. In a secondary battery, of course, all capacity lost by self-discharge according to reaction (14) is, in principle, retrievable on charge.

4. Summary and Conclusion

The feasibility has been demonstrated of a high energy density Li battery with a Li_2S_n positive electrode dissolved in an organic electrolyte. Discharge is flat, at ∿2V, and can be carried out in prototypes of practical cells with 75% cathode utilization at 3-4 mA/cm^2 and at 50°C. Further improvements in discharge rate/capacity should be possible if an electrolyte additive can be found to solubilize Li_2S, the primary discharge product, which precipitates in the cathode matrix, and/or appropriate acidic S_n^{-2} complexing agents can be found which do not aggravate cathode passivation and are also compatible with Li. These improvements would be necessary for the production of high rate batteries operating at room temperature and below.

---

*The basis for these calculations is the $Li/SOCl_2$ high rate cell, for which considerable design work has been published (45,46). Replacing $SOCl_2$ with 6M S (as Li_2S_n, 1M $LiAsF_6$, THF electrolyte), a practical energy density (sans container) of ∿300 $Wh\text{-}kg^{-1}$ is obtained for a 1.5 e^-/S utilization at 2.0V. At this utilization, the specific capacity of the catholyte is 0.26 $Ah\text{-}cm^3$.

Li metal is quite stable to very concentrated solutions of Li_2S_n in THF and other aprotic organic solvents. As reported in the next section, this stability is highlighted by the possibility of recharging the cell, at least partially, with high efficiencies and correspondingly low self-discharge rates. In fact, the anode efficiencies characteristic of such cells are as good or better than the cycling efficiencies of Li in the absence of dissolved Li_2S_n (49). These results, along with the discharge rate and capacity results, suggest that previous interpretations of poor performance of Li/solid S batteries due to escape and self-discharge of S_n^{-2} may be misleading. Total or partial solubility of the cathode material may, in fact, be the key to its efficient utilization.

E. Rechargeability of Li_2S_n Cells

1. Summary of Cell Rechargeability Behavior

The rechargeability of Li/Li_2S_n cells was described in detail in the Semiannual Progress Report (50) covering the first half of 1977. Some of the earlier progress in this area is also reviewed in Appendix C as a paper presented at the IECEC meeting in August 1977. These results are also briefly summarized below.

Most of the rechargeability experiments reported in reference (50) were at 50°C in 3C/2Li cell packages containing 4-5M S, 1M $LiAsF_6$, THF electrolyte. These "baseline cells" were cycled galvanostatically, in both asymmetric and symmetric regimes, as illustrated in Figure 14.

The high reversibility of the polysulfide electrode is evidenced by the low overvoltage exhibited in the charging curve shown in Figure 15. One striking aspect of the charging behavior of these cells is that, in most cases, a charging end point cannot be achieved. Exceptions are found when dilute Li_2S_n catholytes are employed, when the interelectrode spacing is large, or occasionally when Li alloy anodes are used. Although the evidence is indirect, it appears that cathode material produced toward the end of charge may react at a nearly diffusionally controlled rate with electrodeposited Li. This explanation is supported by the following experiment: a cell containing the S initially as $\sim Li_2S_{10}$ can be charged indefinitely. The same fresh cell, if first discharged completely, then charged with a capacity equivalent to $\sim$1 e^-/S, then discharged completely again, will show an efficiency for this first cycle of 95-100%. Clearly the self-discharge rate during charge of the Li_2S_{10} is equivalent to the charging rate, typically $\sim$2 mA/cm^2. However, the self-discharge rate during charge of the initially discharged cell can be calculated to be, typically, 0 to 60 μA/cm^2.

Another important observation is that "baseline cells" decline in efficiency with increasing cycle number. This behavior is illustrated in Figure 16. Here, two "baseline" cells were cycled at 50°C at 1 mA/cm^2

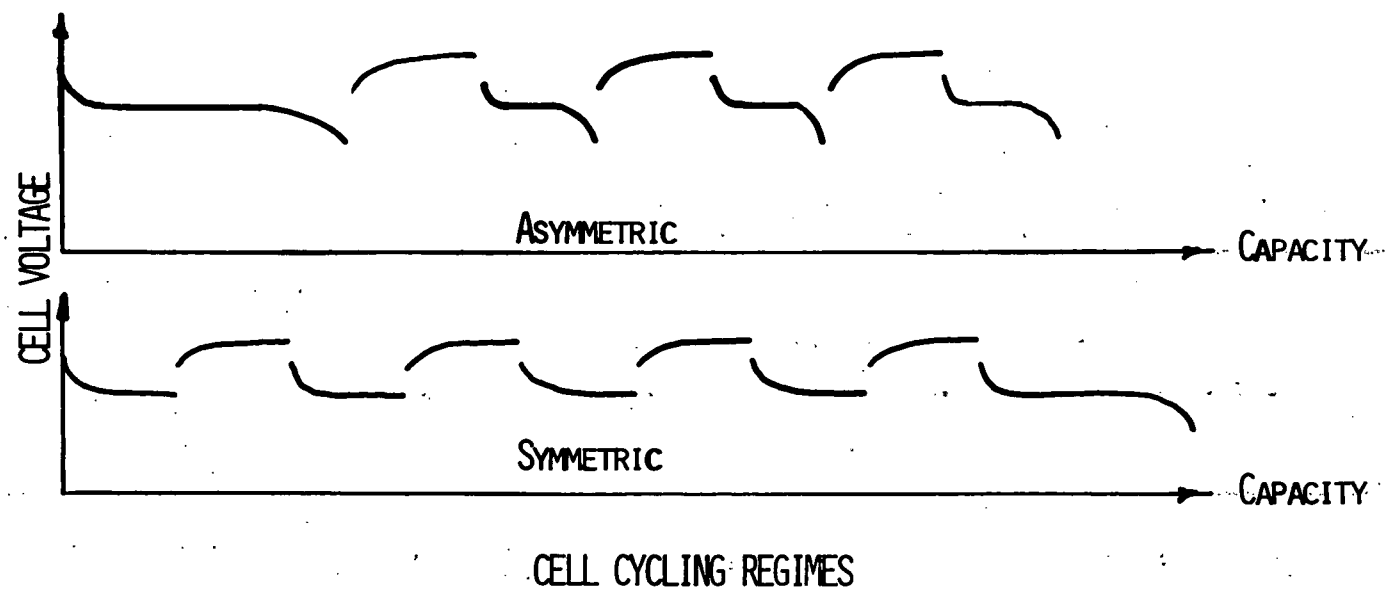

Fig. 14: Cycling regimes for studying the rechargeability of Li/Li_2S_n cells. Asymmetric regime: discharge is terminated at 1.5V cutoff, charge capacity constant. Symmetric regime: discharge, charge capacities constant.

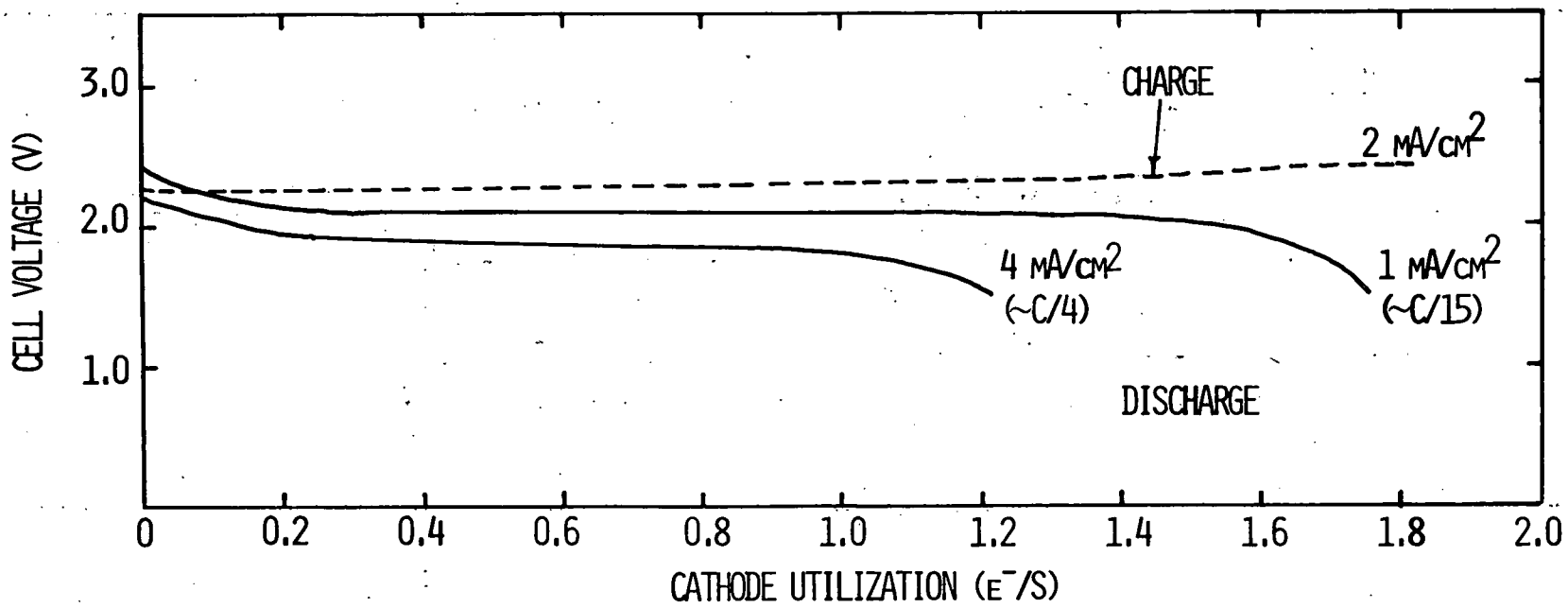

Fig. 15: Galvanostatic charge and discharge curves for Li/5M S (as Li_2S_8), THF, 1M $LiAsF_6$/C. T = 50°C.

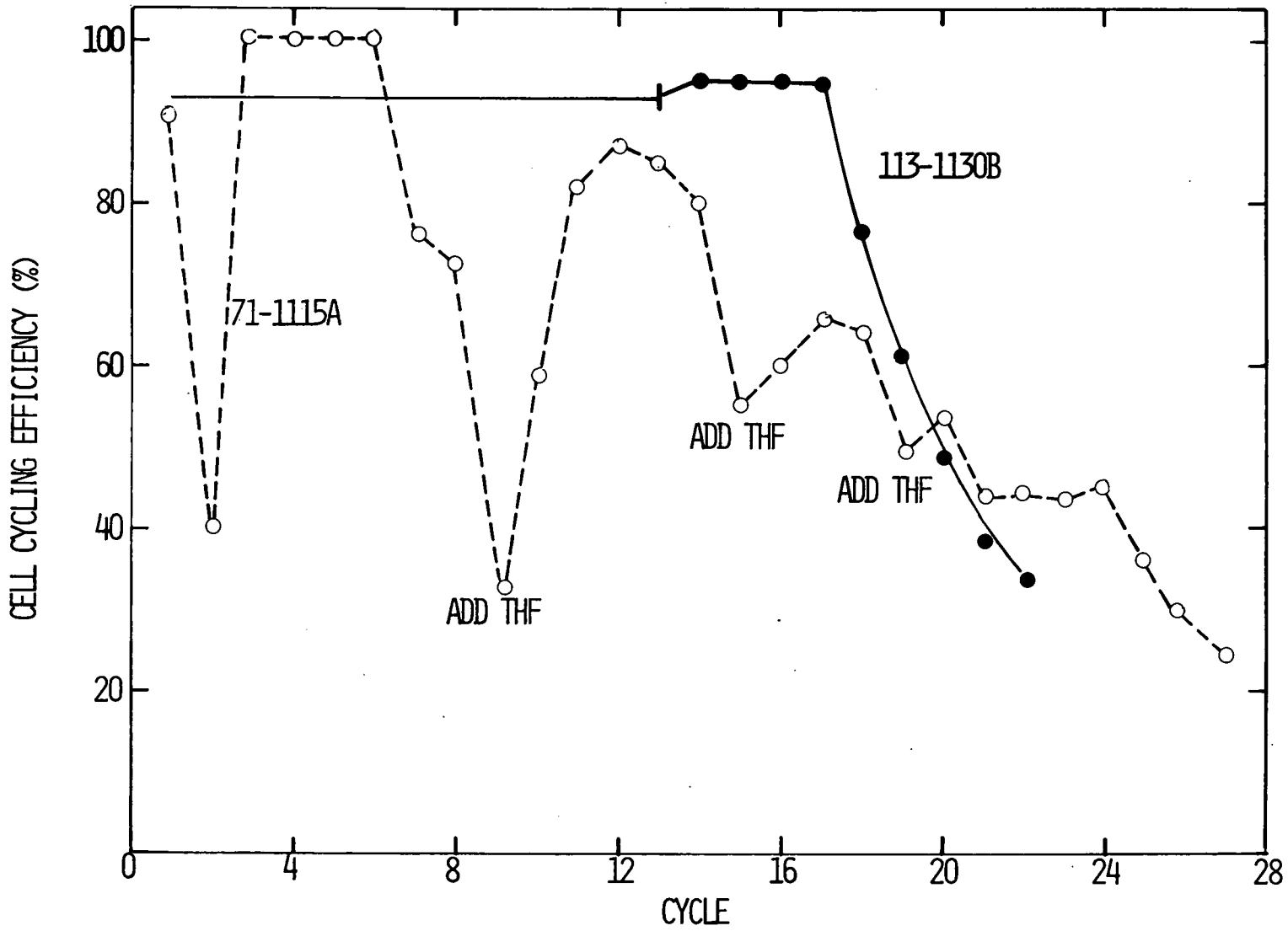

Fig. 16: Cycling efficiencies of Li/Li_2S_n (THF) cells. Current = 1 mA/cm^2, capacity = $0.5e^-/S$, T = 50°C. Electrolyte contains 4.27M S as Li_2S_n. Cell 71-1115A was cycled 12 times before discharge to a 1.5V cutoff, after which cycling continued. Cell 113-1130B was discharged initially to 1.5V, before cycling.

and a depth of 0.5 e^-/S. One cell was cycled symmetrically, starting at full charge. The 12th discharge of this cell was extended to a 1.5V cutoff, and cycling was then continued (asymmetrically) for the fully discharged cell. After several asymmetric cycles of 95% efficiency, the efficiency dropped off sharply until it reached ∿30% by cycle 22.

The second cell was first discharged to 1.5V, then cycled asymmetrically until failure. Although the efficiencies were somewhat erratic, the same trend toward deteriorating efficiency is evident. The erratic behavior of the asymmetrically cycled cell has several possible origins. During the later phases of discharge, the cell resistance increases, leading to some local distillation of the solvent out of the cell package into recesses of the cell holder. Thus, the cell had to be replenished several times with THF. In addition, when charge and discharge are of equal coulombic capacity, as with cycles 1-12 of the first cell, the inefficiency in each cycle is adjusted by stripping away part of the Li anode substrate. This probably has a way of reconditioning the substrate, which could lead to an improved morphology of the subsequent deposit.

A third important aspect of the rechargeability of the Li/Li_2S_n cell relates to the functioning of the Li anode in the highly oxidizing environment of the polysulfide catholyte.

Most previous work on the secondary Li electrode has been carried out in inert, aprotic electrolytes such as propylene carbonate (51-53) and methyl acetate (54,55). In these solvents, electrodeposited Li cannot be stripped efficiently due to encapsulation of granules with thin films of Li-solution reaction products. Encapsulation leads to permanent loss of Li from the system, and can have dire consequences with regard to the cycle life of a secondary Li battery (53).

In the Li/Li_2S_n battery, a self-discharge reaction is provided. Although self-discharge detracts from the cell cycling efficiency, the materials balance is maintained. An experiment was developed to test whether, during cycling of the Li/Li_2S_n cell, any Li is lost to encapsulation, or whether unstrippable Li is returned to the system via self-discharge.

A cell was therefore designed with an anode containing a known charge of Li. The cell was cycled symmetrically ten times, each cycle having a capacity of 0.51 e^-/S. The cell was then discharged totally, to determine the remaining capacity, after which the remaining Li was stripped from the anode. These data allowed the calculation of the average efficiencies of the total cell and the anode alone. They turned out to be equal, ∿83% in this particular experiment. Thus, there can be no Li loss through encapsulation. Rather, all of the anode inefficiency is realized as cell self-discharge, i.e., electrodeposited Li which is not stripped on discharge reacts with dissolved Li_2S_n during the cycle. In principle, this should allow the construction of a cell without the

necessity of using excess Li in the anode, as Li is conserved with each cycle. The contrasting cases of Li cycled in "inert" and oxidizing polysulfide electrolytes are schematized in Figure 17.

Experiments were also performed to determine the effects of temperature, geometry, charge density, current density, polysulfide concentration, and Li/Al alloy anodes on the cycle life of the cell. In general, the cycle life of the cell is extended at lower charge and current density, as well as at lower temperature. It is logical that these factors should influence the self-discharge rate. For example, as the charge on the anode is increased, the electrodeposit probably becomes more dendritic and of higher surface area, enhancing its susceptibility to attack by dissolved Li_2S_n. Higher temperatures also increase this attack rate. Similarly, deposits may be more dendritic at higher plating currents. Going from 1 mA/cm^2 to 2 mA/cm^2 nearly doubles the self-discharge rate in these cells. However, this result could also indicate that a reactive species is produced as a constant fraction of each charge, and therefore the self-discharge rate is higher only because the cycles are shorter.

Anodes comprised of Li/Al were used because cycling studies of these electrodes in concentrated polysulfide solutions have shown that they afford the Li electrodeposit some degree of cathodic protection (48,50). In full cells, this appears also to be true in the early cycles. On charging at 50°C at currents higher than $\sim$4 mA/cm^2, a charging end point can be attained. However, self-discharge appears to compete with alloying of the electrodeposit and efficiencies decrease with cycle, as in the baseline cell. Thus, no fundamental advantage was realized in using an Al alloy anode, particularly considering the penalty of $\sim$0.35V which it incurs.

To summarize the earlier rechargeability results, the "baseline cell" operating at 50°C and at a current density of 1.0 mA/cm^2 has been shown to undergo 135 cycles at 0.1 e^-/S and 17 cycles at 0.4-0.5 e^-/S, at efficiencies exceeding 90%. At 2 mA/cm^2, about 11 such cycles are observed. In all cases, the efficiency then deteriorates catastrophically. Following this decline, little revival of the cell is noted on standing, heating or adding more solvent. Therefore, a large portion of the effort during the second semiannual period had been devoted to determining the reasons for cell failure and to testing ways of extending the cycle life.

2. Assessment of Failure Modes

During the last two years, extensive investigations of the rechargeability of Li/Li_2S_n cells were undertaken in order to comprehend the dramatic decline in efficiency with cycle. In addition, the effects on cycle life of various electrode pretreatments and electrolyte additives were investigated.

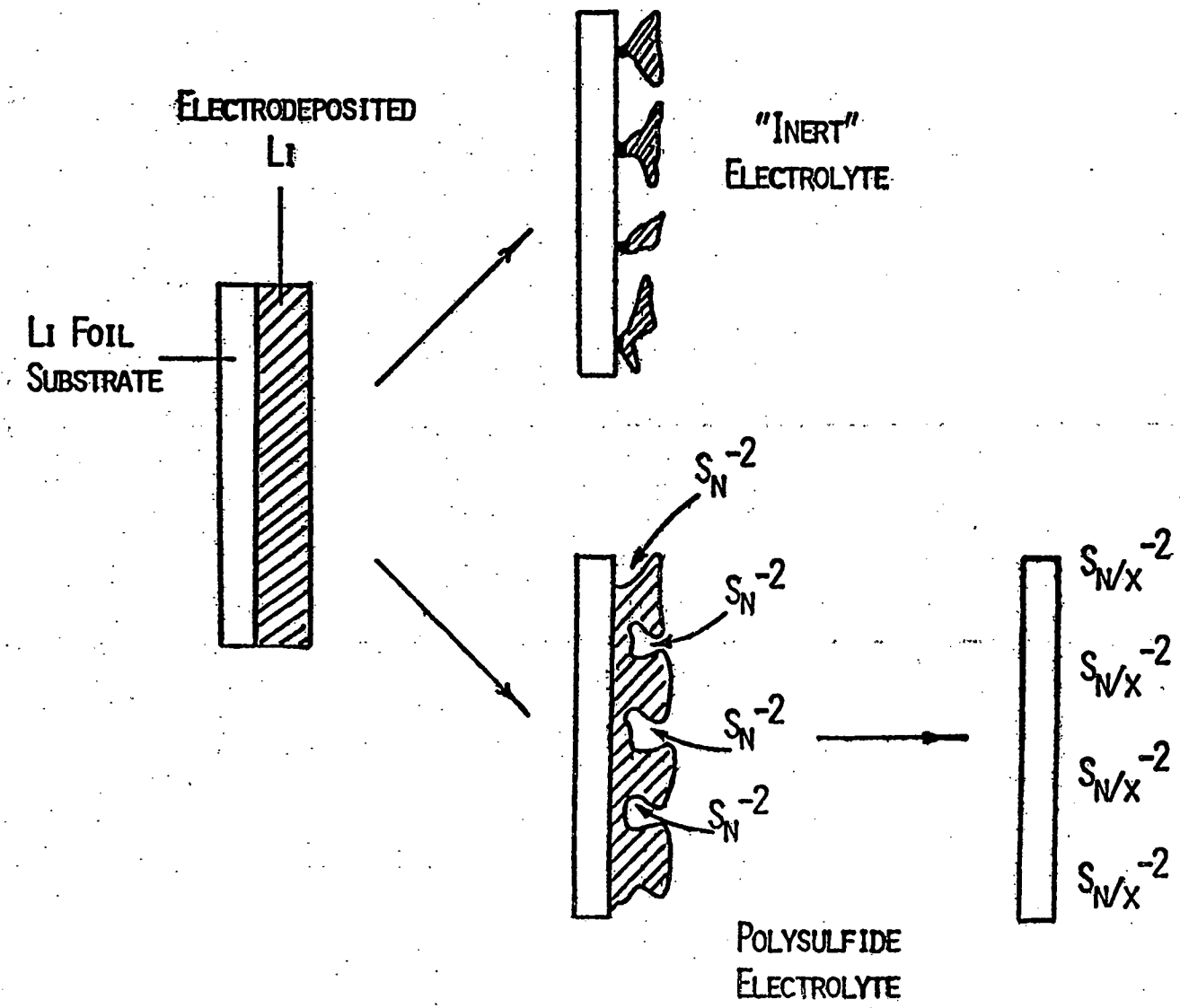

Fig. 17: Results of electrochemically stripping electrodeposited Li in an "inert" electrolyte and in an oxidizing polysulfide electrolyte. In the former case, some Li is left behind with each cycle, encapsulated by insulating reaction products. In the case of the polysulfide electrolyte, self-discharge can redissolve any Li not removable electrochemically during cell discharge.

Cell Description and Baseline Experiments. For these studies, both high rate and flooded cell configurations are employed. The high rate cells were assembled with 0.70 mm thick carbon electrodes in the 3C/2Li electrode configuration. The cell package was contained in a 4 mm wide rectangular glass vial. It accommodated 1.2 ml of electrolyte and had an A/V ratio of 15.7 cm^{-1}. The flooded cell contained one Li and one carbon electrode. These were placed against the interior faces of a 7 mm wide rectangular vial. The cells utilized 3.0 ml of electrolyte.

The purposes for using the "high rate" cells were to shorten the time required for each experiment and to carry out experiments in a geometry with a "practical" A/V ratio (cf. Appendix A). The cycling performance of such a cell is shown in Figure 18A. This cell, containing 1.2 ml of a solution 4.2M in S as $\sim Li_2S_8$ in THF/1M $LiAsF_6$, was cycled from the top of charge at 2.0 mA/cm^2. Each charging half-cycle was of 2-hour duration, corresponding to a capacity of 75.2 mAh or 0.55 e^-/S. Cycling was symmetric until the sixth discharge, when the voltage limit of 1.5V was attained. By the 12th cycle, the efficiency had dropped to $\sim$16%. In addition, the cell polarized to 3V at the end of the 13th charge. This indicated a possible depletion of active cathode material.

In order to compare the flooded electrolyte cell to the high rate cell, the former was filled with 3.0 ml of electrolyte 0.43M in S (as $\sim Li_2S_8$). This cell was also cycled at 2 mA/cm^2 and 50°C. Each half cycle was also 2 hours in duration. The specific charges carried by the electrodes were thus equal for both cells, and corresponded in both cases to 0.55 e^-/S. Results of efficiency vs. cycle number are shown in Figure 19, while the cycling behavior of the two cells are compared in Table 5.

The flooded cell underwent 21 symmetrical cycles before reaching the discharge limit of 1.5V. This converts to an average cycling efficiency of 85-90% and an average self-discharge rate of $\sim$130 $\mu A/cm^2$. As can be seen in Figure 19 and Table 5, the "high rate" cell polarized after $\sim$7 such cycles, averaging 70-75% efficiency and $\sim$230 $\mu A/cm^2$ self-discharge rate.

Unlike the high rate cell, the flooded cell readily reached a charging end point. This is ascribed to the large interelectrode separation, preventing reactive electrogenerated oxidized sulfur species from migrating to the anode. A sharp increase in voltage was noted toward the end of each 2 hour charging cycle, the polarization voltage becoming larger in the later cycles. In cycles 24 to 34, a charging cutoff voltage of 4.0V was imposed instead of the 2 hour time limit. By cycle 30, the cell capacity became very low (<5 mAh), indicating a depletion of active material.

The cell was terminated and the contents examined. The electrolyte was light green in color, with an analyzed S^0/S^{-2} ratio of $\sim$5. In this

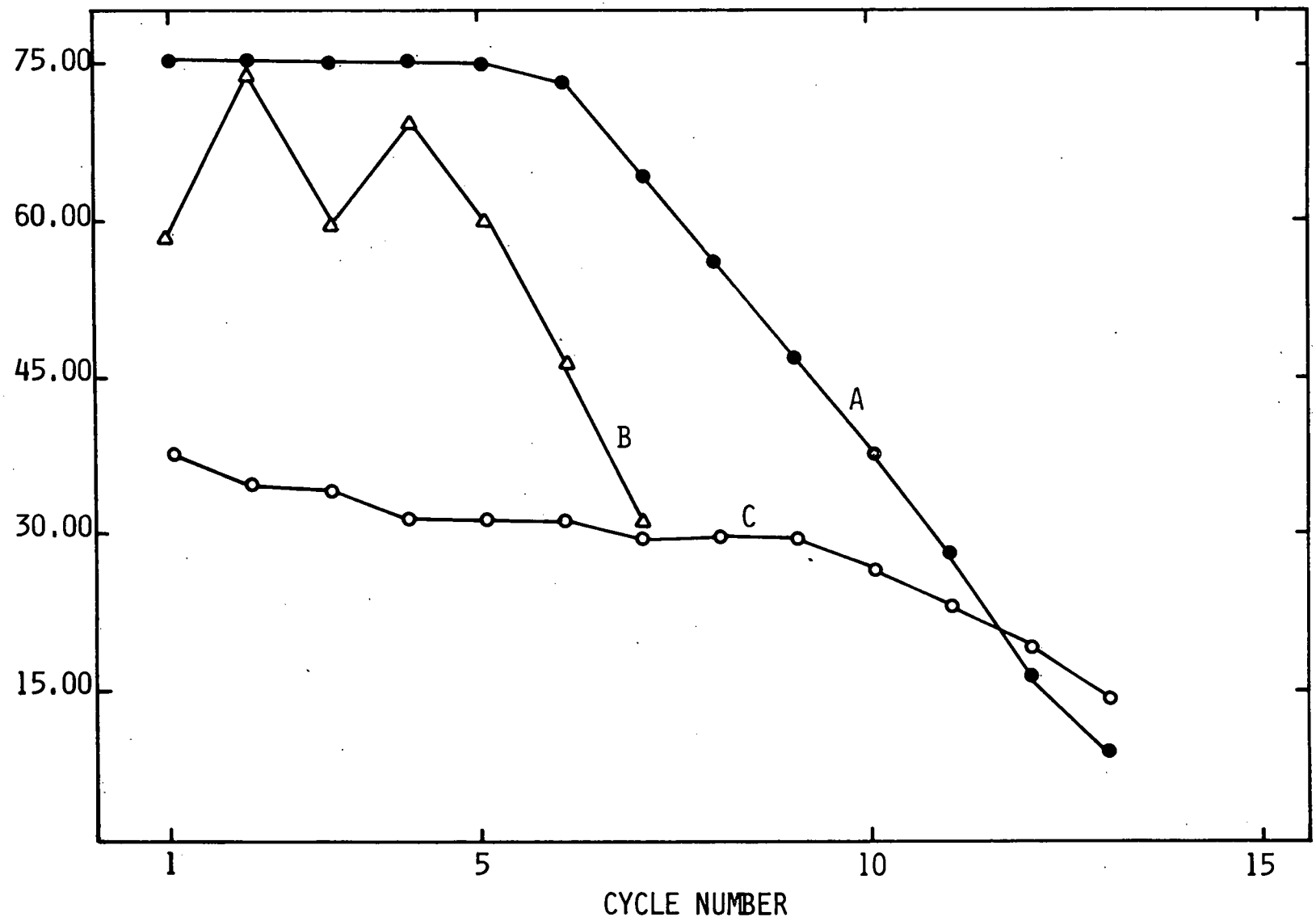

Fig. 18: Discharge capacity vs. cycle number of Li/Li_2S_n, THF cells at 50°C; current density , $i_c = i_d$ = 2 mA/cm^2; charge capacity = 75 mAh (0.556 e^-/S). A, cell 142-0606; B, cell 142-0608; C, cell 142-0613B.

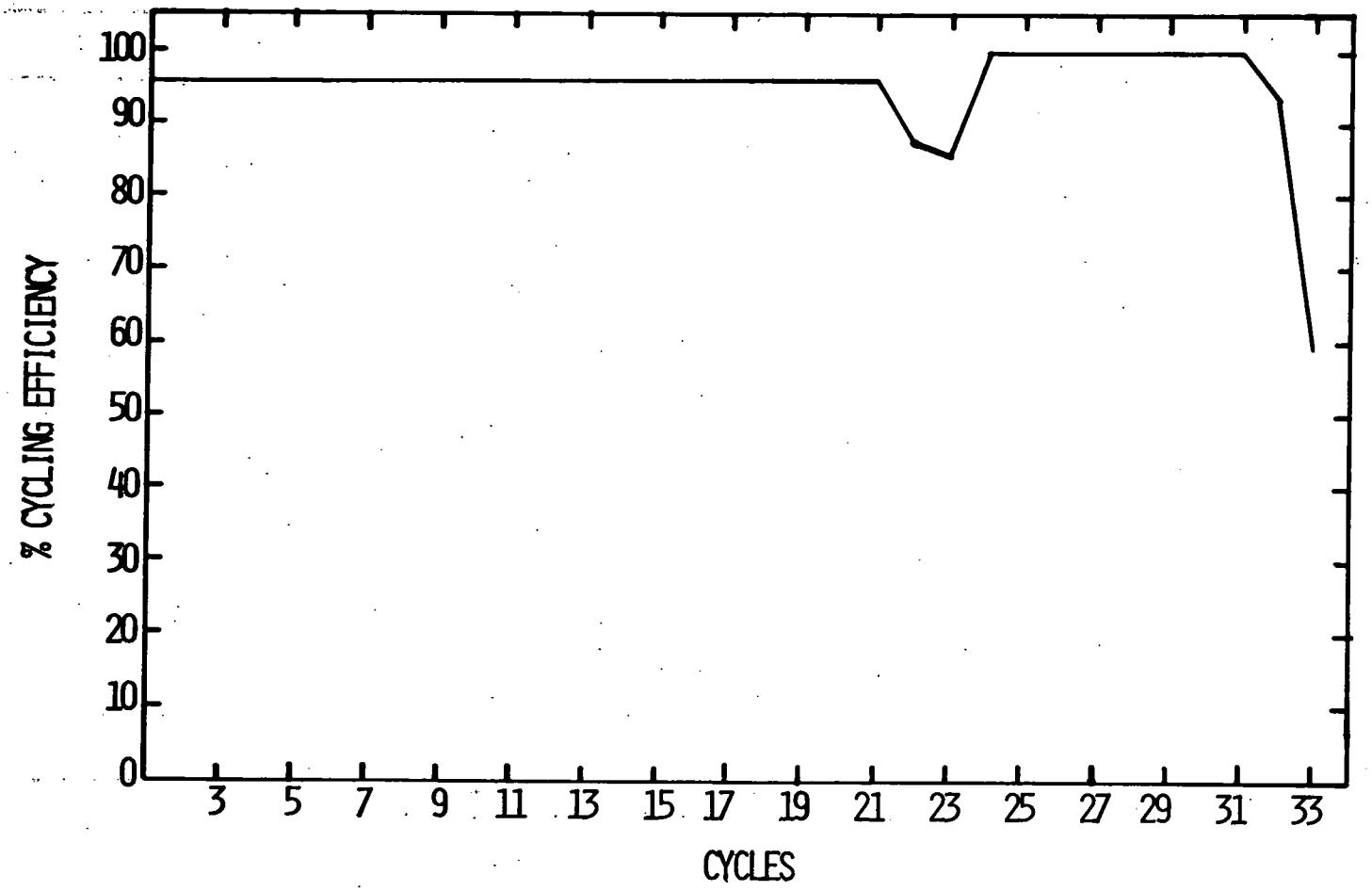

Fig. 19: Efficiency of cycling flooded Li/Li_2S_n cell (No. 113-0923) vs. cycle number. See Table 5 for details. Current = 2.0 mA/cm^2; T = 50°C.

TABLE 5

CYCLING CHARACTERISTICS OF Li/Li_2S_n CELLS
AS A FUNCTION OF A/V RATIO

Cell	Baseline Capacity	mAh/2-hr Half Cycle	Cycles Until Polarization	Avg. Eff. Per Cycle	Avg. SDR ($\mu A/cm^2$)
3.0 ml of 0.43M S as Li_2S_8 in THF, 1M $LiAsF_6$. A = 4.7 cm^2; A/V = 1.56 cm^{-1} (Cell 113-0923)	34.6 mAh/e^- = 51.9 mAh (1.5e^-/S)	18.8 mAh	21	87%	131
1.2 ml of 4.3M S as Li_2S_8 in THF, 1M $LiAsF_6$. A = 18.8 cm^2; A/V = 15.6 cm^{-1}	138.3 mAh/e^- = 138.3 (1.0e^-/S)	75.2 mAh	7	75%	262

experiment, the absolute S concentration in the failed electrolyte was not measured, although it was apparently quite low. The electrodes were also extracted with THF yielding a suspension having $S^{\circ}/S^{-2} \approx 1.0$, indicating primarily Li_2S.

Although the cycle life of the flooded cell is longer than that of the "high rate" cell, the ultimate failure mechanisms appear similar in both cases. The electrolyte level could be easily monitored in the flooded cell, and was never observed to change over its cycle life. This seems to eliminate solvent loss or deterioration as a major contributor to cell failure. The latter had been a concern with the "high rate" cells.

When these are filled, the electrolyte is not completely absorbed by the electrodes. Initially, some liquid occupies spaces between the edges of the anode and cathode. However, after ~30 hours of cycling at 2 mA/cm^2, the excess disappears. There are several possible causes for this, among them absorption by the electrode, reaction of the solvent, or distillation of electrolyte into remote parts of the housing due to local IR heating.

Although it does not appear that this phenomenon is the specific cause of cell failure on cycling, it may enhance the self-discharge rate due to poor current distribution. Cells were designed in which any distillate would drip back into the package, and in which liquid seals reinforced the usual O-ring seals, as added insurance against solvent evaporation. Cells 161-0912, 0915, 0919, 0921 and 1020, all containing 4.3M S in THF, 1M $LiAsF_6$, were assembled in this way and cycled at ± 2 mA/cm^2 at a depth of 0.5 e^-/S. The cells gave essentially the same efficiency vs. cycle behavior as the "baseline cells." The electrolyte still appeared to soak completely into the C electrodes after ~30 hours cycling. After cell failure, adding more THF did not revive the cycling efficiency. These results appear to rule out solvent distillation or evaporation as a cause of any apparent decrease in electrolyte volume with cycling.

Electrode Exchange Experiments. Our initial hypothesis was that the cells failed due to an increasing self-discharge rate aggravated by morphological deterioration at the anode. To test this hypothesis, the "high rate" cell which had been cycled to failure in Figure 18A was terminated and its Li electrodes were carefully replaced with fresh ones. Sufficient care was taken during this operation to avoid any loss of active cell materials. The cell was also replenished with 0.5 ml of THF. After reequilibrating the cell at 50°C, cycling was continued. The charge/discharge curves of the first and last cycle with the old electrodes and the initial cycle with the new electrodes are shown in Figure 20C. It can be seen that there is no improvement in capacity with the new electrodes and the charge/discharge curves are a virtual continuation of those of the 12th cycle of the original cell. This seems to indicate that the cell ran out of capacity at the 12th cycle, not primarily because

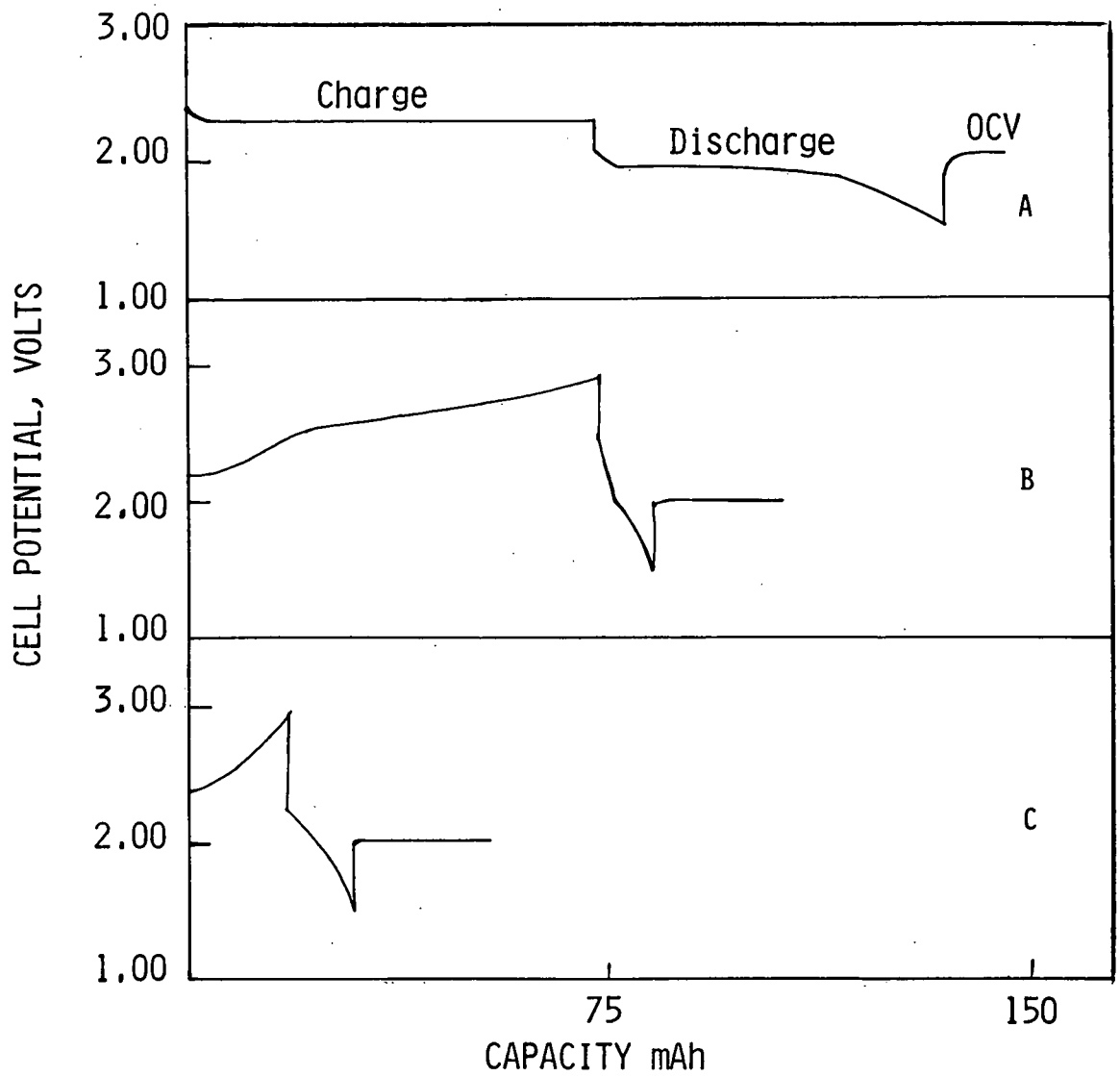

Fig. 20: Charge/discharge curves for cell 142-0606 at various stages of cycling. A, 6th cycle; B, 12th cycle; C, 13th cycle obtained after replacement of the Li electrodes with fresh ones.

of the Li electrode inefficiency, but rather due to loss of active cathode materials. As mentioned earlier, an examination of the charge curve at the 12th cycle also indicates this. Unlike the charge at the 6th curve (curve 20A), the charge at the 12th cycle (curve 20B) reached an upper limit of 3.0V with two plateaus indicating that rechargeable cathode material in the cell is quite sparse at this stage.

In order to confirm further the conclusions drawn above, the original Li electrodes used in the first 12 cycles in the above cell (142-0606) were incorporated into a new cell (142-0608) along with fresh carbon electrodes and catholyte. This cell was then cycled under identical conditions to the previous one. The plot of discharge capacity vs. cycle number for cell 142-0608 is shown in Figure 18B. In the seven cycles shown, the overall performance of the cell is not as good as cell 142-0606. But considering the fact that the Li electrodes have already been used in another cell, this performance is quite impressive. It tends to confirm the earlier conclusion that cathode deactivation is the primary rechargeability limiting factor in this battery.

There are two ways in which cathode inefficiency can occur in these cells. First, Li_2S can gradually accumulate on the carbon electrodes during continued cycling making eventual cell charging difficult; i.e., inefficiency of the carbon electrodes. Second, continued loss of S can occur due to self-discharge which makes most of the S accumulate gradually on the anode as Li_2S. To distinguish between these, a fresh cell was assembled using the carbon electrodes from the failed cell. The plot of discharge capacity vs. cycle number for this cell is shown in Figure 18C. Although the cycling efficiencies are not as high as for a totally fresh cell, they are high enough to show that deterioration of the carbon electrodes are not the primary cause of cell failure. Rather, Li_2S isolation on the anode is supported as the likely cause.

Analysis of Sulfur Distribution in Failed Cells. In order to understand further the cause of cell failure, an analysis of the anode surface products was undertaken. It was to be determined whether any Li-THF/$LiAsF_6$ reaction products were on the anode surface, as had been identified in other work on nonpolysulfide containing electrolytes (56).

A Li/Li_2S_n (THF) cell which had undergone 135 symmetrical cycles at 0.1 e^-/S (see Ref. 50) was disassembled for this analysis. The anode contained a layer of electrodeposited Li which had a slight brownish coloration. However, the electrolyte itself is brown-red. This layer of material was scraped from the Li electrode and left in a watch glass in the open atmosphere until all of the Li had been converted to LiOH. The solubility of this reacted mixture was qualitatively evaluated in H_2O, MeOH and toluene. In each case, the insoluble portion was separated, dried at ∿50°C, and incorporated into a KBr pellet for infrared spectral analysis.

The air-reacted anode extract gave 14 major infrared peaks, listed in Table 6. Some of the peaks can be ascribed to LiOH, formed by reaction of a sample of the Li used for the anode with air. Others, including a major OH stretching vibration from H_2O, arise from Li_2S which had also been allowed to hydrolyze partially in the open atmosphere. Unlike the brown reaction products typical of Li in the nonpolysulfide-containing solution, no significant H_2O-insoluble material was present in the extract. In addition, no infrared-active substance dissolved in toluene, although the presence of S_8 cannot be ruled out. A small amount of $LiAsF_6$ is indicated in the anode residue. There were only 2 weak absorption peaks of unknown origin, at 1000 and 957 cm^{-1}, both from H_2O soluble substances. In no case was the brown, H_2O insoluble, THF, $LiAsF_6$ plus Li reaction product detected, with its characteristic infrared absorption of 400 cm^{-1} (56).

The primary reason for Li stability in polysulfide solutions must be the formation of a passivating film, probably of Li_2S or Li_2S_2. This reaction appears to dominate the surface chemistry of the anode and either occurs at a much higher rate than the Li-THF, $LiAsF_6$ reaction or protects the Li against it.

For the purpose of determining the sulfur distribution in failed cells, a flooded cell configuration was employed. This was similar to the cell described previously, but had a larger volume to facilitate analysis. The cell contained 12 ml of electrolyte initially 1.0M in S as Li_2S_{10}. It was cycled at 50°C at ± 2 mA/cm^2 until failure. The cycle depth was 0.5 e^-/S. The cycling behavior was similar to that illustrated in Figure 19 for the baseline flooded electrolyte cell.

The cell was terminated when it displayed less than 10% of its original capacity and polarized rapidly on charge. The Li electrode and C electrode were extracted separately with THF, to dissolve Li_2S_n, and then with propanol, to dissolve Li_2S. The analyses of the electrolyte and various extracts are recorded in Table 7. The results show clearly the isolation of >90% of the cathode material on the anode, as Li_2S and perhaps some Li_2S_2. The cell was terminated after a discharge, as reflected by the low chain length of what little polysulfide was left in solution. Very little S was found in the C electrode, and its analysis probably contains substantial errors.

The results of these experiments overwhelmingly show that cell failure is manifested by isolation of the cathode material in the anode compartment, as Li_2S. The Li_2S is accumulated due to self-discharge, and is apparently insoluble in the electrolyte at the time of cell failure. It therefore cannot be transported to the carbon electrode for recharge. Ways to lessen this problem would be to decrease the self-discharge rate or to solubilize the Li_2S.

TABLE 6

INFRARED ANALYSIS OF Li ANODE EXTRACT FOLLOWING CONTINUED CYCLING OF A Li/Li_2S_n, 1M $LiAsF_6$, THF CELL AT 50°C. PEAK FREQUENCIES ARE IN cm^{-1}. SAMPLES INCORPORATED INTO KBr PELLETS.

Air-reacted Li Anode Extract	H_2O Insoluble (very little)	H_2O Soluble (evaporated supernatant)	Toluene Insoluble	LiOH (Li + moist air)	Li_2S Partly Hydrolyzed	$LiAsF_6$	Remarks
3640	-	3640	(3600)	3640	3630	-	LiOH
3380	-	3400	3380	-	3360	-	Li_2S, hydrated
1615	1615	1615	1615	-	1615	-	Li_2S
1495	-	-	1470	-	-	-	LiOH
1432	-	1400-1500	1420	-	1432	-	Li_2S, LiOH, H_2O
1280	-	-	(1280)	-	1280	-	Li_2S
1130	-	1120	1130	-	(1130)	-	Li_2S?
1080	-	-	1080	1080	-	-	LiOH
1000	-	1000	1000	-	-	-	?
957	-	940	970	-	-	-	?
866	860	858	866	860	860	-	LiOH
705	-	698	698	-	-	700	$LiAsF_6$
500-600	515	500	500	-	600,510,495	-	LiOH
420-460	-	380	400	400-500	440,410	398	$LiAsF_6$, Li_2S

Li_2S Solubilization by Li_2S_n. Although we have described the final condition of this cell at failure, we are unsure of the details of the mechanism leading to that condition. One question is the extent to which Li_2S can be solubilized by reaction with polysulfides dissolved in the electrolyte. Therefore, the rate of this reaction was investigated in some detail.

The kinetic studies were conducted with Li_2S_{10} solutions in THF at a total sulfur concentration of 0.93 and 4.65M. In actual experiments, 2.54g (54.4 mmols) of solid Li_2S were added to 40 ml of the polysulfide solution in a 50 ml Erlenmeyer flask that was kept stirring in a magnetic stirrer inside a dry box. Following the addition of Li_2S the flask was capped and the stirring continued. At intervals of 20 min, 1, 2, 4 and 24 hours, samples of the suspension were removed during stirring and centrifuged. The supernatant was analyzed for total S and sulfidic S using our standard procedures. The Li content of the prepared samples, with appropriate dilution when necessary, was determined by atomic absorption at 670.8 nm wavelength and a band width of 0.7 nm. The instrument used was a Perkin-Elmer 460 with an oxygen acetylene flame and an integrating time of 30 sec. The results are summarized in Table 8 and are assumed to represent the progress of reaction 18:

$$Li_2S_n + mLi_2S \rightarrow (1+m)Li_2S_{(n+m/1+m)} \qquad (18)$$

As can be seen from the table, most of the reaction in both solutions is over in the first interval. After the average polysulfide order has reached $\sim Li_2S_5$, little or no further reaction occurs, despite a continued excess of Li_2S. Thus, polysulfides of order less than 5 would have little effect in solubilizing anode-isolated Li_2S, while polysulfides of greater order react very rapidly.

In principle, then, the cell cycle life should be increased by imposing an overcharge following each cycle. This will ensure the continued presence of long chain polysulfides in solution. Thus, two cells were cycled in an attempt to demonstrate the effects of overcharge. It must be remembered that overcharging this cell can be carried on indefinitely, maintained by a very high self-discharge rate when the polysulfide order becomes high, making such overcharge possible. Both cells were assembled in the C/Li/C/Li/C configuration, and contained 1.2 ml of 4.1M S as $Li_2S_{8.4}$. Cell 113-0906A was cycled at 2 mA/cm^2. Discharge capacities were 0.5 e^-/S and charge capacities were 1.0 e^-/S. The cell polarized to 1.5V after 9 such asymmetric cycles. The second cell, run as a control, was cycled symmetrically at $\mp$ 0.5 e^-/S, also at 2 mA/cm^2. This too polarized after 9 cycles. The latter cell was then overcharged by 5 e^-/S, but continued cycling at 0.5 e^-/S caused the efficiency to decline rapidly. These results are recorded in Figure 21.

TABLE 7

RESULTS OF ANALYSIS OF COMPONENTS OF FAILED Li/Li_2S_n (THF) CELLS

	Millimoles S^{-2}	Millimoles S	n	% of $[S]_{tot}$ in Failed Cell
Starting Electrolyte	1.2	12	10	-
Final Electrolyte	0.25	0.48	1.9	4.5
Li Anode:THF Extract	1.31	1.54	1.2	14.1
Li Anode:PrOH Extract	8.0	8.3	1.0	78.1
C Cathode:THF Extract	∿0.05	∿0.2	∿4	1.9
C Cathode: PrOH Extract	∿0.02	∿0.1	∿5	0.9

TABLE 8

ANALYTICAL RESULTS OF THE SOLUBILIZATION OF Li_2S BY Li_2S_{10} SOLUTIONS IN THF AT 25°C. SOLUTION A INITIALLY CONTAINS 0.93M S; B INITIALLY CONTAINS 4.65M S.

Time (hr)	[Li] M/ℓ		[S] M/ℓ		Average Polysulfide Order, n	
	A	B	A	B	A	B
0	0.188	0.898	1.05	4.65	9.90	10.35
1/3	0.391	1.623	1.16	-	5.27	6.18
1	0.396	1.744	1.20	5.11	5.32	5.82
2	0.381	1.789	1.10	-	5.38	5.70
4	0.391	1.803	-	5.17	5.27	5.66
24	0.395	1.848	1.13	-	5.23	5.55

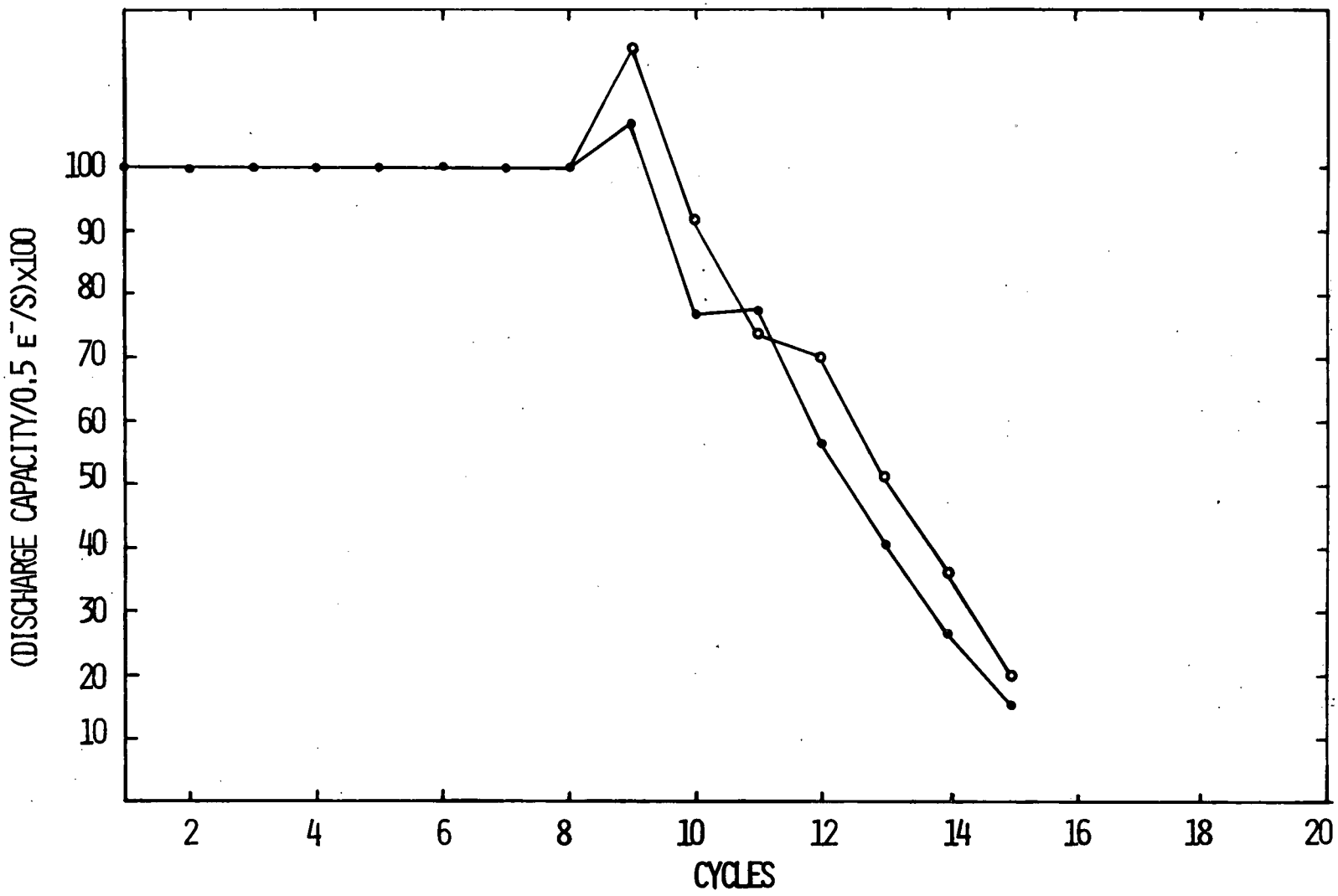

Fig. 21: Effects of overcharge on Li/Li_2S_n (THF) cell cycle life. Solutions are 4.11M S as $Li_2S_{8.4}$; charge/discharge current densities = 2 mA/cm^2. T = 50°C. Cells are of the 3C, 2Li configuration containing 1.2 ml of solution.

o = Cell 113-0906A - charge, 0.5 e$^-$/S; discharge 1.0 e$^-$/S.

● = Cell 113-0906B - charge, 0.5 e$^-$/S; discharge 0.5 e$^-$/S. Cycle #10, charge 5 e$^-$/S.

Clearly, these results run counter to our hypothesis. One possibility is that overcharge might produce S_n° species which react rapidly with both electrodeposited and substrate Li to yield unusually large amounts of anode-precipitated Li_2S which, as indicated above, could be very slow to redissolve. Thus, overcharging could ultimately cause the cell to undergo total self-discharge. Three cells were therefore assembled to assess the effect of overcharge. Cells 113-0825A, B and C were assembled in the same 3C/2Li configuration as described previously, and contained 1.2 ml of the same 4.1M S solution. Cell A was overcharged at 2 mA/cm^2 by 0.4 e^-/S, and yielded 1.0 e^-/S on subsequent discharge, also at 2.0 mA/cm^2. Cell B was overcharged by 5.0 e^-/S and yielded 1.24 e^-/S on discharge. Cell C, without any overdischarge, gave 0.92 e^-/S. Thus, in freshly assembled cells at least, overcharge increases the cell capacity by yielding a net increase in the average polysulfide order. No rise in cell resistance or other evidence of cell deterioration was noted.

The fact that overcharge does not revive spent cells indicates that self-discharge is favored over Li_2S resolubilization at this point. In fact, the material prepared on overcharge (S_n°?) must always prefer to react with electrodeposited Li -- hence the ineffectiveness of overcharge in extending the cycle life. It is likely that insoluble Li_2S is formed by reaction between Li and S_n^{-2}, particularly when n is low.

Effects of Electrode Pretreatments. A series of experiments were carried out on the effects of anode and cathode pretreatments on the cycle life and efficiency of Li/Li_2S_n secondary cells. In one such investigation, the C electrodes were impregnated with elemental S while the Li electrodes were treated with $SOCl_2/LiAlCl_4$ electrolyte. In actual experiments, the C electrodes were kept immersed for 10 min in 5 ml of CS_2 containing 100 mg of pure S followed by evaporation of CS_2 and baking at 80°C for 2 hours. The S loading on each of these electrodes is estimated to be 4-5 mg. The Li electrodes were soaked in the electrolyte for 20 and 125 hours following which the dried electrodes were submerged in THF for 10 min and rinsed with fresh THF prior to their use in fabricating the cells in the usual 2Li/3C assembly with 1.25 ml of Li_2S_{10}/1M $LiAsF_6$ electrolyte.

Cells 161-1003A and 161-1003B were comprised of freshly prepared Li metal electrodes and S loaded C electrodes. These cells were cycled in a galvanostatic mode at 2 mA/cm^2 current density and 2-hour half cycle time starting with a discharge half cycle. The cycle efficiencies of these cells dropped to 30% in 5 and 3 cycles, respectively.

Cells 161-0927 and 161-1012 consisted of Li electrodes soaked in $SOCl_2/LiAlCl_4$ electrolyte for 20 and 125 hours and untreated C electrodes. A thin uniform greyish-white film was observed on all the Li electrodes which was not analyzed but was assumed to be of either LiCl or $LiAlCl_4$. On assembly of the cell and addition of Li_2S_{10} electrolyte, a cell voltage of 2.37V was observed without any time delay. These cells were cycled at

2 mA/cm^2 current density and 2 hour discharge/charge half cycles in the usual manner. The cycle efficiency of cell 161-0927 remained ≥80% for 15 cycles followed by a sharp decrease to a 20% value after the 20th cycle. Cell 161-1012 had a cycle efficiency of ≥85% for the first 13 cycles followed by a slow decline reaching a value of 20% after the 19th cycle.

Based on the above study, though limited in scope, it is concluded that elemental S is strongly adsorbed on the carbon electrodes. The anticipated leaching of S in the electrodes to replenish polysulfide species in the electrolyte thus compensating for the loss of active species in galvanostatic cycling was not observed. In addition, the loading of C electrodes with S appears to be detrimental for improved cycle efficiency and life.

The chloride films on the Li electrodes on the other hand seem to improve slightly the cycle life of these cells. It seems appropriate, therefore, to investigate further the possibility of improving the cycle life of these cells by preformed protective films on the Li electrodes that are preferably permeable to Li atoms and/or ions. Two further experiments were conducted on the effects of anode pretreatment on cell rechargeability, using the flooded configuration. In cell 170-1208, the anode was immersed in 5M S as Li_2S_8 in THF for 48 hours at 50°C. As shown in Figure 22, the cell using this anode cycled with a nearly constant efficiency of ∿50% after polarization occurred on the 3rd discharge. Therefore, this anode pretreatment served to increase the self-discharge rate. This result is in contrast to anode pretreatment with $SOCl_2$, a procedure which we have shown to extend the rechargeability. Another anode pretreatment was the formation of Li_3N on its surface, by passing over it a stream of dry N_2 at room temperature for ∿2 hours. The Li_3N is known to be an excellent Li^+ conductor. However, cycling results with this anode were indistinguishable from those obtained without pretreatment (Figure 19).

The following additional experiments were carried out on Li/Li_2S_n (THF) cells with electrolytes containing 4.5M S and 1M $LiAsF_6$:

- Cells 161-1003A and B were assembled using C electrodes which had been impregnated with ∿20 mg of elemental S. These cells, cycled at ∿2 mA/cm^2 and 0.5 e$^-$/S, yielded only ∿30% efficiency after 3 and 5 cycles respectively (compared to >10 cycles for baseline cells).

- Cells 161-1028 and 161-1031 and C electrodes impregnated with $LiAsF_6$. These cells reached an end point on the first charging cycle, but not thereafter. Cycling efficiencies remained >50% for at least 20 cycles carried out at ± 2 mA/cm^2 and 0.5 e$^-$/S per cycle. Similar improvements were noted for cell 161-1107, where the C electrodes were impregnated with Li_2S.

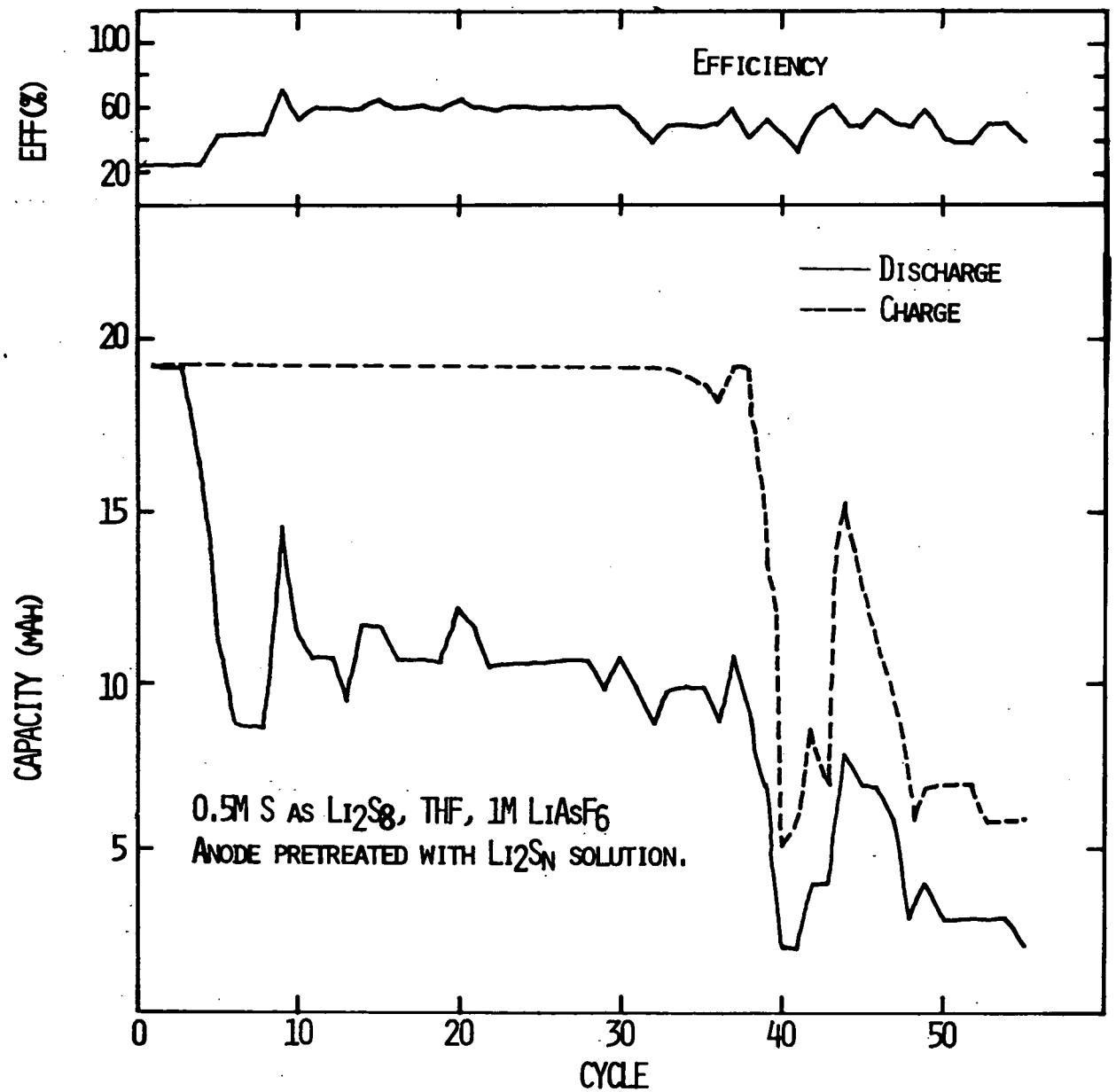

Fig. 22: Effect of anode pretreatment with 5M S as Li_2S_8 in THF on the capacity and efficiency of cycling flooded Li/Li_2S_n cell (No. 170-1208). Current = 2.0 mA/cm^2; T = 50°C; half-cycles are 18.8 mAh, unless voltage limits of 1.5 or 3.5V are attained.

3. Attempts to Extend Cycle Life with Lewis Acids

Demonstration that the failure of Li/Li_2S_n cells on extended cycling is due chiefly to the accumulation of insoluble Li_2S on the anode making it unavailable for recharge, led us to search for means of dissolving Li_2S in THF, for the purpose of enabling its transport to the carbon current collector. As shown in Table 9, several Lewis acids were discovered which appeared to form soluble complexes with Li_2S, notably $B(OAc)_3$, BBr_3 and $SiCl_4$. A Li/Li_2S_n cell containing $B(OAc)_3$ as an additive to the electrolyte was shown to have an increased cycle life over the baseline cell. Linear and cyclic voltammetric experiments indicated that oxidation rates of S_n^{-2} species appeared to be retarded by $B(OAc)_3$ complexation, while reduction rates were enhanced.

Eventually, however, we found that many of these Lewis acids actually oxidize Li_2S_n, contrary to our earlier hypothesis. This was determined by performing analyses for total sulfidic sulfur (S^{-2}) on solutions of Li_2S_4 before and after additions of excesses of various Lewis acids. The results are given in Table 10. It is seen that BBr_3 totally oxidizes S_4^{-2}, while partial oxidation is observed for $B(OAc)_3$ (with and without Li salts present), BF_3 and $SiCl_4$. No oxidation occurred with $B\phi_3$, in accordance with our earlier results. However, $B\phi_3$ has a minimal effect on Li_2S solubility. A voltammogram of $B(OAc)_3$ reduction shows a significant current rise only at $\sim$1V vs. Li^+/Li. However, in concentrated $B(OAc)_3$ solution in THF (0.1-0.5M), a reduction tail out to $\sim$2.6V is observed. The very low electrochemical reduction rate near its equilibrium potential led to our earlier misconception concerning its stability to reducing agents like Li_2S. Although employing Li_2S solubilizing agents may still be a viable approach to extending the cycle life of this battery, it now appears that none of the present group of Lewis acids can function in this capacity.

4. Effects of Intermediate Redox Species on Polysulfide Rechargeability

The basic principal of the anodically generated redox "scavenger" is to generate at the carbon electrode a highly oxidized species at the end of charge which will then migrate to the Li and oxidize in turn any isolated Li_2S. As the onset potential for Li_2S oxidation is $\sim$2.5V in THF, a material with a more positive oxidation potential will be required. Cyclic voltammetry on a vitreous carbon working electrode revealed that in THF, $LiAsF_6$, the reversible couples I_2/I^-, chloranil/[chloranil]$^{-2}$, ferricenium/ferrocene and Br_2/Br^- all have reversible potentials between 3.1 and 4.1V (Table 11).

Several experiments were carried out to demonstrate the reaction between I_2 and Li_2S_n. It was found that the reaction between I_2 and Li_2S in THF was rapid and vigorous, the product spectrum matching that of a high order polysulfide. In dilute solutions with excess I_2, this reaction

TABLE 9

SOLUBILITIES OF Li_2S IN SOLUTIONS OF LEWIS ACIDS AS DETERMINED BY $[S^{-2}]$ ANALYSES

Lewis Acids LA	[LA] (M/ℓ)	[Li_2S] (M/ℓ)	Comments
None	0	$\sim 5 \times 10^{-4}$	
$B(OAc)_3$	0.2	0.1(1)	
	2.0	0.66	
BF_3	0.2	0.03	insoluble gel formed
	2.0	0.02	
BBr_3	0.2	0.1(5)	
	2.0	-	
$B\phi_3$	1.0	<0.01	insoluble complex formed
$SiCl_4$	0.2	0.1(4)	
	2.0	0.8	
$Sn\phi_4$	0.2	-	
	2.0	$\sim 5 \times 10^{-3}$	

TABLE 10

EFFECT OF ADDITION OF EXCESS LEWIS ACID ON THE $[S^{-2}]$ CONCENTRATION IN Li_2S_4/THF SOLUTIONS

Lewis Acid	Original $[S^{-2}]$	$[S^{-2}]$ after Adding Lewis Acid
$B(OAc)_3$	0.075	0.034
$B(OAc)_3$	0.5	0.22
$B(OAc)_3$, 1M $LiAsF_6$	0.037	0.019
$B(OAc)_3$, 1M $LiClO_4$	0.037	0.019
BF_3	0.074	0.04
BBr_3	0.065	0.0
$SiCl_4$	0.074	0.058
ϕ_3B	0.075	0.077

TABLE 11

REST POTENTIALS OF REDOX COUPLES IN THF, 1M $LiAsF_6$ MEASURED BY CYCLIC VOLTAMMETRY ON A VITREOUS CARBON ELECTRODE AT AMBIENT TEMPERATURE

Couple	E (rest) vs. Li^+/Li
Chloranil/$[Chloranil]^{-2}$	3.15
Ferricenium/Ferrocene	3.43
I_2/I^-	3.56
Br_2/Br^-	∿4.1

proceeds all the way to neutral sulfur. The reaction also occurs, although more slowly, with polysulfides. Decolorization of S_n^{-2} solution with chloranil and ferricenium have also been demonstrated.

The reaction of S_n^{-2} with I_2 was investigated in more detail using cyclic voltammetry, and is summarized in Figure 23. Figures 23a and 23b present the CVs of S_n^{-2} and I_2 along in THF, 0.5M $LiAsF_6$ (anodic sweep first). The oxidation reactions of both I_3^- and I^- occur positive of 3V. The reduction of I_2 and I_3^- occur at E_{max} = 3.4 and 2.1V, respectively. The effects of incremental additions of I_2 to a 4 mM S_{10}^{2-} solution are shown in Figures 23c and 23d. Here the nearly complete oxidation of S_{10}^{-2} by the I_2 is clearly demonstrated. A CV of the I_2-Li_2S reaction products is similar to Figure 23d.

Potentiostatic reduction of the 1:1 I_2/S_{10}^{-2} solution was carried out at 2.2V for ∿0.8 e^-/S. The CV (Figure 23e) of the product was typical of a mixture of I_2, I_3^-, S_n^{2-} and neutral sulfur formed on the anodic sweep. Steady state oxidation of this mixture at 3.8V appeared to yield I_3^-, neutral S and S_n^{-2} (Figure 23f), although the implications of differences between 23d and 23f are yet to be resolved.

The evaluation of potential Li_2S oxidants in flooded cells was carried out for I_2 and chloranil. These cells contained 0.5M S as Li_2S_{10} in THF, 1M $LiAsF_6$, and 0.1M of the additive. The results of cycling these cells are compared to a baseline cell in Figure 24. In each case, during normal cycling, the charging capacity was maintained at 0.5 e^-/S, unless an end point was reached first. The latter usually occurred only later in the cycling history, indicating a depletion of cathode material.

It can be seen in Figure 24a that the baseline cell went 50 cycles before polarization occurred on charge. After that, the charging capacity

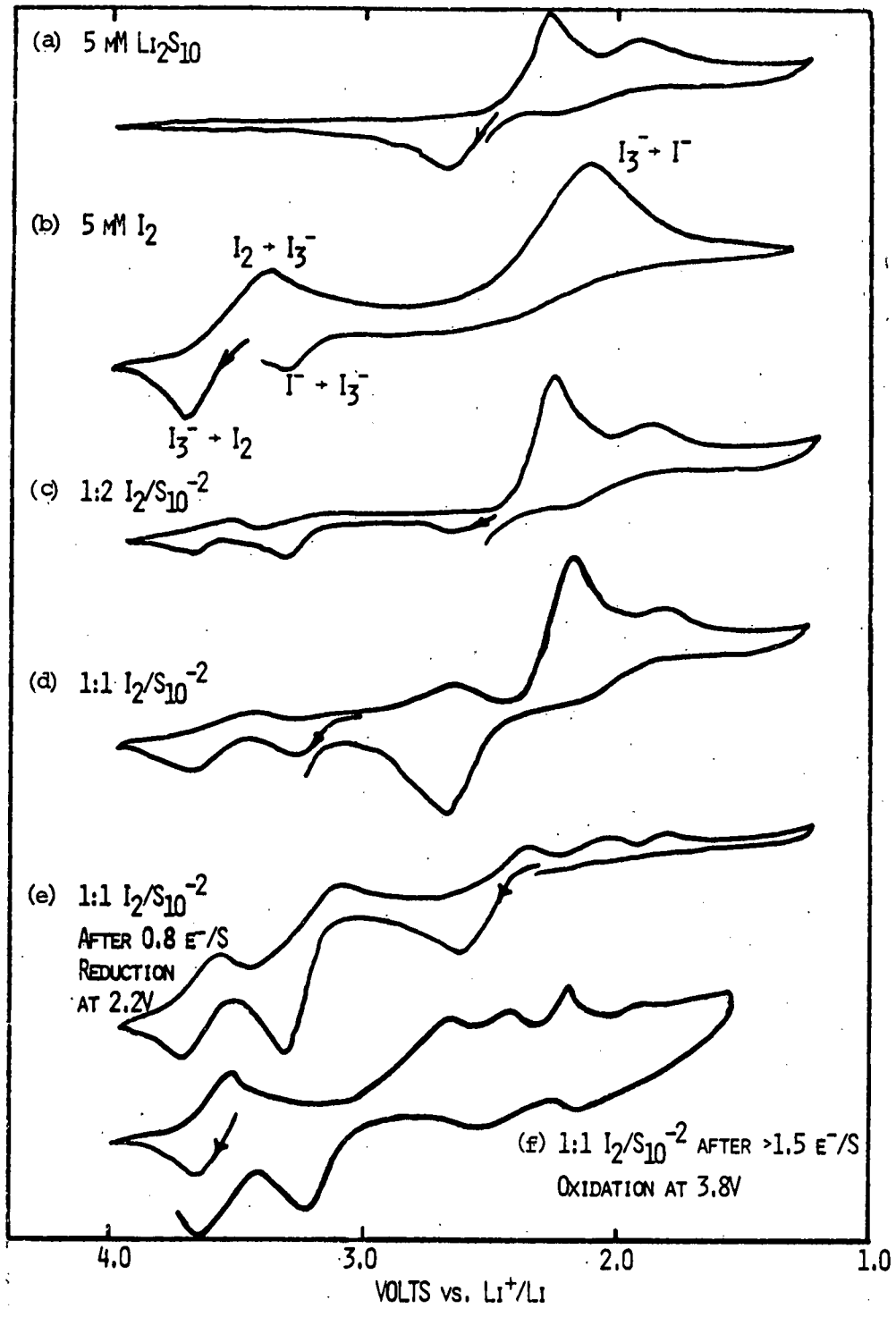

Fig. 23: Cyclic voltammogram of I_2, S_{10}^{-2} and their solutions on vitreous C at 25°C. Sweep rate = 0.1V sec^{-1}.

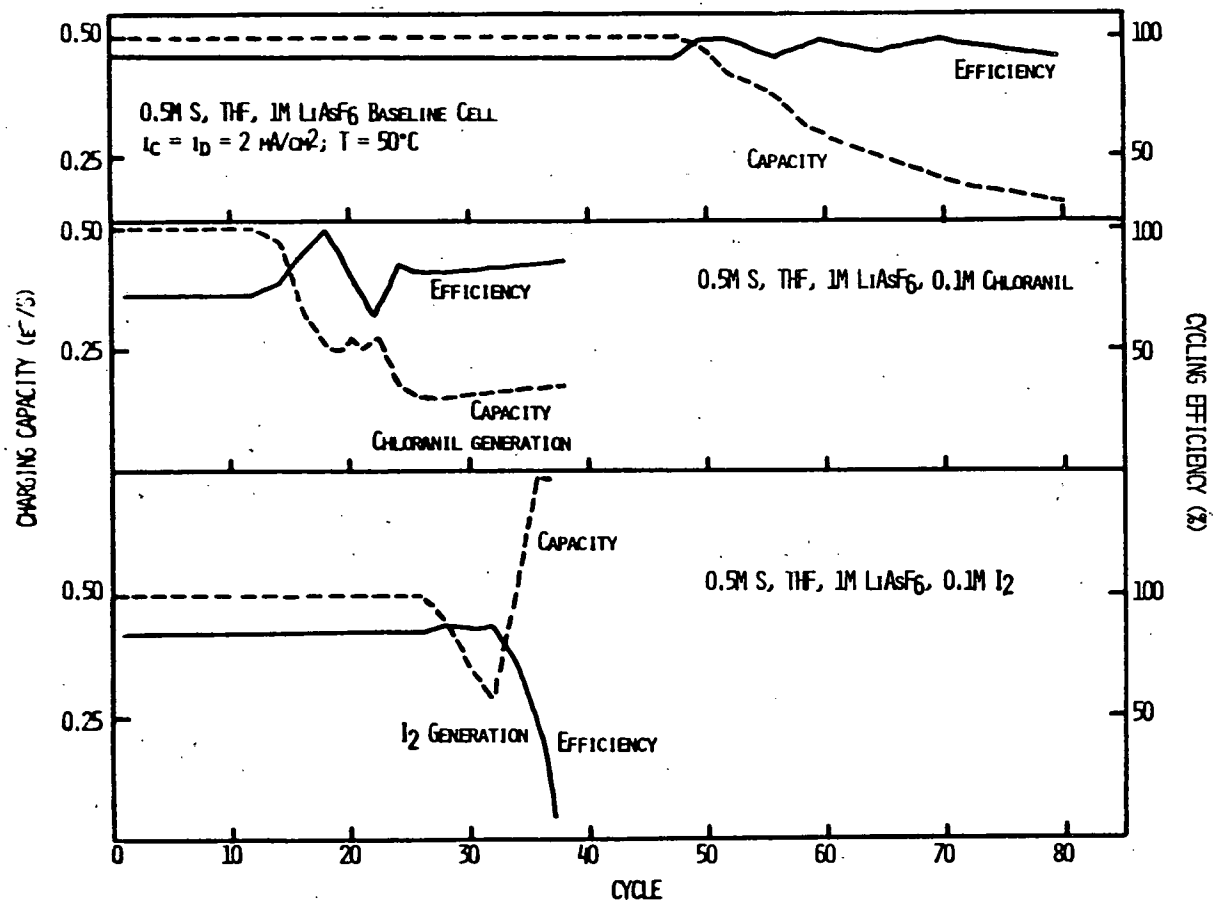

Fig. 24: Efficiencies of cycling Li/Li_2S_n cells (flooded configuration) in the presence and absence of redox scavengers.

decreased although the cycling efficiency remained near 100%. With I_2 added to a similar cell cycled under similar conditions, polarization on charge occurred after the 26th cycle, with a subsequent decrease in both capacity and efficiency (Figure 24b). On cycles 33-37, varying amounts of I_2 were generated at 3.5V. In the last two cycles, a standing time of 24 hours was observed following I_2 generation. Yet, no revival of cell performance was observed. The results using chloranil in a similar experiment were also not encouraging, as indicated in Figure 24c, although the decline in efficiency was not as catastrophic as for I_2.

The electrolytes in the failed baseline and I_2-enhanced cells were analyzed and found to contain little sulfur. The I_2 in the second cell could be nearly accounted for, however. This is in accordance with our earlier findings of Li_2S isolation on the anodes of failed cells. The surface of the anode of the failed baseline cell was scraped, and the scrapings were divided into two portions. The first was extracted with THF and the second with a THF/I_2 solution. Very little reaction or polysulfide dissolution was observed in either case. This rather surprising result indicates that the Li_2S on the anode is rendered inactive to I_2, thus explaining the ineffectiveness of I_2, or chloranil, in reviving failed cells.

The effects of redox scavengers ferrocene/ferricenium and Br^-/Br_2 were also investigated. To separate cells containing initially 0.5M S as S_{10} and 1M $LiAsF_6$ were added to 0.1M of ferrocene and 0.2M LiBr, respectively. Cycling was carried out at 50°C and ± 2 mA/cm^2 to a charge capacity of 0.5 e^-/S until cathode depletion became evident on the charging half cycle. Following cell failure, i.e., when the voltage limited charge and discharge capacity was ∿0.1 e^-/S, the cells were allowed to "overcharge," so that the secondary oxidized species could be generated (ferricenium or Br_2). As shown in Figure 25, this procedure had little effect on the ferrocene cell, although it appeared to revive the Br_2 cell. It should be noted that in the latter cell, following Br_2 generation at 4.0V, the subsequent discharge occurred at the S_n^{-2} potential (2.1V) rather than the Br_2 or Br_3^- potentials, which are considerably higher (57).

As indicated above, the cathode material isolated on the anode on cell failure appears to be quite inactive to oxidizing agents like I_2, while Li_2S alone reacts rapidly with such reagents in THF solution. However, all analyses to date indicate the anode-isolated species indeed to be Li_2S mixed in with finely divided Li. No products of solvent degradation have yet been detected.

To further specify the possible reactions between the catholyte and the anode, incubation experiments were carried out on the electrolytes with and without Li. The results are given in Table 12. These were introduced into break-seal tubes (Figure 26) and sealed in vacuo. The sealed tubes were incubated at 68°C for 21 days. They were then opened

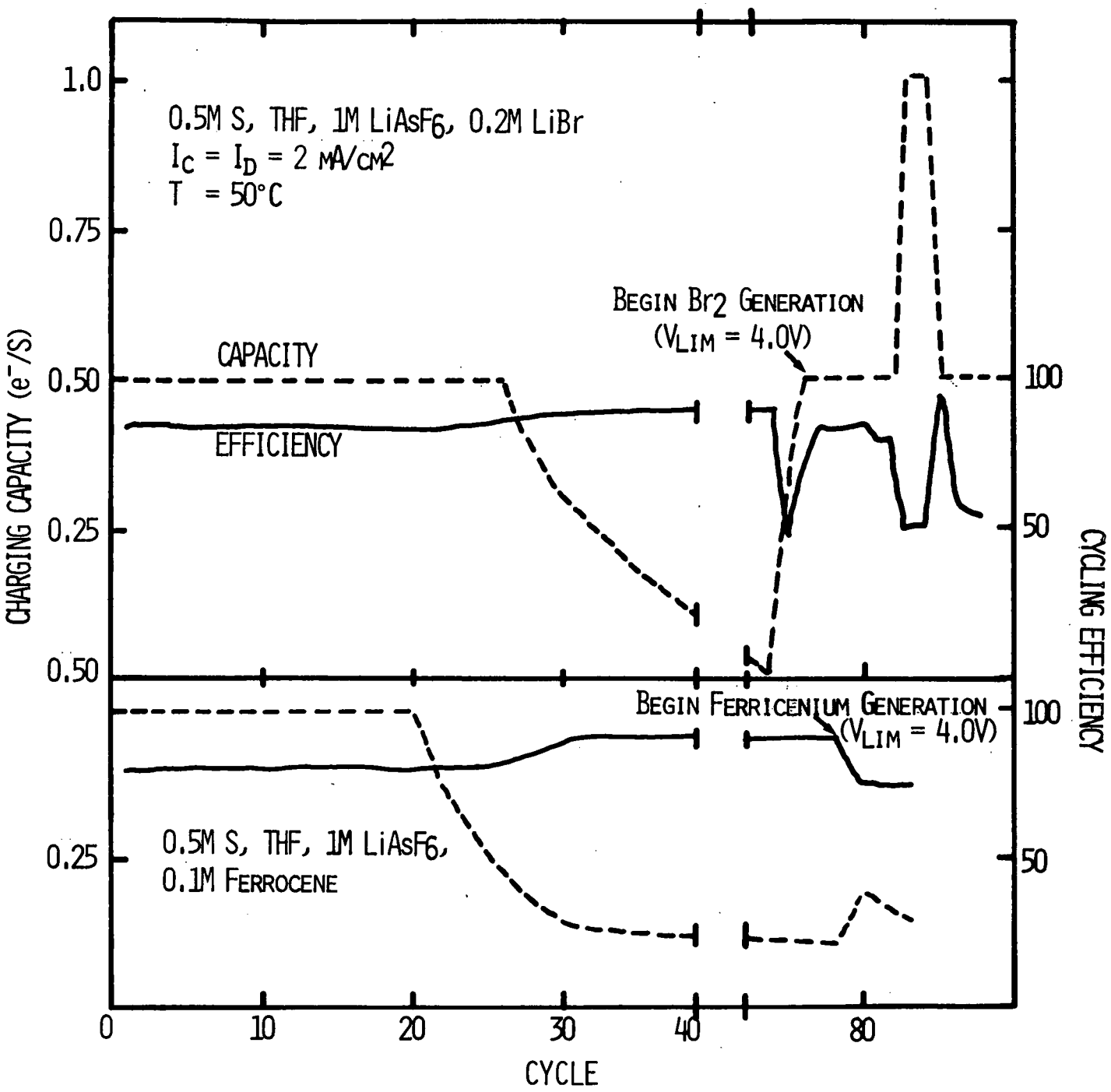

Fig. 25: Cycling behavior of Li/Li_2S_n cells (flooded configuration) in the presence of added redox reagents.

TABLE 12

RESULTS OF STORAGE TESTS OF POLYSULFIDE SOLUTIONS
IN EVACUATED SEALED AMPOULES

Storage*	Storage Time	Storage Time (°C)	Gas Pressure (mm) at 0°C	Extent of Li Corrosion
A - 1M S as S_8^{-2}	21 days	68	100	--
B - Sol'n A + Li	21 days	68	130 @ 25°	Most Li reacted
C - 1M S as S_4^{-2}	21 days	68	65	--
D - Sol'n C + Li	21 days	68	48	Most Li reacted
E - 1M S as Li_2S	21 days	68	60	--
F - Sol'n E + Li	21 days	68	50	Mild attack due to S_n^{-2} impurities
G - 1M S as S_8^{-2} + 1M $LiAsF_6$ + Li	21 days	68	60	Moderate attack

*In B, D, F and G, Li surface area to solution volume ratio is $\sim$2 cm^{-1}.

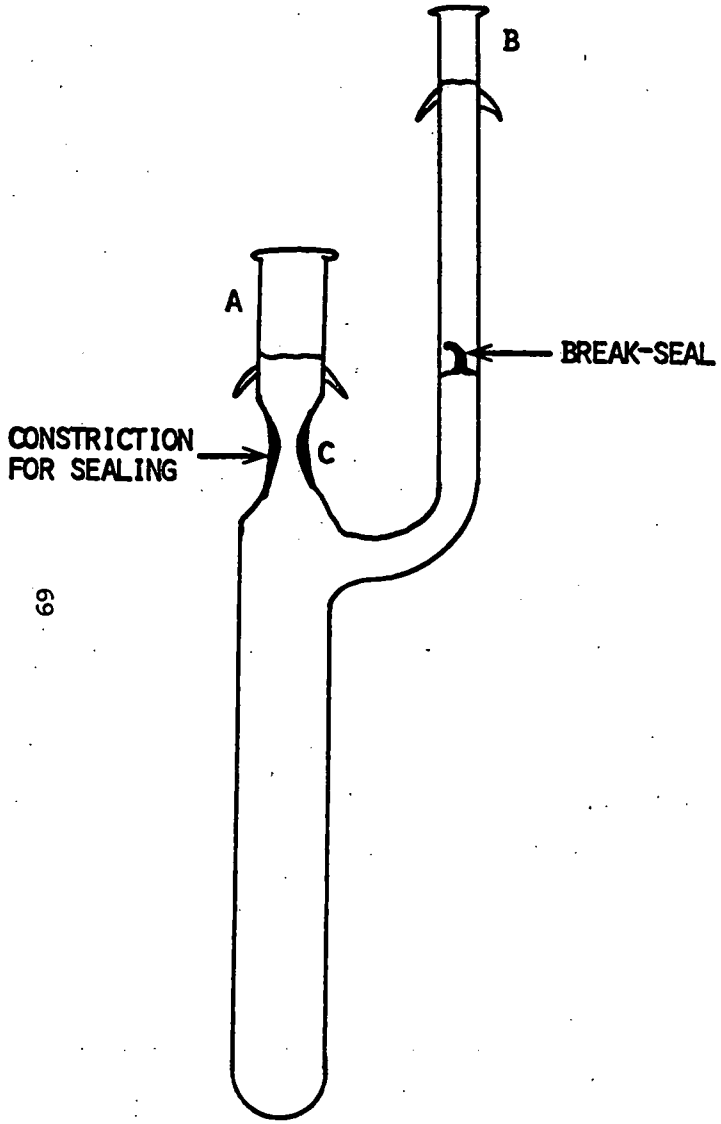

Fig. 26a: Sample tube for stability test.

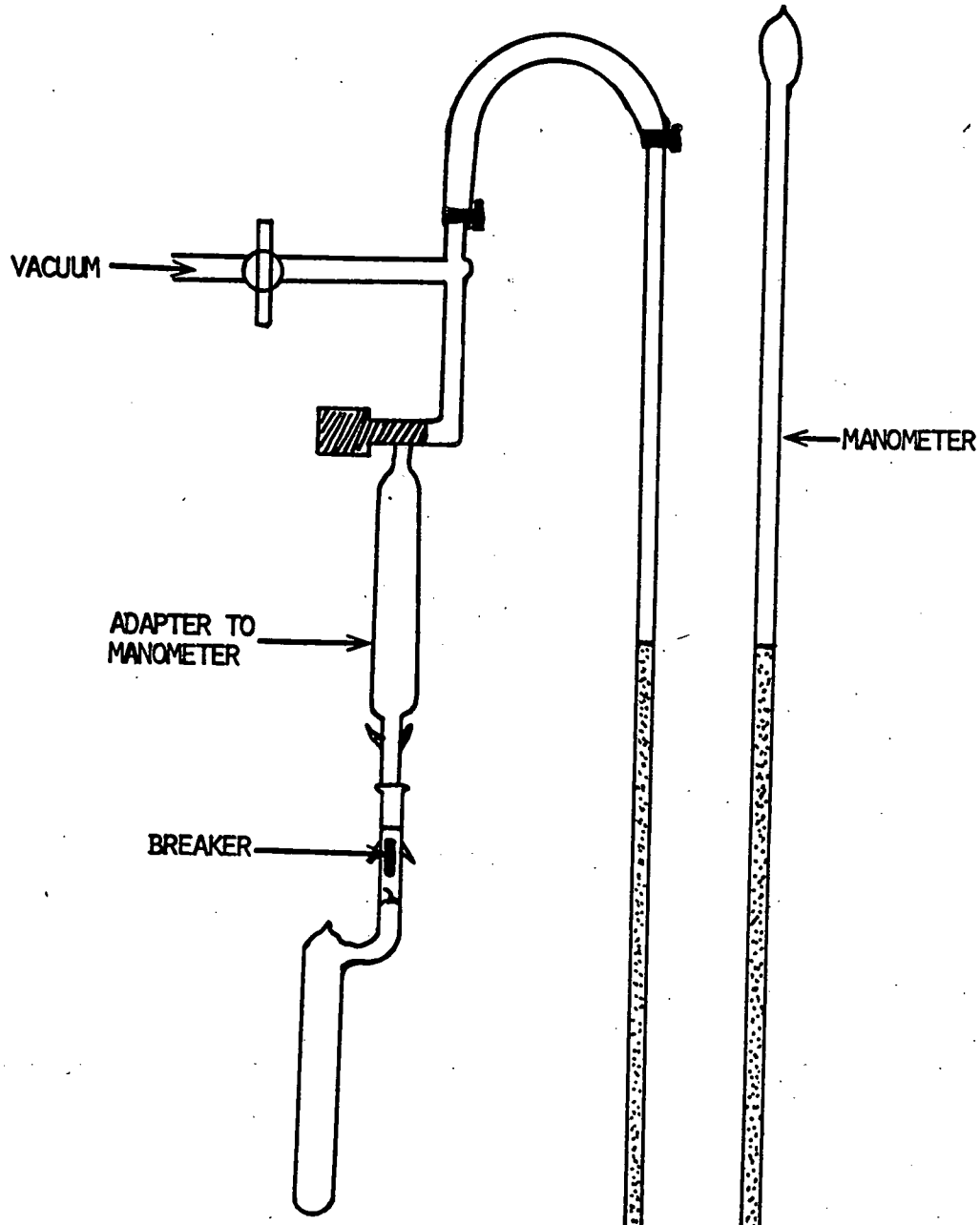

Fig. 26b: Manometer Assembly

on the vacuum line. Any accumulation of gas pressure was measured with a mercury manometer attached to the vacuum line, and the atmosphere above the solutions were sampled in a gas-phase ir cell. Following gas analysis, the solutions were transferred to centrifuge tubes under Ar, and centrifuged to separate out solid components. These solids were repeatedly washed with THF to remove polysulfides. In the tubes containing Li, it is anticipated that these solids contain the apparently "inert," anode isolated cathode material.

The supernatants were diluted 5:1 with Et_2O and extracted with aqueous base, again to remove S_n^{-2}. The ether layers were then concentrated and subjected to gas chromatographic and ir spectral analysis. Any organic solvent decomposition products should be in this fraction.

The results, however, gave no indication of solvent decomposition in polysulfides with or without Li. No significant pressure accumulations were noted in any of the tubes, the pressures corresponding well to the THF vapor pressure at the sampling temperature, 0°C. The gas phase ir spectra of the gaseous atmosphere within these tubes revealed only THF. In the Li_2S_8, Li_2S_4 and $Li_2S_8/LiAsF_6$ solutions in contact with Li metal, the Li became quite corroded over the storage period, particularly in the first two solutions. The presence of $LiAsF_6$ appeared to offer some protection. Where Li was corroded, a black-gray sediment was noted, similar to the material found on the anodes of failed cells. When it is washed continuously with THF, highly colored polysulfide is extracted from the residue leaving behind a white material, probably Li_2S, and a lesser black component, as yet unidentified. Finally, the concentrated ether extracts of the reacted solutions showed only THF in both the ir and gas chromatographic analyses.

In all of our experience, the Li/Li_2S_n cell performs best when $LiAsF_6$ is used as an electrolyte. An attempt to replace the 1M $LiAsF_6$ with 1M LiBr in a flooded cell configuration (0.5M S as Li_2S_{10}) with our usual cycling regime resulted in cell failure by the 10th cycle. The generation of Br_2 had no effect on increasing the capacity, so it can be inferred that the self-discharge rate is inherently very high in this electrolyte, probably due to poor Li electrodeposit morphology. A high rate package cell containing 5M S and 1M LiBr and cycled at a capacity of 0.5 e^-/S at ± 2 mA/cm^2 failed after 4 cycles.

The problem with LiBr electrolytes may be due, in part, to low purity and dryness of the salt (the reagent grade salt was dried <u>in vacuo</u> at 100°C for 24 hours previous to dissolving in the THF). To avoid the salt altogether, flooded cells were prepared using 0.5M <u>neutral</u> S as a slurry in a THF, 1M $LiAsF_6$ electrolyte both with and without 0.1M Br_2. The results of cycling these cells to a depth of 0.5 e^-/S at ± 2 mA/cm^2 and 50°C are presented in Figure 27. In the baseline cell, a few initial cycles were run at 0.5 mA/cm^2 in order to bring enough S_n^{-2} into solution to carry the higher current. After these "priming" cycles, the

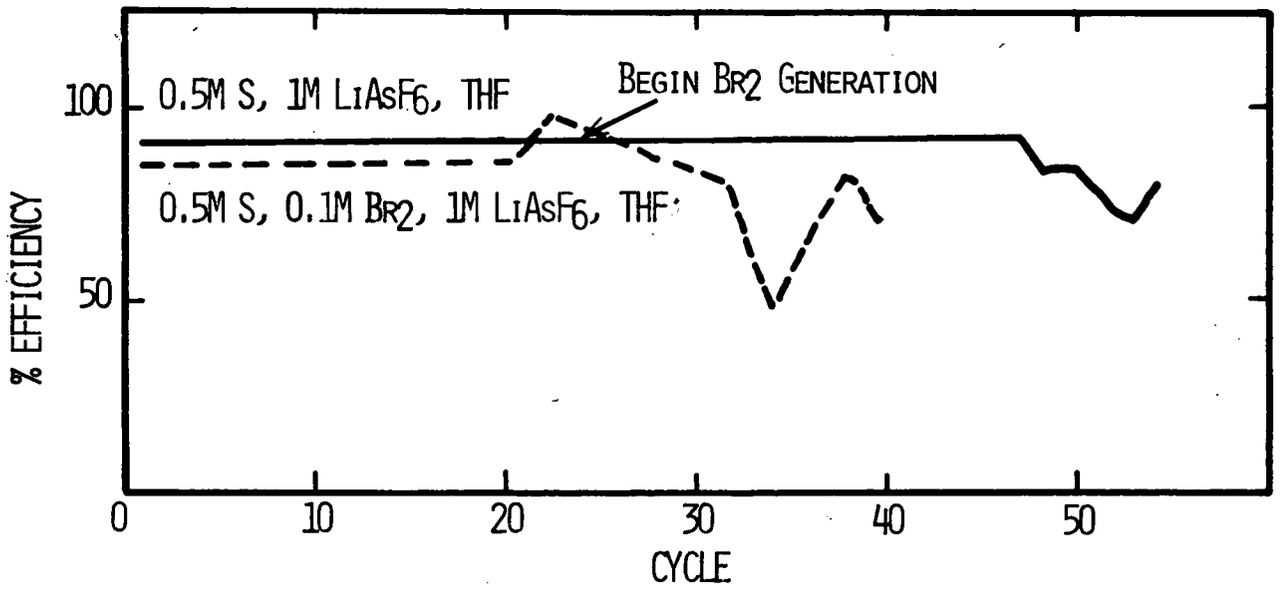

Fig. 27: Results of cycling flooded cells at a constant charging capacity of 0.5 e^-/S. Sulfur initially present as S°.

cell went over 50 cycles before the efficiency began to decline. The same cell with Br_2 added went only ~25 cycles. Following the 21st cycle, some Br_2 was generated on each charging half-cycle, which appeared to keep the cycling efficiency from declining rapidly. The cell cracked on cycle 39, so the experiment had to be terminated there.

Another complication is the physical state of the electrolyte following complete self-discharge when ~5M S is present. To illustrate this, a tube containing 5M S as Li_2S_{10} in THF was sealed with Li foil in vacuo in a glass tube and stored for 3 weeks at 71°C. Following this period, the electrolyte had become a dark green-black paste. However, an infrared spectrum of the paste showed only THF (the S_n^{-2} bands are very weak and at low energies in the "fingerprint" region). It is likely that the solvent becomes occluded in the massive amount of Li_2S and lower polysulfide precipitate. The pure Li_2S appears to become freed on continued washing of the paste with THF, the supernatant, by its visible spectrum, containing polysulfides and an unidentified product with $\lambda_{max} \approx 800$ nm.

Finally, a 1M solution of Br_2 in THF allowed to stand for a week in the dark gradually decolorized. It is possible that sites with labile hydrides, such as the α position in THF, are susceptible to reaction with Br_2. However, this reaction with solvent appears to be much slower than the reaction between Br_2 and Li_2S, and hence may not present a large problem.

More detailed analysis of the products of the reaction between Li foil and 5M S as Li_2S_{10} in THF was carried out. In carrying out this experiment, 10 ml of the 5M S and 120 cm^2 of Li foil cut into 6 x 0.5 cm strips were sealed in vacuo in a break-seal tube. In the tube, the solid Li was completely submerged beneath the liquid. As reported above, the tube was stored at 71°C for 21 days, after which a sludge-like paste remained surrounding the partially corroded Li. After this reaction period, the tube contained no free liquid. The residue reacted readily with Br_2.

The break-seal tube was opened in a vacuum line equipped with a mercury manometer for detecting pressure build-up. No unusual increase in pressure within the tube was detected. A gas phase infrared spectrum of the atmosphere within the tube revealed only THF. H_2S was definitely not present.

The residue was washed 5X with 10 ml aliquots of THF. All manipulations were carried out in an Ar-filled glove box. Each washing step lasted 24 hours, with intermittent agitation. At the end of each wash, the tube was centrifuged and the supernatant decanted. After the first wash, the strands of unreacted Li were easily removed.

Figure 28 shows the visible absorption spectrum of the first wash, diluted 1:10 with THF. The spectrum of the muddy green solution contains maxima or shoulders at 800, 760, 550, 470 and 420 nm. Addition of Br_2 reduced all these features to a broad tail extending out to ~780 nm, part of which may be due to Br_2 itself.

A cyclic voltammogram of this wash made 0.5M in $LiAsF_6$ is shown in Figure 29. The general features of the CV correspond to S_n^{-2} in THF, with a peak corresponding to S° being present on the second sweep. Thus, the species giving rise to the anomalous spectral features are either electrochemically inactive or have the same redox properties as S_n^{-2}.

By the fifth wash, the supernatant was nearly colorless. Each washing had spectral features similar to Figure 28. The remaining solids had a fine, powder-like consistency, and were comprised of a gray upper layer and a black lower layer. Both layers dissolved slowly in MeOH and rapidly in H_2O. Some gas evolution was observed during dissolution of the darker solid. Spectra of the reddish MeOH solutions were identical, and are shown in Figure 28. Shoulders were observed at 365, 500 and 600 nm.

Infrared spectra of the solid residue before and after the five washings were obtained in a KBr matrix. The spectrum of the final solid residue is quite featureless, with weak, structural transitions at 1625 cm^{-1} and 1450 cm^{-1}, and a broad water peak centered at 3200 cm^{-1}. It is very similar to the spectrum of hydrated Li_2S recorded previously.

Some exploratory investigations were performed to develop electrolytes to THF. In particular, we are interested in only partial Li_2S_n solubility and in electrolytes where the self-discharge products have a crystalline rather than a paste-like consistency.

With this goal in mind, we studied the mixed propylene carbonate (PC)/THF electrolyte. Since S_n^{-2} is completely insoluble in PC, it was anticipated that such mixtures would afford the desired partial solubility along with the Li stability characteristic of the components. A detailed analysis of Li_2S_n solubility in such mixtures were therefore conducted. Various amounts of PC were added to 1.5M (as Li_2S_n)/THF solutions. After at least 6 hours, the solutions were centrifuged and the supernatant analyzed for total S and S^{-2}. The results are summarized in Table 13, with the PC concentration expressed as its ratio to the S^{-2} concentration. The sharpest decrease in Li_2S_n solubility occurs between 0.5:1 and 2:1 PC/S^{-2}. Accompanying this decrease is an increase in the average chain length of the remaining dissolved S_n^{-2}. It was also apparent that the solutions containing higher PC concentrations were unstable, giving rise to continued precipitation on long-term stand. The effect of PC is assumed to be due to a shift in the disproportionation equilibrium,

$$2Li^+ + S_n^{-2} \rightleftarrows Li_2S + \frac{n-1}{8} S_8 \qquad (19)$$

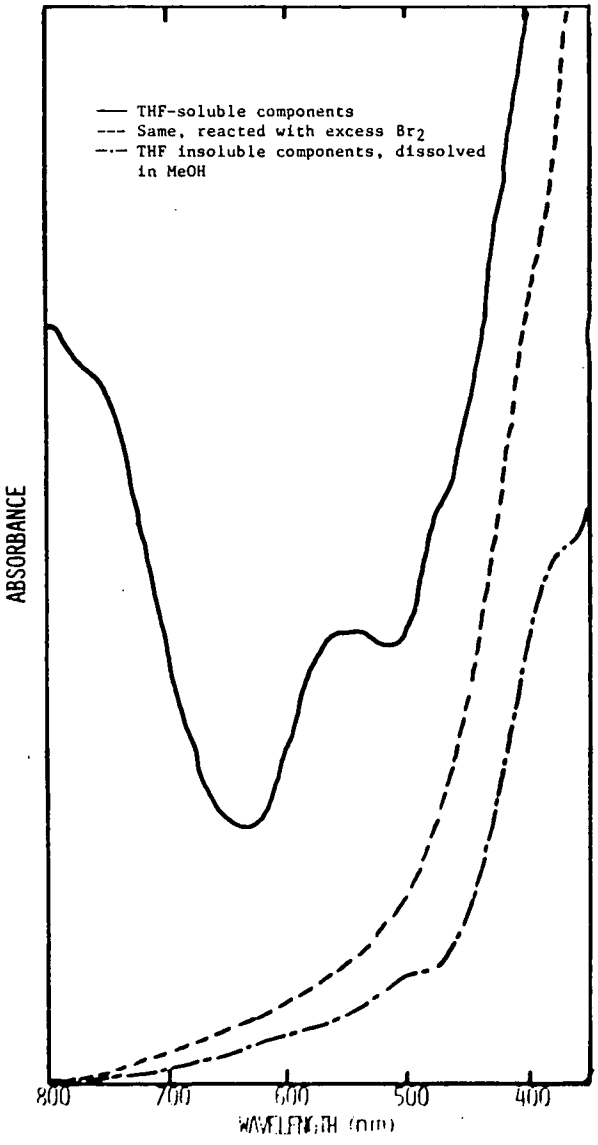

Fig. 28: Spectra of Li + Li_2S_n (THF) self-discharge products.

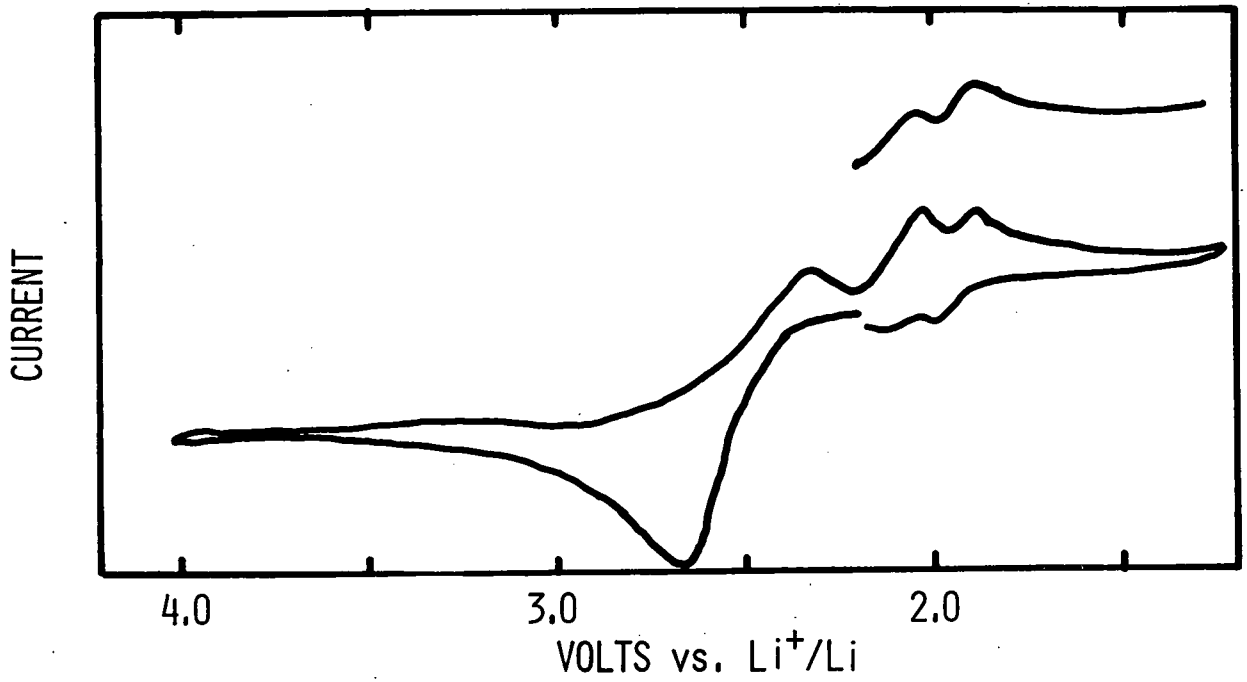

Fig. 29: Cyclic voltammogram on vitreous C of THF soluble reaction products of Li + Li_2S_n in THF. Sweep rate = 0.1V sec^{-1}.

Furthermore, the solubility studies indicated that this shift may arise from a specific PC/S_n^{-2} interaction rather than from a change in such a macroscopic property as dielectric constant. PC therefore may be an effective additive to Li/Li_2S_n cells if, during cycling, it can keep equilibrium moderately shifted to the right. Thus, enough S_n^{-2} is retained in solution to carry the cathode charge/discharge current, but most of the cathode material is stored in the carbon electrode as Li_2S and S_8 during all phases of charge and discharge.

TABLE 13

SOLUBILITY STUDIES OF POLYSULFIDES IN PROPYLENE CARBONATE/THF

Ratio of PC:$S^=$	Sulfide Analysis	Total Sulfur	Ratio of Sulfide:Sulfur
0.1:1	0.148	1.48	0.1
0.25:1	0.135	1.54	0.088
0.5:1	0.094	1.40	0.67
1:1	0.081	0.90	0.09
2:1	0.019	0.56	0.034
3:1	0.015	0.49	0.0306
4:1	0.011	0.36	0.0305
5:1	0.013	0.49	0.026
6:1	0.014	0.35	0.04

Discussion of Cell Rechargeability. The process of recharging a Li/Li_2S_n cell depends on being able to electrodeposit Li from a highly oxidizing environment. In terms of current research on the secondary Li electrode, our success in this area has been quite remarkable. In this cell, Li has been cycled on a Li substrate at greater than 90% efficiency for 135 cycles of ∿7 coul/cm^2 (0.1 e^-/S) at 50°C, and for at least 40 cycles five times that charge at ∿85% efficiency. This performance exceeds that of the Li electrode in "inert" media, such as propylene carbonate (51-53), methyl acetate (54,55) or tetrahydrofuran (39).

The additional feature which separates the Li/Li_2S_n battery from devices using "inert" electrolytes is the presence of a true self-discharge mechanism. If the self-discharge rate can be controlled, it should be possible to develop a battery which uses only a stoichiometric amount of Li on the anode. In the Li/Li_2S_n battery, no Li is actually lost from the system by encapsulation, at least under the symmetrical cycling regime. The most probable Li-resolubilizing self-discharge reactions are

$$2Li \text{ (electrodeposited)} + Li_2S_n \text{ (dissolved)} \rightarrow 2Li_2S_{n/2} \quad (20)$$

$$2Li \text{ (electrodeposited)} + S_n^{\circ} \text{ (electrogenerated)} \rightarrow Li_2S_n \quad (21)$$

It is also self-discharge which gives rise to cell failure via eventual Li_2S isolation on the anode. Studies of the effects of overcharge in fresh cells on the subsequent baseline capacity indicate that reaction (21) is not a source of Li_2S, but probably only of soluble S_n^{-2} species. Although the details of reaction (20) are not known at this time, it is likely to be the main route to Li_2S formation.

A remaining question is whether Li_2S, once formed on the anode, is ever resolubilized via the reactions

$$Li_2S + Li_2S_n \text{ (dissolved)} \rightarrow 2Li_2S_{n+1/2} \text{ (dissolved)} \quad (22)$$

$$Li_2S + S_n^{\circ} \text{ (electrogenerated)} \rightarrow Li_2S_{n+1} \text{ (dissolved)} \quad (23)$$

We do know that reaction (22) becomes very slow for $n \leq 5$. We also know that depleted cells cannot be revived by overcharge. In this case, reactions (20) and (21) must supersede reactions (22) and (23). Indeed, the reverse can be true only under a rather restrictive set of circumstances, judging from the results, i.e., when $n > 5$ of S_n^{-2} and when Li is passivated or otherwise protected relative to Li_2S. Overcharging of failed cells does not establish a shuttle mechanism for redissolving Li_2S specifically because the freshly deposited Li always reacts more rapidly.

It has been seen from studies of prefilming the Li anodes that in certain cases cell failure can be postponed by decreasing the self-discharge rate. Presumably, the LiCl film is Li^+-permeable, allowing deposition to proceed beneath it while continually affording protection for the new deposit. Prefilming the anodes with Li_2S, however, appears detrimental to cycle life; however, unlike LiCl, Li_2S should be partly soluble in the fresh, highly oxidizing electrolyte.

The problem of increasing the cycle life of this cell must therefore be addressed in two areas. One area is to reduce the self-discharge rate and thus to prevent or delay Li_2S formation on the anode. This approach was explored by using alloy anodes. However, the Li/Al alloy, while giving rise to reduced self-discharge compared to an inert substrate such as Ta, afforded little advantage over a Li substrate. In addition, it has been shown in other work (48) that it is difficult to maintain the mechanical integrity of alloy electrodes due to volume changes on cycling.

It must be stressed that, in order to achieve the positive benefits of avoiding Li encapsulation and maintaining the materials balance, the

self-discharge reaction should not be eliminated. Rather, it should occur at a reasonable rate and not give rise to sulfur species isolated on the anode. An extremely convenient solution, and a second major area of investigation, would be to find a way to dissolve Li_2S. To date, we have found no unreactive Li_2S solubilizing agents. Lewis acids which appeared to dissolve Li_2S were actually being irreversibly reduced. Internally generated "scavengers" such as ferricenium, Br_2 or S_n^{-2} itself either react preferentially with Li instead of Li_2S or, at very best, are ineffective at extending rechargeability. It is clear, however, that this approach merits further investigation.

A further modification of the cell configuration is still being investigated, that of partially soluble sulfur-containing cathodes. Studies with methyl acetate indicate that this approach can give rise to enhanced discharge rates due to lower electrolyte viscosities. What is not yet known is how these systems behave under extended cycling using a solvent more compatible with Li than MA.

REFERENCES

1. K. M. Abraham, R. D. Rauh and S. B. Brummer, Electrochim. Acta, 23, 501 (1978).

2. W. Giggenbach, Inorg. Chem., 10, 1306 (1971).

3. W. Giggenbach, Inorg. Chem., 11, 1201 (1972).

4. W. Giggenbach, Inorg. Chem., 13, 1724 (1974).

5. T. Chivers and I. Drummond, Chem. Soc. Rev., 2, 233 (1973).

6. F. Seel and G. Simon, Z. Naturforsch, 27B, 1110 (1972).

7. F. Seel and H. Güttler, Agnew. Chem. Int. Ed., 12, 421 (1973).

8. W. Giggenbach, J. Inorg. Nuc. Chem., 30, 3189 (1968).

9. W. Giggenbach, J. C. S. Dalton, 1973, 729.

10. M. Merritt and D. Sawyer, Inorg. Chem., 9, 241 (1970).

11. R. Martin, W. Doub, J. Roberts and D. Sawyer, Inorg. Chem., 12, 1921 (1973).

12. R. Bonnaterre and G. Cauquis, J. C. S. Chem. Comm., 1972, 293.

13. J. Badoz-Lambling, R. Bonnaterre, G. Cauquis, M. Delamar and G. Demange, Electrochim. Acta, 21, 119 (1976).

14. T. Chivers and I. Drummond, Inorg. Chem., 11, 2525 (1972).

15. T. Chivers and I. Drummond, J. C. S. Dalton 1974, 631.

16. H. Lux, S. Benninger and E. Bohm, Chem. Ber., 101, 2485 (1968).

17. R. Maccoll and S. Windever, J. Phys. Chem., 74, 1261 (1970).

18. G. Schwarzenbach and A. Fischer, Helv. Chim. Acta, 43, 1365 (1960).

19. T. Pickering and A. Tobolsky in Sulfur in Organic and Inorganic Chemistry, A. Senning ed. (New York: Marcel Dekker Inc., 1972), Vol. 3, p. 27.

20. J. Letoffe, J. Blanchard and J. Bousquet, Bull. Soc. Chim. 1976, 395.

21. D. Sawyer and J. Roberts, Jr. in Experimental Electrochemistry for Chemists (New York: John Wiley & Sons, 1974), pp. 172-175.

22. V. Gutmann, Electrochim. Acta, 21, 661 (1976).

23. S. B. Brummer, R. D. Rauh, J. M. Marston and F. S. Shuker, Semiannual Progress Report, Contract E(11-1)-2520, July 1975.

24. M. Delamar, J. Electroanal. Chem., 63, 351 (1975); M. Delamar and J. Marchon, ibid., 63, 351 (1975).

25. Z. Kovacova and I. Zezula, Coll. Czech. Chem. Comm., 39, 722 (1974).

26. M. L. Rao, U.S. Patent 3,413,154 (1968).

27. J. R. Coleman and M. W. Bates, Power Sources 2, ed. D. N. Collins (1969).

28. D. Nole and V. Moss, U.S. Patent 3,532,543 (1970).

29. G. Eichinger and J. Besenhard, J. Electroanal. Chem., 72, 1 (1976).

30. Varta Batterie, Fr. Demande 2,236,285 (1975).

31. J. Auborn, K. French, S. Lieberman, V. Shah and A. Heller, J. Electrochem. Soc., 120, 1613 (1973).

32. W. Behl, J. Christopulos, M. Ramirez and S. Gilman, J. Electrochem. Soc., 120, 1619 (1973).

33. J. R. Driscoll, G. L. Holleck and D. E. Toland, Proc. 17th Power Sources Symposium, Atlantic City, N.J., June 1976.

34. D. Maricle and J. Mohns, Fr. Demande 2,015,160 (1970).

35. P. Bro, R. Holmes and H. Taylor, 9th Intern. Power Sources Symposium, Brighton, Paper 44 (1974).

36. R. D. Rauh, J. M. Marston and S. B. Brummer, Fall Meeting of The Electrochem. Society, Dallas, 1975, Abstract No. 33.

37. R. D. Rauh, F. S. Shuker, J. M. Marston and S. B. Brummer, Spring Meeting of The Electrochemical Society, Washington, D.C., 1976.

38. R. D. Rauh, F. S. Shuker, J. M. Marston and S. B. Brummer, J. Inorg. Nuc. Chem., 39, 1761 (1977).

39. V, R. Koch and J. H. Young, J. Electrochem. Soc., 125, 1371 (1978).

40. J. A. Christopulos and S. Gilman, Proc. 10th IECEC Conference, Newark, Delaware (1975).

41. F. W. Dampier, unpublished results.

42. S. B. Brummer, R. D. Rauh, K. M. Abraham, J. M. Marston, G. F. Pearson and F. S. Shuker, Semiannual Progress Report, Contract EY-76-C-02-2520, September 1976.

43. S. B. Brummer, R. D. Rauh, J. M. Marston and F. S. Shuker, Annual Progress Report, Contract EY-76-C-02-2520, April 1976.

44. K. M. Abraham and R. D. Rauh, Fall Meeting of The Electrochemical Society, Atlanta, 1977, Abstract No. 2.

45. A. N. Dey, Electrochim. Acta, 21, 377 (1976).

46. A. N. Dey and P. Bro, 10th Intern. Power Sources Symposium, Brighton, England, Paper 32, September 1976.

47. Z. Kovacova and I. Zezula, Coll. Czech. Chem. Comm., 40, 1279 (1975).

48. S. B. Brummer, F. W. Dampier, V. R. Koch, R. D. Rauh, T. F. Reise and J. H. Young, Final Report, NSF Grant AER75-03779, January 1978.

49. R. D. Rauh, T. F. Reise and S. B. Brummer, J. Electrochem. Soc., 125, 186 (1978).

50. S. B. Brummer, R. D. Rauh, K. M. Abraham, G. F. Pearson and J. K. Surprenant, Semiannual Progress Report, Contract No. EY-76-C-02-2520, December, 1977.

51. R. Selim and P. Bro, J. Electrochem. Soc., 121, 1457 (1974).

52. R. D. Rauh and S. B. Brummer, Electrochim. Acta, 22, 75 (1977).

53. R. D. Rauh, T. F. Reise and S. B. Brummer, J. Electrochem. Soc., 125 (1978).

54. R. D. Rauh and S. B. Brummer, Electrochim. Acta, 22, 85 (1977).

55. F. W. Dampier and S. B. Brummer, Electrochim. Acta, 22, 1339 (1977).

56. V. R. Koch, J. Electrochem. Soc., 126, 181 (1979).

57. J. Weininger and F. Secor, J. Electrochem. Soc., 121, 315 (1975).

III. INSOLUBLE SULFIDE POSITIVE ELECTRODES FOR ORGANIC ELECTROLYTE LITHIUM SECONDARY BATTERIES

A. Background

Simple sulfides of the transition metals such as CuS and NiS have been extensively studied as positive electrodes for primary Li/organic electrolyte cells (1-7). Primary Li-CuS batteries have been developed by several battery manufacturers (1,6) and 112 Whr/lb has been achieved (1) for D-size cells. The monosulfides previously have been considered (8) of minimal reversibility because it was thought that they lacked a crystal structure favoring the intercalation of Li^+ similar to TiS_2. However, CuS as covellite has a layer structure as indicated by several crystallographic studies (9,16). Since initial exploratory work with the Li-CuS cell showed that the cell is reversible, it was decided to investigate the behavior of other insoluble sulfides as positive electrodes. In this section results are presented of an investigation of the behavior of CuS, NiS, SiS_2, MnS_2, FeS and Bi_2S_3 positive electrodes in rechargeable Li cells. The findings are evaluated in terms of the merits of each material for practical application in high energy density secondary batteries.

The selection of the most promising sulfides for investigation was made on the basis of the specific energy calculations presented in Table 14, cost and previous work reported in the literature. Although CuS is the most attractive sulfide positive electrode listed in Table 14, both in terms of specific energy and cost, its experimental discharge potential ($\sim$1.7V) is rather low. In principle, metal disulfides should have much higher potentials because it is much easier to reduce a metal disulfide to a monosulfide, than to reduce a monosulfide, most of which are extremely stable, to the elemental metal and Li_2S. To illustrate this point, in Table 14 the cell potentials vs. Li are presented for a number of disulfide positive electrodes.

Since the high cell potentials and large specific energies (e.g., 1037 Whr/lb for SiS_2) calculated for the disulfides are almost unbelievably attractive, some comments concerning the limitations of the calculations are in order. For the calculations, it was assumed that the discharge products for the reduction of metal disulfides are the monosulfide and Li_2S. However, the discharge products are probably "intermediate" Li compounds, analogous to the intercalation compounds formed with TiS_2 (11,12), and therefore the actual cell potentials will be lower than the calculated values. In the case of TiS_2, the observed cell potential ($\sim$2.6V) is about 30% lower than the calculated value.

TABLE 14

SPECIFIC ENERGIES OF INSOLUBLE
SULFIDE POSITIVE ELECTRODES

Compound	Eq.Wt.[a]	No. of Electrons	E°[b]	Whr/lb
A. Complete Reduction				
NiS	52.32	2	2.022	470
CuS	54.74	2	2.231	496
FeS	50.89	2	1.98	473
MnS	50.44	2	1.39	335
MnS_2	66.47	4	0.759	138
Ag_2S	130.84	2	2.28	212
VS	48.44	2	1.523	382
CoS	52.44	2	2.056	477
B. Partial Reduction to Monosulfide				
SiS_2	53.10	2	4.54	1037
TiS_2	63.00	2	3.73	720
MnS_2	66.52	2	5.29	967
FeS_2	66.98	2	5.69	1033

[a] Includes weight of required Li.

[b] The cell potentials were computed from the free energies of formation at 25°C tabulated by Gibson and Sudworth (10).

B. Experimental

1. Cell Construction

Cells were either constructed as in Section II, or were of a larger design. These larger cells consisted of two Li negative electrodes (3.5 x 3.5 cm) on either side of the sulfide positive electrode, separated by two layers of a 0.025 mm thick polypropylene separator (Celgard 2400). Cells were assembled by wrapping the positive electrode in a "U" fold of two layers of separator, then sandwiching the wrapped electrode between two Li electrodes. The element was then inserted into a rectangular glass cell case (inside L x W x H: 4.5 x 1.5 x 7.0 cm), using polypropylene shims to insure a snug fit.

The Li electrodes (3.5 x 3.5 cm) were prepared by pressing a layer of 0.38 mm thick Li foil (Foote Mineral Company) on both sides of a 0.08 mm thick 3 Ni 10 - 3/0 grid (Exmet Corp.). Either pressed powder or Teflon-bonded positive electrodes were used depending on the properties of the sulfide active material and the purpose of the particular test. Pressed powder sulfide positives were prepared by pressing a blend of 50% active material, 45% graphite (No. 1651, Southwestern Graphite Co.) and 5% polyethylene powder (Microthene FN-500, U.S. Industrial Chemicals) onto a 3 mil thick Ni5 - 4/0 grid)(7).

The Teflon-bonded positive electrodes (2.54 cm^2) were prepared by pressing a mixture of 50% sulfide active material, 50% Shawinigan carbon black and DuPont No. 30 Teflon dispersion on an Exmet 5 Ni5 - 5/0 grid and sintering the dried (overnight at 105°C) electrodes at ∿300°C for 20 minutes under flowing argon. The procedure was similar to the one described earlier by Driscoll and co-workers (13).

2. Electrolyte Preparation

Tetrahydrofuran (THF)(MC/B, Chromatoquality) was dried by passage through a glass column (height, 38 cm) filled with Linde 4A molecular sieves. The solvent was then passed through a second 38 cm column of fresh sieves, to achieve a water adsorption capacity equivalent to a 76 cm column. Lithium hexafluoroarsenate ($LiAsF_6$, electrochemical grade) was obtained from U.S. Steel, Agri-Chemicals Division, and was used as-received.

The preparation of the electrolyte and the construction of cells were all carried out in an argon-filled glove box with a relative humidity maintained at less than 0.002% (0.5 ppm), as measured by a dew point hygrometer (Alnor Instrument Co., Niles, Illinois).

3. Positive Electrode Materials

The CuS, SiS_2, Bi_2S_3 and FeS used to prepare positive electrodes were obtained commercially in highly pure form. However, the NiS and MnS_2 used in the present work were synthesized.

Nickel sulfide (NiS) was formed by reacting 146g of $NiSO_4 \cdot 6H_2O$ (Harshaw) with 170 ml of 24% $(NH_4)_2S$ solution (Fisher Certified). The $NiSO_4 \cdot 6H_2O$ was dissolved in 600 ml of distilled water to which 100 ml of 14M NH_4OH was added. The NiS precipitate was filtered and washed until the wash water gave a negative test with dimethylglyoxime (0.16 µg detection limit). The precipitate was then dried at 120°C for 48 hours in a tube furnace flushed with N_2.

Manganous disulfide (MnS_2) was prepared using the procedure developed by Biltz and Wiechmann (14). In brief, 5g of $MnSO_4 \cdot H_2O$ (Fisher, Certified) was dissolved in 20 ml of water, then 20 ml of a boiling potassium polysulfide solution was added. The potassium polysulfide solution was prepared by dissolving 25g of anhydrous K_2S (Fisher) in 100 ml of water, bringing the solution to a boil, then adding 25g of sulfur (Ventron Corp.) in small portions over a 20-hour period. The slurry thus obtained was evaporated to dryness under vacuum in a glass tube, sealed, then heated to 170 ± 10°C. After 60 hours at this temperature the tube was broken open and the product was collected, washed first with 1 liter of hot water then with methanol without exposing it to air. Excess S was next removed from the MnS_2 by treatment with CS_2 in a Soxhlet extractor for 24 hours. Finally the compound was vacuum dried for 24 hours over NaOH at 100°C and transferred under vacuum into the glove box.

C. Results

1. Copper Sulfide

The capacity change as a function of cycle number for Li-CuS cells using a 1M $LiAsF_6$/THF electrolyte and discharged to 1.5 and 1.45V are shown in Figures 30 and 31 respectively. Over 300 cycles were obtained for the Li-CuS cell described in Figure 31 by replacing the Li electrodes and the electrolyte after cycles 41 and 204. Since the capacity was greatly improved for more than 30 cycles each time the cell was refurbished, there is no indication that a cycling limit was reached for the CuS electrode even after 300 cycles. The capacity decrease observed after extensive cycling thus appears in large part due to failure of the Li electrode.

The CuS electrodes used in Cells 1-3 were of the Teflon-bonded type described earlier and contained 49% CuS in Cells 1 and 2 and 73% CuS in Cell 3. The nominal capacities of the electrodes were calculated on the basis of a 1.0 eq/mole CuS utilization and 6.45 cm^2.

The decline in capacity with cycle life observed for the Li-CuS cell as shown in Figure 30 demonstrates that with $LiAsF_6$/THF the cell cycles quite well with little loss in capacity for about 35 cycles after which the capacity rapidly falls. This same basic trend is seen in Figure 31 although the voltage limits are slightly different and the Li

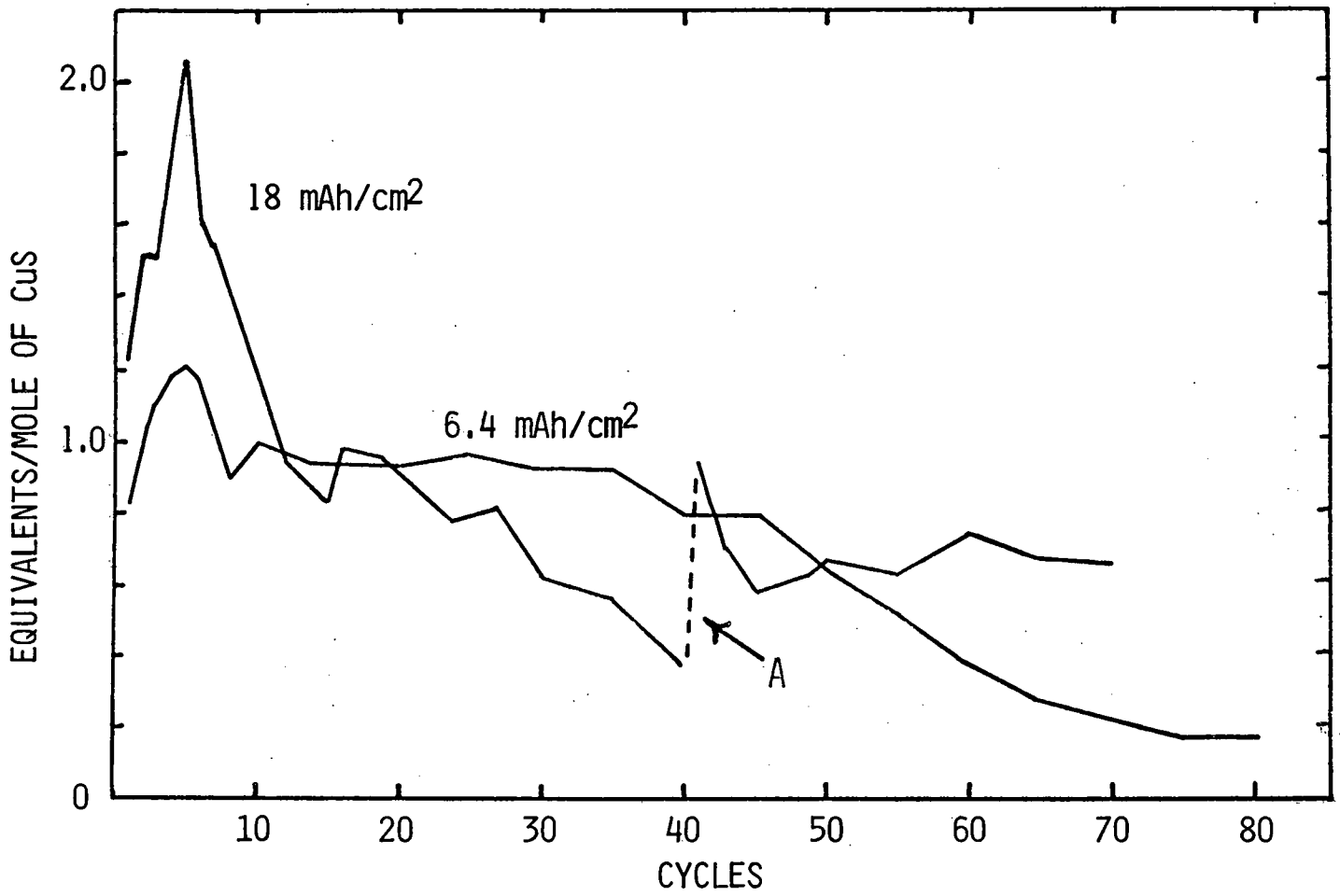

Fig. 30. Capacity of Li/CuS cells as a function of cycle number. Nominal capacities of 6.4 mA/cm^2 and 18 mA/cm^2 for cells 1 and 3, respectively. Cycling carried out at 1.0 mA/cm^2, with discharge and charge limits of 1.5V and 2.9V.

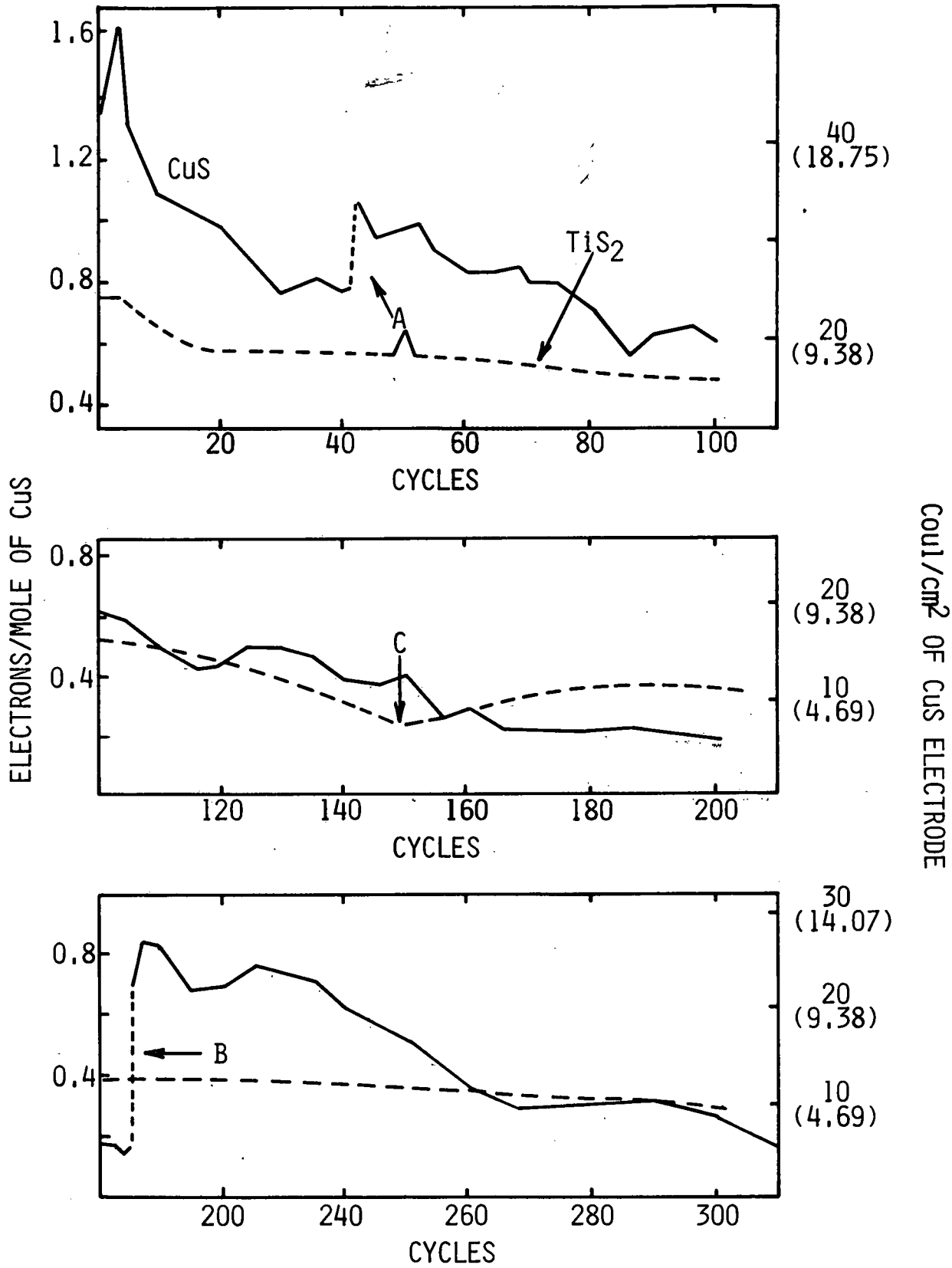

Fig. 31: Capacity changes of a Li/CuS cell as a function of cycle number, Cell #2. Voltage limits: 1.45V on discharge, 2.90V on charge, $i_d = i_c = 1$ mA/cm^2. A, B: Li electrodes and electrolyte replaced. For comparison, data on TiS_2 from ref. (12) are also included (coul/cm^2 capacities in parentheses). C: Li electrodes replaced.

electrodes were replaced. The voltage limits for Cell 1 (Figure 30) were initially 1.5V on discharge and 3.0V on charge but near the end of the fifth charge, the cell potential suddenly became erratic and failed to reach an end point, behavior typical of dendrite shorting. The charging voltage limit was then set at 2.90V and no further problems with dendrite shorting were encountered.

Because the Li-CuS cell has a long sloping discharge curve extending below 1.3V at 1 mA/cm^2 (Figure 32) it was thought that a 1.50V discharge cutoff might needlessly sacrifice capacity. Thus, for Cell 2 the discharge cutoff was extended to 1.45V, and as Figure 31 shows, considerably more capacity was obtained without any sacrifice in cycle life.

Typical charge-discharge curves for the Li-CuS cell at 1.0 mA/cm^2 are shown in Figures 32 and 33. The discharge curve for CuS shows a plateau which ends at 0.3 eq/mole for the first discharge. However, on the second discharge, the end of the plateau occurs at 0.4 eq/mole which suggests that the Cu(II) content is increased by the first charging. Previous workers (3) have postulated that the overall cell reaction involves a stepwise reduction of CuS to metallic Cu corresponding to the two voltage plateaus:

$$2Li + 2CuS \rightarrow Cu_2S + Li_2S \qquad (1)$$

$$2Li + Cu_2S \rightarrow 2Cu + Li_2S \qquad (2)$$

Since mineralogical examinations carried out in our laboratory (15) revealed that the CuS used in the present work (Fisher, ACS Reagent) contained ∿89% CuS as covellite and 10% Cu_2S as chalcocite, only one-third of the Cu is present as Cu(II). Investigations (9,16) of the structure of covellite using X-ray diffraction techniques have shown that it is not a simple cupric salt but a more complex compound which could be represented as $Cu_4^{I}Cu_2^{II}(S_2)_2S_2$. Therefore in Figure 33, because only one-third of the Cu was present as Cu(II) one would expect the first plateau to end at 0.30 eq/mole taking into account that the CuS active material was ∿89% covellite. As Figure 33 shows, the first plateau actually ends at 0.3 eq/mole for the first discharge, which yields a utilization efficiency of ∿100% for Cu(II).

During cycling, the charge time for the Li-CuS cell is conspicuously shorter than the discharge time yielding Ah efficiencies greater than 100% (see Figure 33 and Table 15). The fact that after five cycles both the Li-CuS cells tested yielded more capacity on discharge than the sum of the capacity initially present and the recharge indicates the possibility of solvent reduction. Since it is known from previous voltammetric work (17) that 1M $LiAsF_6$/THF resists reduction down to the Li potential on a Ni working electrode, the only explanation remaining to account for the extra discharge capacity is that the electrolyte is either being reduced on the CuS or the carbon black added to the electrode to increase its conductivity.

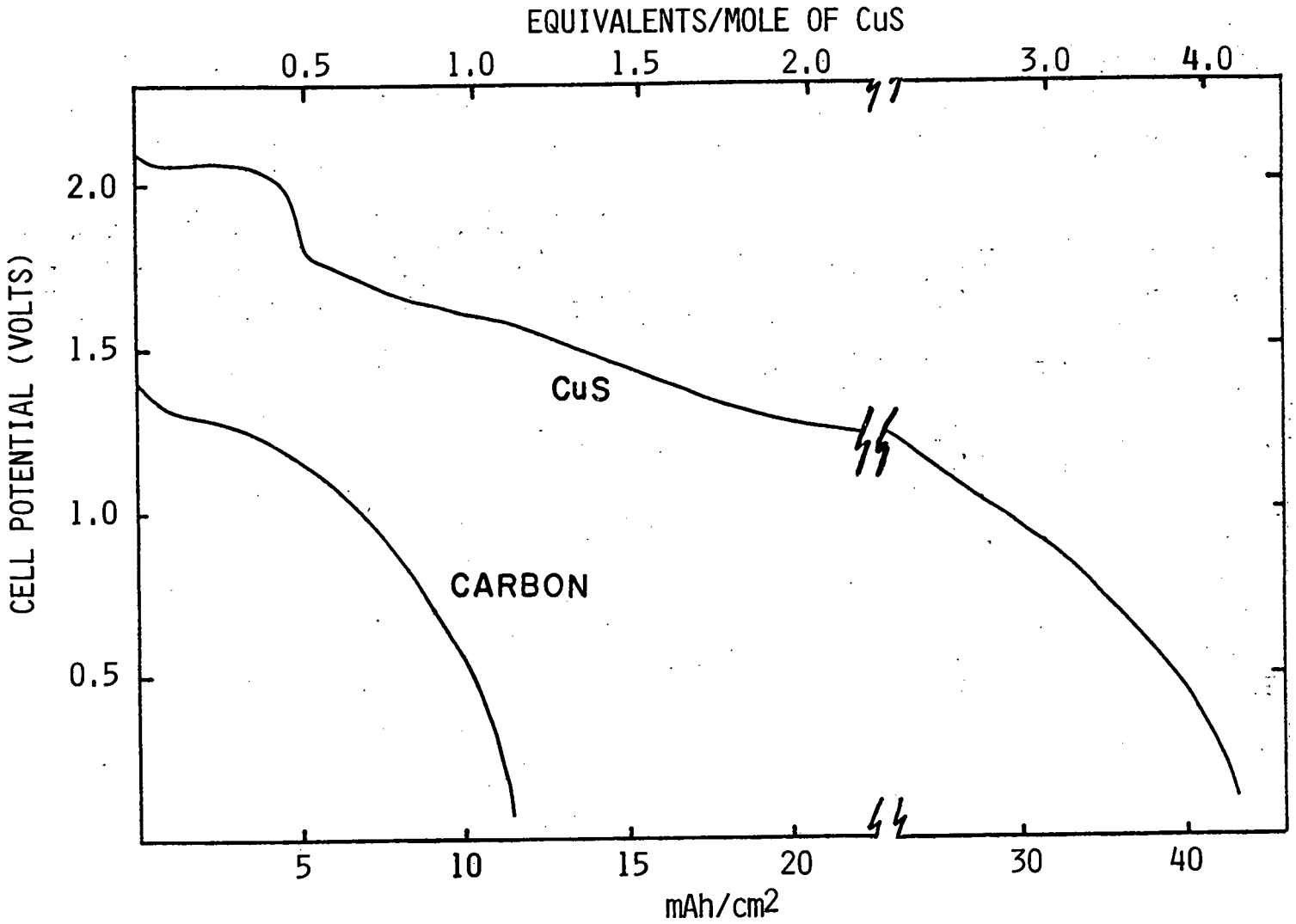

Fig. 32: Electrolyte reduction compared at Teflon-bonded carbon black and CuS electrodes. i = 1.0 mA/cm^2; 1M $LiAsF_6$/THF; CuS electrode capacity 20.4 mAh/cm^2 at 1.0 eq/mole CuS.

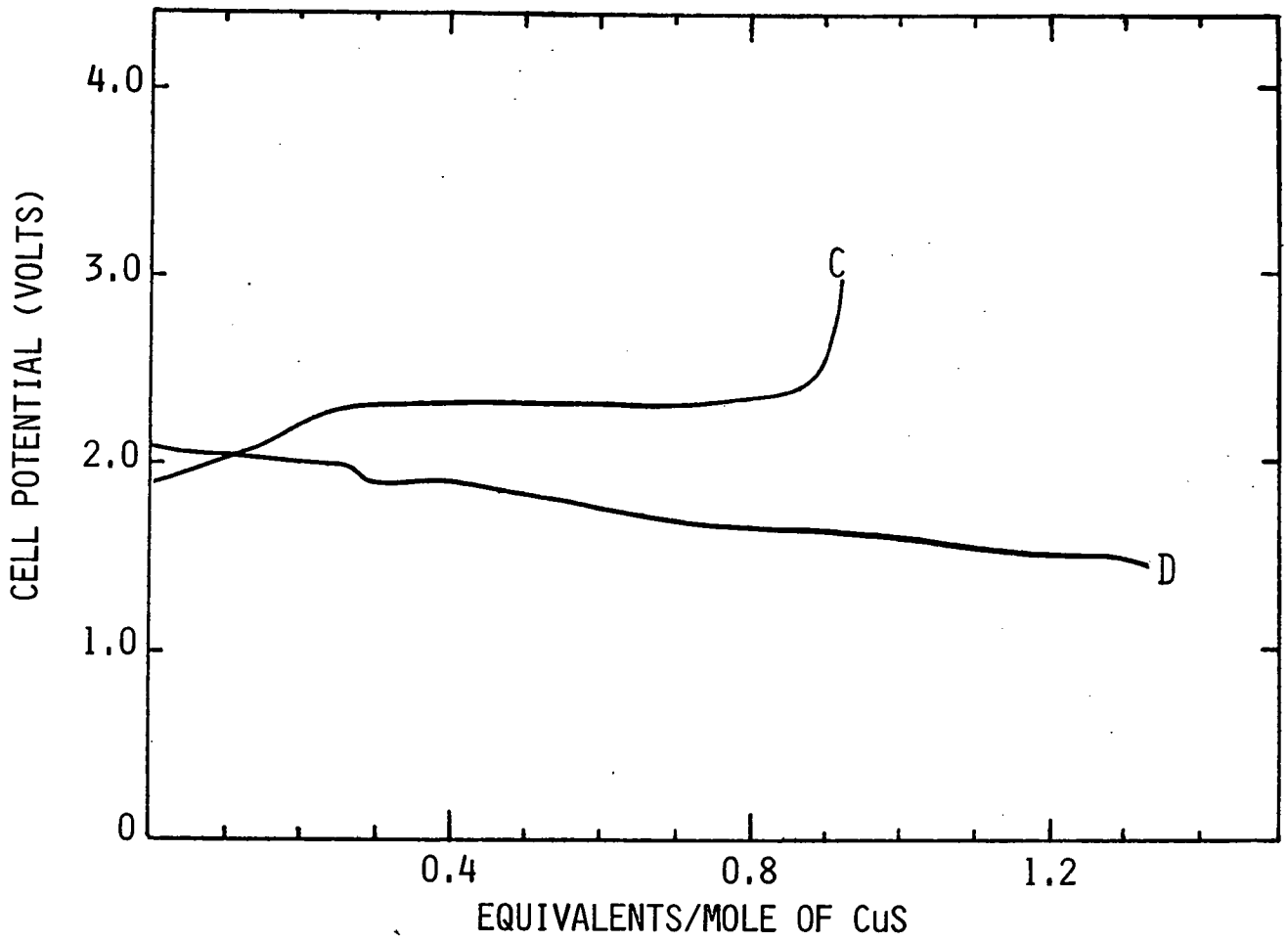

Fig. 33: Charge and discharge curves for the first cycles of Li/CuS Cell No. 2.

TABLE 15

Ah EFFICIENCIES DURING CYCLING OF
Li/CuS AND Li/NiS CELLS*

Cycle No.	CuS Ah Efficiency (%)	NiS Ah Efficiency (%)
1	138	123
2	-	110
3	140	111
4	119	119
5	107	114
6	106	117
7	103	118
10	92	112
20	101	144
30	90	110
40	104	142

*CuS efficiencies for Cell No. 2.

To determine the extent of electrolyte reduction at CuS and Shawinigan carbon black, Teflon-bonded electrodes made of each of these materials were discharged to 0.10V vs. Li. The discharge curves are compared in Figure 32. On carbon, ∿11 mAh/cm^2 discharge capacity is obtained below 1.5V, derived from the electrolyte alone. On the CuS electrode, 2.0 eq/mole are passed down to 1.33V. Beyond that, an additional ∿20 mAh/cm^2 of electrode is passed, double that on the carbon. Since a greater capacity would be expected at the carbon black electrode with its high surface area and capacity, it seems likely that CuS may be a catalyst for reduction of the solvent or supporting electrolyte. The discharge products on the CuS may shorten its cycle life, as intermittent rinsing of the CuS with fresh THF appears to revive its capacity after the latter had been allowed to deteriorate by extended cycling. Further investigation is required to determine whether additional solvent purification (e.g., preelectrolysis on C electrodes) or use of a different supporting electrolyte or solvent can lead to an extended cycle life for CuS.

The other major factor reducing cycle life of the Li-CuS cell is deterioration of the Li electrode. The Li electrodes removed from Li-CuS, Cell No. 2, after 41 cycles were found to be shiny except for the part opposite the CuS positive which was dark brown. Although the Li in this dark area opposite the CuS electrode was heavily corroded, when the surface film was scratched away it was found that considerable Li remained and the 0.38 mm thick Li foil was in no place eaten through to the Exmet

grid. Since a total of approximately 630 coul/cm^2 of Li would have been anodically dissolved during the 41 cycles, even if the 0.38 mm thick layer of Li foil had been consumed down to the grid on both Li electrodes (i.e., 284 coul/cm^2 each), 346 coul/cm^2 of Li would have been plated. Thus the average cycling efficiency of the Li electrode during the 41 cycles was greater than 50%. The brown film on the Li electrode was analyzed (ir, flame tests, m.p.) and found to be similar to the $Li_{1.2}F_{1.2}As_{0.66}O_{1.1}$ polymer reported by Koch (18,19).

Despite the decrease in capacity of the CuS electrode with extended cycling in the THF/1M $LiAsF_6$ electrolyte, it is instructive to compare its performance with TiS_2, the most actively studied cathode for Li secondary batteries. A Li/TiS_2 battery discharges at 2.0 to 2.1V at moderate rates. At EIC, Holleck and Driscoll (12) have demonstrated over 360 cycles of such a cathode. With a light loading (4.2 mAh/cm^2), the initial discharge gave 75% utilization, based on 1 e^-/mole. By cycle 339, this utilization was 25%. Whittingham has, however, determined the ultimate chemical reversibility of TiS_2 (20,21). Declines of utilization with cycle can probably be attributed to changes in the physical structure of the cathode rather than to TiS_2 chemistry. Despite the attention paid to TiS_2, it is remarkable no real data on capacity vs. cycle for practical loadings have appeared besides ref. (12).

In Figure 31, we have also plotted the TiS_2 cycling data from ref. (12) on the graph of CuS capacity vs. cycle. The CuS loading in these experiments is ∿2X the TiS_2 loading. Despite this difference, the CuS compares very favorably with TiS_2 under equivalent conditions. In addition, although CuS has a somewhat lower discharge voltage than TiS_2 (1.7V), CuS has a slightly higher gravimetric density. In addition, it has a very considerable economic advantage over TiS_2. These comparisons are summarized in Table 16.

2. CuS Discharge and Cycling Mechanism

The CuS discharge curves exhibit two plateaus, at ∿2.0V and 1.7V; the OCV also shows two plateaus (Figure 34), with approximately 0.5 e^-/mole being consumed at each voltage. From Figure 34, it is also evident that the cathode resistance is higher during the second half of discharge. These results indicate that the two plateaus are chemical in origin, rather than resulting solely from physical changes in the electrode structure.

There is considerable ambiguity in the literature regarding the mechanism of CuS electroreduction. A commonly held mechanism for the discharge of CuS is:

$$\text{Plateau \#1:} \quad 2CuS + 2e^- \rightarrow Cu_2S + S^{-2}$$

$$\text{Plateau \#2:} \quad Cu_2S + 2e^- \rightarrow 2Cu + S^{-2}$$

TABLE 16

COMPARISON OF PROPERTIES OF TiS_2 AND CuS AS CATHODE MATERIALS

	TiS_2	CuS
Molecular Weight	112.03	95.61
Density	3.2 g/cm^3	4.6 g/cm^3
Discharge Voltage vs. Li (1 mA/cm^2)	2.0	1.7
Utilization (1 mA/cm^2)	0.6-0.8[a]	0.8[b]
Weight Energy Density	0.28-0.37 Wh/g	0.38 Wh/g
Volume Energy Density	0.9-1.2 Wh/cm^3	1.7 Wh/cm^3
Unit Cost, from elements	\$3.084/eq[c] to \$0.154/eq[d]	\$0.086 eq[c]

[a] Extensively developed.
[b] As yet unoptimized.
[c] Calculated from costs of elements (Ti metal @ \$28/lb).
[d] Calculated from $TiCl_4$ as Ti source.

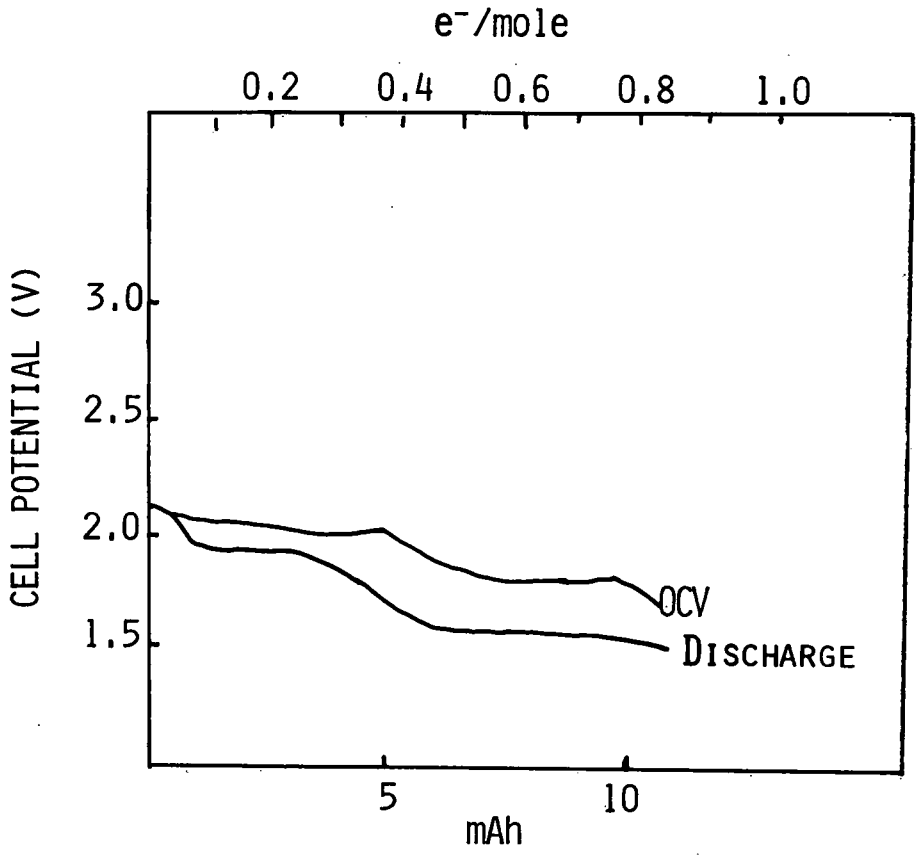

Fig. 34: Comparison of open circuit voltage with discharge curve of Li/CuS Cell No. 5E. Rate = 0.5 mA/cm^2.

However, Eichinger and Fritz (22) observe the second plateau in DMF, but not in PC, and assign it to solvent reduction on high surface area Cu formed during CuS reduction. We also observe the second plateau in THF/$LiAsF_6$ at 1.7V, while solvent reduction on high surface area carbon is not observed above 1.40-1.45V. In this solvent, a transition between the 1.7V plateau and the region of solvent reduction is also quite distinct at low discharge rates. Finally, the 1.7V plateau appears to be quite reversible, as our cycling studies of the CuS electrode demonstrate. For these reasons, we feel that the second discharge plateau originates from the cathode and not from the electrolyte, at least down to ∿1.5V.

The first four charge and discharge curves for a Li/CuS cell are shown in Figure 35. It is evident that the first discharge plateau decreases relative to the second during these cycles. The charge curves also have at least two plateaus, the higher voltage component also increasing (on a relative scale) with each successive cycle. The total capacities, however, remain at 0.9-1.0 e^-/S, despite the changes in the shapes of the curves. Finally, the fourth discharge was allowed to proceed down to 0.4V, and an additional 1 e^-/mole was passed. However, the subsequent charge yielded only the original 1 e^-/mole, indicating that the second e^-/mole was irreversible (e.g., electrolyte reduction).

Several additional new pieces of information need further resolution. First, "chemically discharged" CuS was prepared by reacting it with N-BuLi. One mole of CuS consumed 1.98 eq. of n-BuLi. The black product, "$Li_{1.98}CuS$" was incorporated into a cell and charged at 0.5 mA/cm^2. It accepted 0.9 e^-/mole, at ∿2.6V, and reached a sharp voltage cutoff. However, the subsequent discharge was of ∿0.1 e^-/mole capacity, and the recharge capacity was even less.

A portion of the "$Li_{1.98}CuS$" was reoxidized by reacting it with I_2 in THF, with the following stoichiometry following a three day reaction period:

$$Li_{1.98}CuS + 0.72I_2 \rightarrow 1.44LiI + Li_{0.54}CuS \qquad (3)$$

This material showed only ∿0.2 e^-/mole discharge capacity and cycled at <0.1 e^-/mole thereafter.

Reagent grade Cu_2S showed two poorly resolved discharge plateaus, with a capacity of 0.3-0.4 e^-/mole, and exhibited poor recharge and subsequent cycling capacity.

3. Nickel Sulfide

The capacity change as a function of cycle number for the Li-NiS cell using a $LiAsF_6$/THF electrode is compared in Figure 36 with results for the Li-CuS cell. The Li-CuS cell is clearly far superior both in terms of cycle life and capacity. The NiS cell described in Figure 36

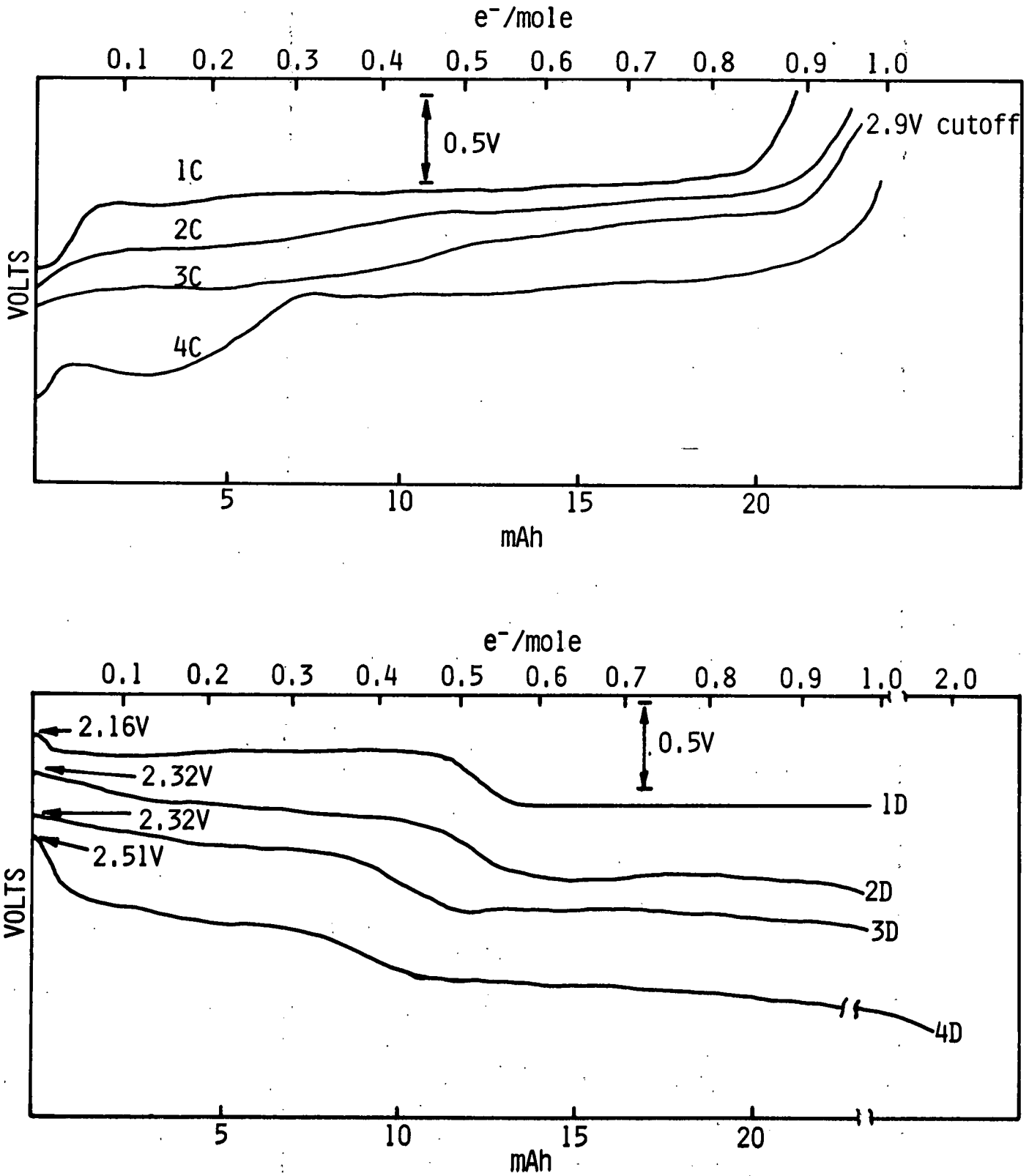

Fig. 35: Charge and discharge curves of Li/CuS Cell No. 3E, $i_d = i_c = 0.5$ mA/cm^2.

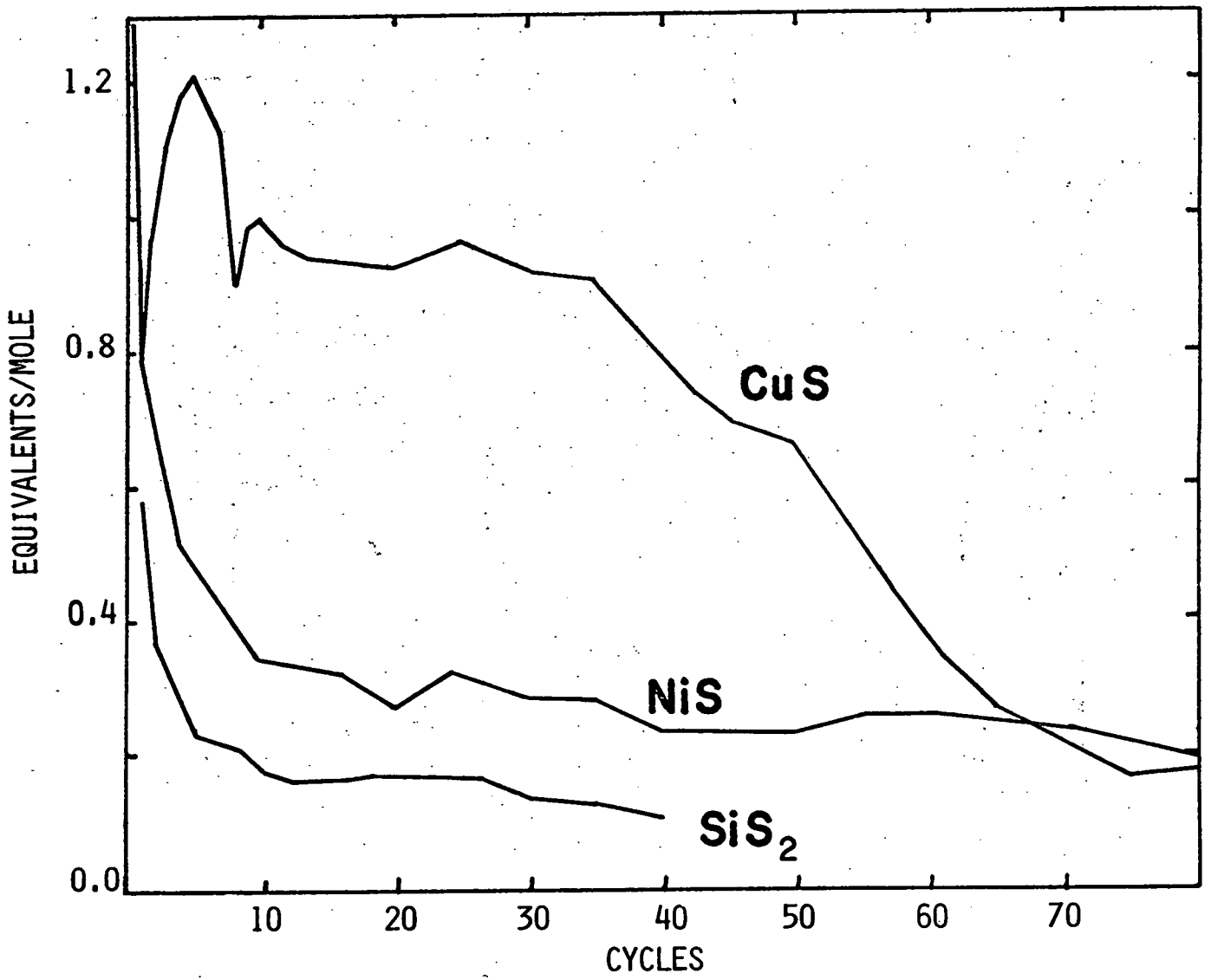

Fig. 36: Comparison of the cycling performance of Li cells with CuS, NiS and SiS_2 positive electrodes. Cycled at 1.0 mA/cm^2.

used a Teflon-bonded electrode (1.1 mm thick) containing 30% NiS and 70% carbon black with a nominal capacity of 6.1 mAh/cm^2 calculated on the basis of 1.0 eq/mole utilization. Pressed powder NiS electrodes (41 mAh/cm^2) were also tested but they cycled poorly, the utilization dropping below 0.2 eq/mole by the eighth discharge.

Similar to TiS_2, NiS gives a high utilization on the first discharge but fails to accept sufficient charge to duplicate the discharge performance during the second and following cycles. Since the discharge curve for the Li-NiS cell shows a single long plateau at ∿1.6V at 1 mA/cm^2 (see Figure 37), the capacity is highly dependent on the value of the discharge cutoff potential. Thus when a Li-NiS cell was discharged to a 1.04V cutoff, a capacity of 2.0 eq/mole was obtained, part of which was probably due to reduction of the electrolyte towards the end of discharge. Another indication of electrolyte reduction, as described earlier for CuS, are Ah efficiencies greater than 100%. A comparison of the Ah efficiencies for NiS and CuS in Table 17 shows that the Ah efficiencies are somewhat smaller for NiS but they remain well above 100% much longer than CuS where they stabilize near 100% after about 10 cycles.

TABLE 17

SPECIFIC ENERGIES ACHIEVED FOR VARIOUS INSOLUBLE SULFIDES AS POSITIVE ELECTRODES FOR RECHARGEABLE LITHIUM BATTERIES*

Positive Electrode Material	Mid Discharge Potential	Whr/lb Achieved at Cycle Number				
		1	4	10	20	30
CuS	1.70	288	348	235	211	164
NiS	1.62	299	110	74	61	61
SiS_2	1.12	86	41	27	24	21
MnS_2	1.85	2	-	-	-	-
FeS	1.86	46	-	-	-	-
TiS_2	2.13	210	175	-	-	-
Bi_2S_3	1.60	138	50	-	-	-

*The specific energies were calculated using only the weight of the positive electrode active material omitting the weight of the Li, grids and hardware.

Charge-discharge curves typical for the Li-NiS cell at 1.0 mA/cm^2 are shown in Figure 37. The discharge curve for NiS has only a single plateau which would be expected since Ni(I) has no appreciable degree of stability. However, the potential fails to show a sharp upturn indicating the end of charge, even for cells charged to 3.80V.

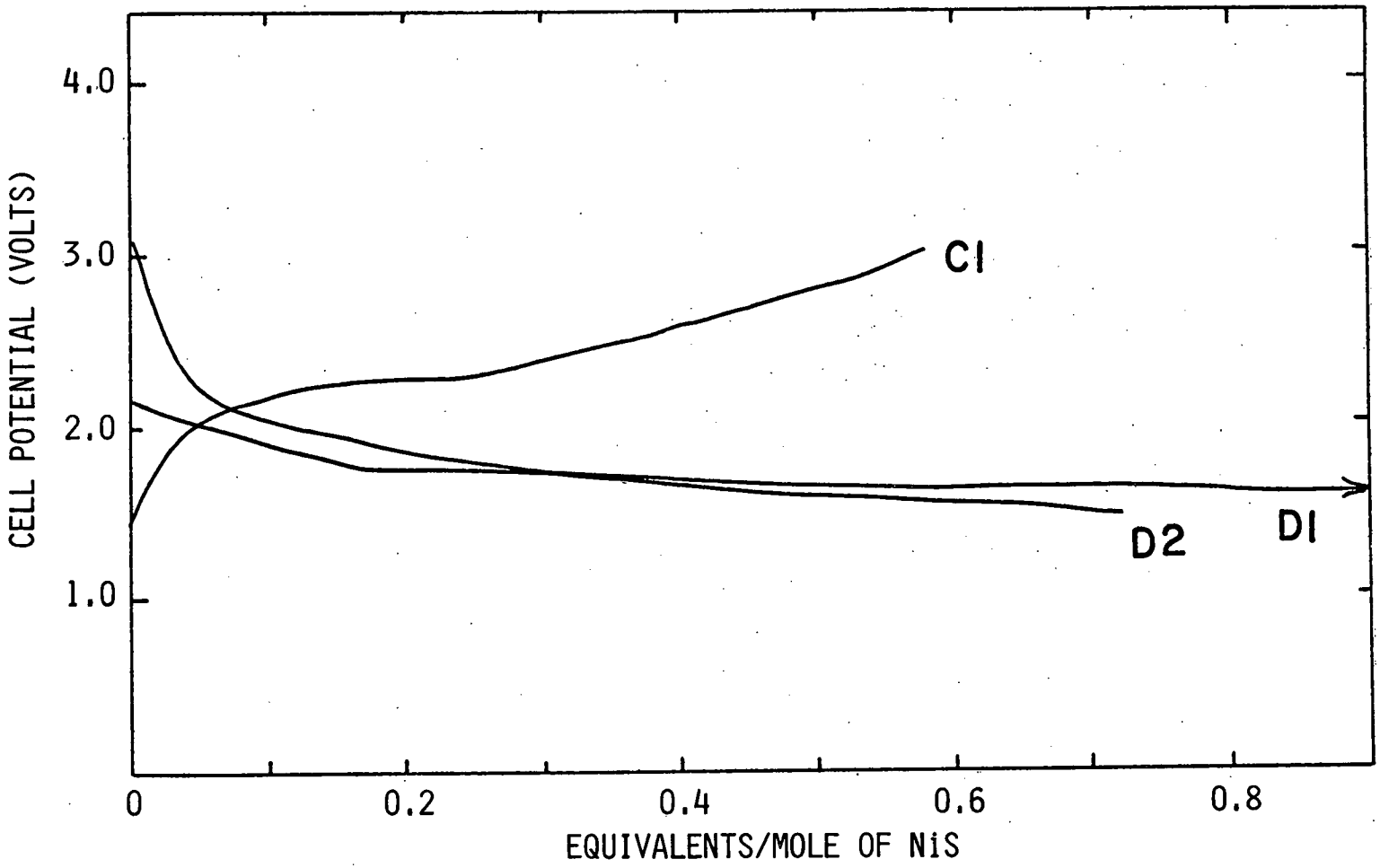

Fig. 37: Charge and discharge curves for the Li/NiS cell. Cycling carried out at 1.0 mA/cm^2, between voltage limits of 1.4 and 3.0V.

Since the NiS used in the present work was synthesized in our laboratory, it is noteworthy that our NiS cells considerably outperformed the cells described by Jasinski (2) [e.g., 1.28 compared to 0.49 eq/mole to a 1.5V cutoff]. Although the superior performance of our cells can be partially attributed to the use of $LiAsF_6$/THF which is much more conductive and less viscous than $LiClO_4$/PC, the potentials reported by Jasinski were for half-cells and measured with a Li^+/Li reference electrode.

4. Silicon Disulfide

The cycling performance for the Li-SiS_2 cell using a $LiAsF_6$/THF electrolyte is shown in Figure 35. Compared to CuS which gives almost ten times the capacity after ten cycles, the SiS_2 electrode is of marginal interest for practical batteries. The SiS_2 electrodes used in this study were of the pressed powder type (0.9 mm thick) described earlier and were 40% SiS_2, 54% graphite and 6% polyethylene. Pressed powder SiS_2 electrodes were used because the preparation of Teflon-bonded electrodes involves the use of a water paste and SiS_2 hydrolyzes very rapidly to form H_2S and SiO_2.

The Ah efficiencies calculated for the Li-SiS_2 cell described in Figure 35 were all less than 100%. Thus, SiS_2 does not appear to act as a catalyst for the reduction of the $LiAsF_6$/THF electrolyte even down to a 1.0V discharge cutoff. The reversible behavior of the SiS_2 electrode may possibly be due to intercalation of Li since it is known to have a layer structure (23).

Typical charge-discharge curves for the Li-SiS_2 cell are shown in Figure 38. The peculiar peak in the first charge curve at 0.22 eq/mole remains well defined for the first 15 cycles after which it weakens until it disappears after 30 cycles. From observations of the SiS_2 as it was received from the manufacturer in large lumps, it was evident that it was a heterogeneous mixture about 90% SiS_2 and 10% impurities. Thus the plateaus in the charge-discharge curves are probably due to the heterogeneous nature of the active material.

5. Manganese Disulfide

The MnS_2 which was synthesized was evaluated using pressed powder electrodes (45.2% MnS_2, 50.1% graphite, 4.6% polyethylene) to avoid the possibility of MnS_2 decomposition if a Teflon-bonded construction was used. The open circuit voltage of the Li-MnS_2 cell was 3.29V immediately after it was assembled. However, when a Li-MnS_2 cell was discharged at 1.0 mA/cm^2 the potential dropped to 2.35V within 30 seconds, and to 1.45V after 5 minutes. On recharge, the potential rose to the 4.00V charge limit within 4 minutes of 1 mA/cm^2. The second discharge was no better than the first, the potential dropping to 1.57V after 3 minutes. The capacity of the MnS_2 electrode tested was 13 mAh/cm^2 based on a 1.0 eq/mole

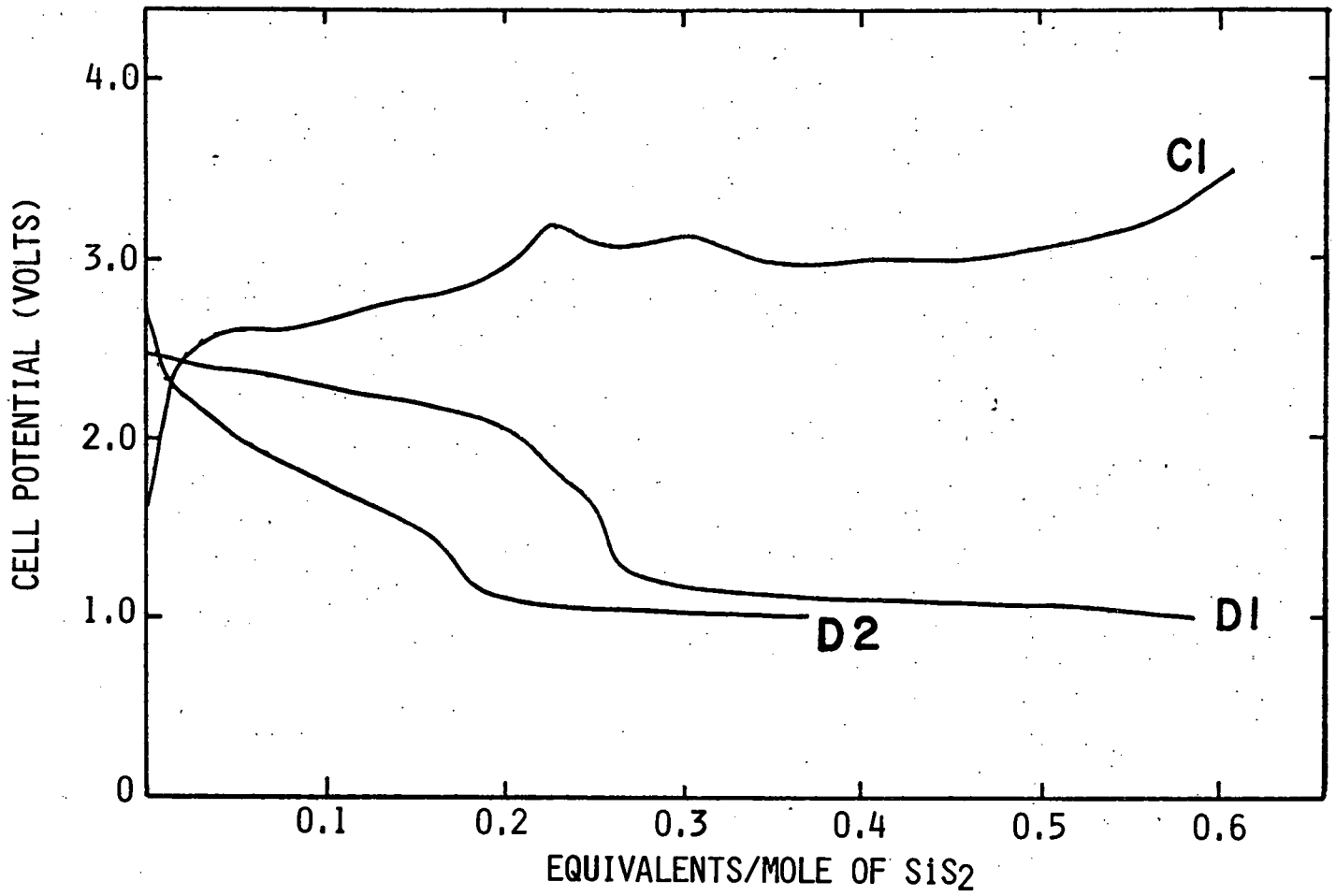

Fig. 38: Charge and discharge curves for the Li/SiS_2 cell. Cycled at i_d = 1.0 mA/cm^2, i_c = 0.75 mA/cm^2. Voltage limits were 1.0 and 3.8V.

utilization. Thus, the first discharge amounted to a utilization of only 0.013 eq/mole which means that MnS_2 is for all practical purposes electrochemically inert.

6. Ferrous Sulfide

When a Li-FeS cell was discharged at 1.0 mA/cm^2, the potential fell from the 3.16V OCV to 1.47V in 18 minutes. On recharge at 1.0 mA/cm^2, the potential rose to the 2.90V limit within less than 2 minutes. The capacity of the Teflon-bonded FeS electrode was 3.4 mAh/cm^2 based on a 1.0 eq/mole utilization. Thus the first discharge yielded only 0.18 eq/mole to a 1.45V voltage limit which indicates that FeS is not a practical electrode material for Li batteries. Even when the current density was lowered to 0.10 mA/cm^2 after two cycles, the utilization for the third cycle was still only 0.12 eq/mole.

These results for the FeS electrode are of some interest because they demonstrate that even at 0.1 mA/cm^2 negligible reduction of the $LiAsF_6$/THF electrolyte occurs down to 1.45V and little capacity can be obtained by cycling just the electrolyte.

7. Bi_2S_3

Bi_2S_3 has been reported recently as a cathode for ambient temperature Li batteries (24). It has been reported that the discharge reaction can involve up to 6 electrons/Bi, with the following stoichiometry:

$$12Li + Bi_2S_3 \rightarrow 2Li_3Bi + 3Li_2S \qquad (4)$$

These workers report that $Bi^{+3} + 3e^- \rightarrow Bi^\circ$ is readily reversible, while $Bi^\circ + 3e^- \rightarrow Bi^{-3}$ is not.

We have prepared cells containing Bi_2S_3 and the following observations can be made (Figure 39). The cell discharge curve is sloping between 2.5 and 1.5V. The lower discharge limit was set at 1.4V and it seems that even lower voltages are attainable, although at these lower voltages, solvent decomposition may occur. At a 1.4V limit, 3.5 e^-/mole are transferred. On charging, the efficiency is around 100%. In the present cathode configuration, the cell gradually fails on cycling, $\sim$1 e^-/mole becoming irreversible on each cycle. Further work is necessary to ascertain whether these phenomena are physical or chemical.

From a practical standpoint, it will be necessary to have high electron yields due to the high (514.14 g/mole) molecular weight of Bi_2S_3. For cells tested, the energy density is 304.54 Whr/kg based on 3.5 e^-/mole. This is somewhat less than the energy density for TiS_2 (449.51 Whr/kg) based on 1 e^-/mole.

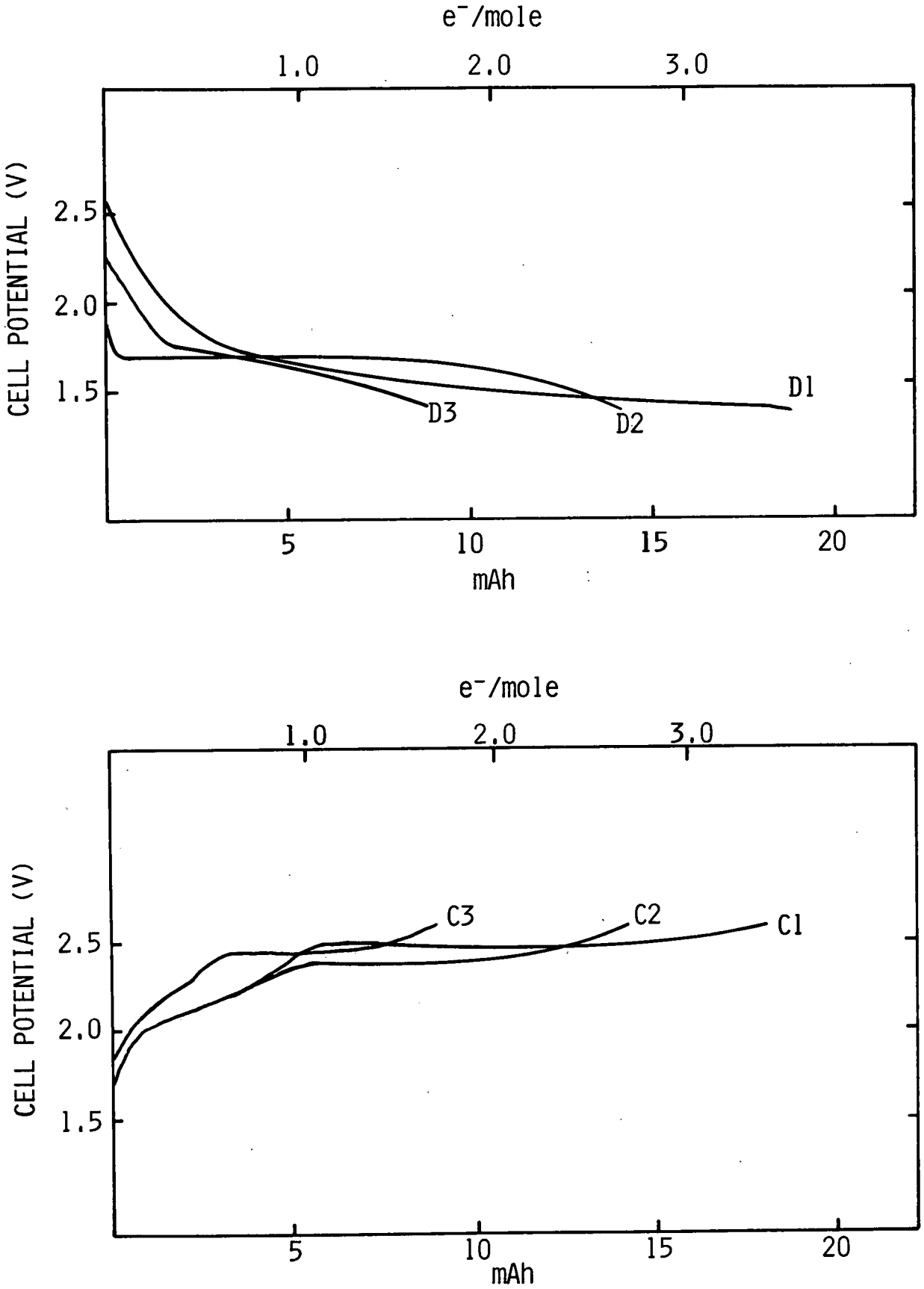

Fig. 39: Cycling curves of Li/Bi_2S_3 Cell No. 2F, $i_d = i_c = 0.5$ mA/cm^2,

8. Conclusions

The practical energy densities obtained for the seven sulfides covered in this study are compared in Table 17. Based only on the weight of active cathode materials, cells of 200-300 Whr/lb were cycled effectively with CuS as the cathode, the results comparing favorably with TiS_2. The lower molecular weight of CuS compared to TiS_2 makes up for the former's lower discharge potential. The complexity of the CuS crystal structure leaves the charge-discharge mechanism open to question. Possibly the method of preparation of the "CuS" could yield material of varying crystal structure and hence with different long range cycling behavior. The economy of CuS makes it a definite candidate for further investigation.

The remaining sulfides were marginal in their behavior as rechargeable cathodes. Only NiS and Bi_2S_3 show some possibilities as cathodes for primary cells, although their voltage is quite low.

REFERENCES

1. J. P. Gabano, V. Dechenaux, G. Gerbier and J. Jammet, J. Electrochem. Soc., 119, 459 (1972).

2. R. Jasinski and B. Burrows, J. Electrochem. Soc., 116, 442 (1969).

3. J. P. Gabano, G. Gerbier and J. F. Laurent, Proc. 23rd Power Sources Symposium, Atlantic City, N.J., 1969, PCS Publication Committee, Red Bank, N.J., p. 80.

4. D. Hebert and J. Ulam, U.S. Patent 3,043,896 (1962).

5. G. Eichinger and H. P. Fritz, Electrochimica Acta, 20, 753 (1975).

6. M. R. Kegelman, U.S. Patent 3,847,674 (1974).

7. F. W. Dampier, J. Electrochem. Soc., 121, 656 (1974).

8. M. S. Whittingham, J. Electrochem. Soc., 123, 315 (1976).

9. L. G. Berry, Am. Min., 39, 504 (1954).

10. J. G. Gibson and J. L. Sudworth, Specific Energies of Galvanic Reactors (London: Chapman and Hall Ltd., 1973).

11. D. W. Murphy and F. A. Trumbore, J. Cryst. Growth, 39, 185 (1977).

12. G. L. Holleck and J. R. Driscoll, Electrochimica Acta, 22, 647 (1977).

13. J. R. Driscoll, G. L. Holleck, D. E. Toland and S. B. Brummer, Eleventh Quarterly Report, U.S. Army ECOM-74-0030-11, October 1976.

14. W. Biltz and F. Wiechmann, Z. Anorg. Allg. Chem., 228, 268 (1936).

15. W. W. Harvey, J. L. Schad and P. H. Yu, Interim Status Report, Contract No. E(11-1)-2730, U.S. Energy Research and Development Administration, December 1975.

16. R. T. Savey in Semiconducting Ore Minerals (London: Elsevier, 1975), Chapter 12.

17. S. B. Brummer, F. W. Dampier, V. R. Koch, R. D. Rauh, T. F. Reise and J. H. Young, Final Report, NSF Grant AER75-03779, January 1978.

18. V. R. Koch, J. Electrochem. Soc., 126, 181 (1979).

19. V. R. Koch and J. H. Young, Abstract No. 5, Fall Meeting of The Electrochemical Society, Atlanta, GA, 1977.

20. M. S. Whittingham, Prog. Sol. State Chem., 12, 1 (1978).

21. M. S. Whittingham, Science, 192, 1126 (1976).

22. G. Eichinger and H. P. Fritz, Electrochimica Acta, 20, 753 (1975).

23. Gmelins Handbuch, System No. 15, Part B, p. 750, Verlag Chemie, Weirheim, 1959.

24. J. O. Besenhard, Z. Naturforsch, 33b, 279 (1978).

IV. SUMMARY AND CONCLUSION

Research has been carried out on this program on the development of rechargeable, ambient temperature Li/(dissolved) Li_2S_n and Li/metal sulfide batteries. In the former system, the variables of capacity, discharge rate, system stability and rechargeability have been explored. In the Li/metal sulfide system, several potentially economical simple sulfides have been tested for their discharge and rechargeability behavior, with particular emphasis paid to CuS. The salient results are summarized below.

- Li/Li_2S_n Rate-Capacity Behavior. Key to achieving high energy densities in this battery is the development of electrolytes containing >4M dissolved S, and achieving a 1.0-1.5 e^-/S utilization on discharge. A study of Li_2S_n solubility resulted in our specification of THF as the best compromise solvent. Capacity-rate studies on test cells containing a THF, 1M $LiAsF_6$, dissolved Li_2S_n electrolyte allowed us to formulate a mechanism of rate limitation.

Capacities were measured as a function of rate and S concentration. All evidence points to cell polarization being a result of Li_2S precipitation on the current collector. The thickness of the Li_2S layer is a function of the discharge current - presumably due to ohmic drop through the thickness of the carbon electrode. Improved rates were therefore obtained by decreasing the thickness of the current collector and increasing the ratio of its area to the solution volume. The results indicate that utilization of 1.0-1.5 e^-/S should be obtainable at 50°C for the discharge of ∿5M S solutions in cells with an A/V ratio of 15. This corresponds to our rate-capacity goal for this battery (>50% utilization at C/3) in its proposed design for vehicle or load-leveling applications.

Even better rates may be obtained with the appropriate catalyst. Lewis acids, such as Ba^{+2} and ϕ_3B, can evidently complex S_n^{-2}. Such complexes display enhanced reduction rates in dilute solutions. Barium ion also increases the discharge rates in full cells, although it has not been tried yet in the high A/V cell configurations. Triphenylboron gives capacities which are better than the baseline cell at high rates. At low rates, it seems to prematurely passivate the electrode by precipitation, probably of salts like $[(\phi_3B)_3S]^{-2}$ $2Li^+$, of high molar volume. Lower molecular weight Lewis acids may well give better results.

- Li/Li_2S_n Rechargeability. For the baseline Li/Li_2S_n cell, 135 cycles of 0.1 e^-/S and ∿45 cycles of 0.5 e^-/S have been demonstrated. At the higher capacities, cell failure is characterized by a rapid decline

in cycling efficiency and eventual polarization during the charging half cycle. This decline occurred both with Li and Li-Al alloy anodes. This failure is not due to specific failure of the Li electrode of the current collector, as they perform well in the construction of otherwise fresh cells. It appears that the active cathode material migrates from the cathode compartment and becomes isolated on the anode as Li_2S, due to cumulative self-discharge. Analyses of products on spent anodes and of the sulfur distribution in failed cells supports this conclusion.

Experiments with limited-Li anodes revealed that the cell cycling efficiency is identical to the anode efficiency, at least in the symmetrical cycling regime. This means that no electrodeposited Li becomes lost through electrical isolation, as in the inert electrolyte case. Instead, all of the anode inefficiency is ascribed to self-discharge, a process which maintains the materials balance within the cell. This is a major positive feature of the Li/Li_2S_n cell, as only stoichiometric amounts of Li may be required in its construction, rather than the large excess needed if some Li is totally lost during each cycle.

Two general approaches have been followed to extend the cycle life of Li dissolved Li_2S_n cells. The first approach is to decrease the self-discharge rate (SDR). Some success was noted by prefilming the anodes with LiCl, by treating them with $SOCl_2$. Impregnating the current collectors with Li_2S also had a positive effect, perhaps by controlling the nature of the S_n^{-2} species diffusing to the anode.

The second approach is to enhance the solubility of Li_2S in THF. This has been attempted by complexing the Li_2S with Lewis acid such as $B(OAc)_3$, BBr_3 and $SiCl_4$. Although these materials appeared to solubilize Li_2S, it was determined that they actually became reduced. Another way to solubilize Li_2S is via a redox scavenger produced during overcharge. This has been attempted with I_2, ferricinium, chloranil, Br_2, with only limited success. To date, the oxidant appears to react preferentially with the Li, if at all. Not all avenues have been pursued, however, in achieving Li_2S solubilization. This could provide fertile ground for further research.

Alternative cell configurations are also being considered. These include the Li/partially soluble polysulfide battery, for which preliminary results were presented in previous progress reports. In addition, methods of immobilizing the S within the carbon structurative are being sought, such as by functionalizing the carbon with S-interactive groups, or by chemically bonding the S to it.

• Li/Metal Sulfide Cells. The discharge and rechargeability of the following metal sulfides were examined: CuS, NiS, SiS_2, MnS_2, FeS, and Bi_2S_3. Of these, the most promising new material in terms of energy density and rechargeability is CuS. A typical Li/CuS cell with a cathode

loading of 8.5 mA/cm^2 averaged well over 0.8 eq/mole over the first 100 cycles, dropping to ∿0.25 eq/mole over the course of ∿300 cycles. The reason for this decline is not yet understood, but is probably associated with deficiencies in the as yet unoptimized electrode structure. CuS compares favorably with TiS_2 in terms of energy density and rechargeability, and is superior in terms of economics.

APPENDIX A

PUBLICATIONS AND PRESENTATIONS

R. D. Rauh, J. M. Marston and S. B. Brummer, "Electrochemistry of Sulfur in Organic Solvents," Fall Meeting of The Electrochemical Society, Dallas, 1975.

R. D. Rauh, F. S. Shuker, J. M. Marston and S. B. Brummer, "The Li/Dissolved S Secondary Battery," Spring Meeting of The Electrochemical Society, Washington, D.C., 1976.

R. D. Rauh, G. F. Pearson and S. B. Brummer, "Capacity, Rate Capabilities and Rechargeability of a Li/Dissolved S Secondary Battery" in Symposium on Electrode Materials and Processes for Energy Conversion and Storage, The Electrochemical Society, 1977.

K. M. Abraham, S. B. Brummer and R. D. Rauh, "A Novel Na/S Battery Using a Soluble S Cathode," ibid.

R. D. Rauh, F. S. Shuker, J. M. Marston and S. B. Brummer, "Formation of Lithium Polysulfides in Aprotic Media," J. Inorg. Nuc. Chem., 39, 1761 (1977).

R. D. Rauh, G. F. Pearson and S. B. Brummer, "Rechargeability Studies of Ambient Temperature Lithium/Sulfur Batteries," Proc. 12th IECEC, Washington, D.C. Aug. 28 to Sept. 2, 1977.

K. M. Abraham and R. D. Rauh, "Studies of Polysulfide Coordination and Electrochemistry in Non-aqueous Solvents," Fall Meeting of The Electrochemical Society, Atlanta, 1977.

K. M. Abraham, R. D. Rauh and S. B. Brummer, "A Low Temperature Na/S Battery Incorporating a Soluble S Cathode," Electrochim. Acta, 23, 501 (1978).

R. D. Rauh, K. M. Abraham, G. F. Pearson, J. K. Surprenant and S. B. Brummer, "A Lithium/Dissolved Sulfur Secondary Battery with an Organic Electrolyte," J. Electrochem. Soc., 126, 523 (1979).

APPENDIX B

SYSTEM CONSIDERATIONS

In this appendix, we consider the practical energy and power densities which can be achieved with a Li battery having a dissolved Li_2S_n positive. The basis for these calculations is the Li/$SOCl_2$ high rate D-cell, for which considerable design work has been published (1-5). Such design involves the basic requirements for high-rate, high-capacity construction and can readily be generalized to ambient temperature Li batteries using other positives.

Design characteristics of a spiral wound Li D-cell, as presented by Dey (3-6), are shown in Table B-1. Both the Li anode and the Teflon-bonded C cathode (∿80% porosity) are supported on expanded Ni mesh. Separators are composed of 5 mil fiberglass paper. The total weight of such a cell filled with 29 cm^3 of $SOCl_2$-based catholyte (ρ = 1.6 g/cm^3) is 105g. A substantial fraction of this weight is that of the Ni container (41g).

A dissolved Li_2S_n battery can make use of the same basic battery structure. Parameters for such a D-cell are given in Table B-2. The catholyte is 6M S (as Li_2S_n) THF, 1M $LiAsF_6$. We have measured the density of this solution to be 1.1 g/cm^3 at 50°C, the normal operating temperature for the cell. Thus, the weight of the electrolyte is 31.9g, compared to 48.9g for $SOCl_2$ electrolyte. The resulting weight of the Li/Li_2S_n D-cell is 88g.

The capacity of the Li_2S_n cathode is known from our previous work on this system (7). Reduction stoichiometries approaching 1.5 e^-/S at 4 mA/cm^2 are observed at a discharge voltage of 2.0V. The corresponding D-cell capacity is 7.0 Ah. The energy density expected for such a D-cell is therefore 72 Whr/lb or 159 Whr/kg. Since the active Li area is 452 cm^2 (Table B-1), the 1-hr C rate for this battery is 15.4 mA/cm^2. The 4 mA/cm^2 discharge rate corresponds then to approximately the 4-hr rate. The ohmic loss at this current density is ∿75 mV, i.e., 3-5% of the output.

As the size of a module increases, so does the practical energy density, since the weight of the container becomes a smaller fraction of the total. Therefore, the energy densities of the Li/Li_2S_n system <u>without</u> the container is also included in Table B-2. Thus, as the cell capacity increases, the energy density of the Li/Li_2S_n cell approaches 135 Whr/lb (298 Whr/kg). For a 1 kWh module, the practical energy densities would be considerably closer to these limits than to those of the D-cells.

TABLE B-1

PARAMETERS FOR $Li/SOCl_2$ D-CELLS

Electrical (10,43)

Open circuit	3.66V
Discharge potential at 2.5 mA/cm^2	∿3V
Capacity at 2.5 mA/cm^2 (≡ C/10 theoretical)*	∿10-15 Ah
Utilization at 2.5 mA/cm^2 (≡ C/10 theoretical)	∿50%-75%
Energy density at 2.5 mA/cm^2 (≡ C/10 theoretical)	∿130-190 Whr/lb

Dimensions

Li - dimension	50.8 x 4.45 x 0.04 cm
- active area	452 cm^2
- volume	9.0 cm^3
Cathode - dimensions	50.8 x 4.45 x 0.04 cm
- volume	10.9 cm^3
- pore volume	8-9 cm^3
- carbon volume	2-3 cm^3
Electrolyte - volume	29 cm^3

Weights

Li	4.8 g
Carbon	5.8 g
Electrolyte	48.9 g
Separator	5.0 g
Can	41.0 g
Total	∿105.0 g

*Theoretical is $2e^-/SOCl_2$.

TABLE B-2

PARAMETERS FOR Li/Li_2S_n D-CELL

Parameters same as for $Li/SOCl_2$ cell, except:

Wt electrolyte	$29\ cm^3 \times 1.1\ g/cm^3 = 31.9g$
Cell voltage	2.0V
Cathode capacity at 1.5 e^-/S utilization	$\frac{29 \times 6 \times 96500 \times 1.5}{3600 \times 1000} = 7.00$ Ah
Cell weight	105g - [48.9 - 31.9] = 88g
Energy density	$\frac{(7.00)(2.0)}{88} \times 453 - 72$ Whr/lb (159 Whr/kg)
Energy density without can	135 Whr/lb
Li capacity	$65.1\ coul/cm^2$
Calculated C rate	$15.4\ mA/cm^2$

It can also be seen in Table B-2 that full cycles correspond to specific charges of 60-70 coul/cm^2 on the Li electrode. Thus, we must seek highly efficient cycling of the Li electrode at this level over the cycle life. With a fivefold excess of Li present initially (300-500 coul/cm^2), less than 0.3 coul/cm^2 can be lost on each cycle, i.e., 99.5% efficiency is required. Of course, lower efficiencies can be tolerated if the Li can be resolubilized by some mechanism, such as the slow self-discharge reaction which characterizes the Li/Li_2S_n cell. In principle, this cell can yield a very long cycle life without the necessity of a large excess of Li.

It should be noted that we have carried out some characterization of materials which might be considered in cell construction (8). In concentrated polysulfide/THF solutions, it was found that Inconel 600, Hastalloy B, and 316 and 446 stainless steel show a negative weight loss ($\leq$0.002%) and remain bright and shiny after being immersed in the solution for 28 days at 71°C. Under the same conditions, Ni showed severe corrosion and pitting, even when placed in contact with Li. It was concluded that 316 stainless steel should be the preferred material for use in Li-polysulfide batteries, because it is less expensive and/or more easily machined than other materials.

In summary, the Li/Li_2S_n battery looks attractive from a technical viewpoint as a candidate for load-leveling and vehicle applications. It has already demonstrated suitable energy density, and rate capability, although long run cost goals may require some improvement. It does cycle, and here improvements are required. The Li_2S_n electrode, being soluble, may well already have appropriate cycle life. However, its contact with high surface area Li may eventually limit its functioning in ways that we are beginning to understand. The understanding and control of this interaction is the key to long-term rechargeability, and constitute the main focus of this program.

REFERENCES

1. N. Marincic, J. Applied Electrochem., 6, 263 (1976).

2. N. Marincic, J. Applied Electrochem., 6, 463 (1976).

3. A. N. Dey, Electrochim. Acta, 21, 377 (1976).

4. A. N. Dey, J. Electrochem. Soc., 123, 1262 (1976).

5. A. N. Dey, Second Quarterly Report, ECOM-74-0109-2, November 1974.

6. A. N. Dey and P. Bro, Paper No. 32, 10th Intern. Power Sources Symposium, Brighton, England, September 1976.

7. S. B. Brummer, R. D. Rauh, K. M. Abraham, J. M. Marston, G. F. Pearson, F. S. Shuker and J. K. Surprenant, "Low Temperature Alkali Metal-Sulfur Batteries," Annual Progress Report for December 1, 1975 to November 30, 1976, Contract No. EY-76-C-02-2520 , June 1977.

8. F. W. Dampier and S. B. Brummer, Fall Meeting of The Electrochemical Society, Atlanta, 1977, Abstract No. 14.

APPENDIX C

RECHARGEABILITY STUDIES OF AMBIENT TEMPERATURE LITHIUM/SULFUR BATTERIES

R. D. Rauh, G. F. Pearson and S. B. Brummer

EIC Corporation, 55 Chapel Street, Newton, Mass. 02158

ABSTRACT

An ambient temperature Li/S battery of the configuration Li/Li_2S_n, organic solvent/C is described, where the cathode material is totally soluble in the electrolyte. For a practical battery, the sulfur concentration must be >5M. Despite the intimate contact between the Li anode and the cathode, the cell can be charged.

Prototype cells have been cycled at 25°C and at 50°C. Charge and discharge rates ranged from 0.5-2.0 mA/cm^2. At least 120 low capacity cycles (0.10e$^-$/S) have been demonstrated at 50°C, with an average efficiency of 95%. Higher capacity cycles are somewhat less efficient. For a cycle depth of 0.5e$^-$/S, efficiencies at 1 mA/cm^2 are 95% at 25°C and 90% at 50°C. The anode cycling efficiency is, within experimental error, the same as that of the total cell. Therefore, any Li dendrites isolated on the anode during cycling are dissolved via the self-discharge reaction. This maintains the materials balance in the cell, a major requirement for its practical success.

INTRODUCTION

A battery based on Li and S is inherently attractive because of its high theoretical energy density (~1300 Whr/lb) and because it utilizes relatively inexpensive materials. A rechargeable battery of this type operating at ambient temperature could be useful in electrical load levelling and for vehicular propulsion, as well as in a variety of smaller size applications.

Ambient temperature primary Li batteries have been developed with both soluble and insoluble cathodes [1]. Those with soluble cathodes, such as Li/SO_2 [2,3] and $Li/SOCl_2$ [4-6] have the advantage of high rate, as good electrical contact is maintained between the positive material and the current collector through all phases of discharge. Early attempts to develop primary Li/S batteries [7,10] with the insoluble S incorporated into the cathode structure have resulted in cells with low rates and/or poor utilization efficiencies, probably because both S and its discharge products are electrical insulators.* Because of these considerations, we have chosen to investigate a Li/S secondary battery in which the S is completely dissolved in an organic electrolyte, as polysulfide, Li_2S_n.

Because S is in a slightly reduced state as S_n^{-2}, there is a small sacrifice in theoretical energy density, to achieve high solubility. The cell reaction becomes

$$2\left(\frac{n}{m}-1\right)Li + S_n^{-2} \rightarrow \frac{n}{m}S_m^{-2} + 2\left(\frac{n}{m}-1\right)Li^+ \qquad (1)$$

If n = 10 and m = 1, the capacity is 1.8e$^-$/S instead of 2.0e$^-$/S for the S/S^{-2} couple. A preliminary battery design has shown that, for a 2 kWhr module, a 5.4M S solution discharged at 2.0V with a utilization of 1.5e$^-$/S is sufficient to yield a practical energy density of 100 Whr/lb.

Solubilities of >10M S as Li_2S_n (n>8) have been achieved in several basic aprotic organic solvents potentially compatible with Li [11]. Best results with regard to Li stability and S solubility have been obtained for tetrahydrofuran, THF. Even 5-10M S solutions in THF are quite stable to Li, presumably due to a passivating film formed on the metal surface. The corrosion rate via reaction (1) of Li metal foil in a 5M S solution, initially as Li_2S_8, is about 7 μA/cm^2 at 25°C and 15 μA/cm^2 at 50°C. In a practical cell, this would correspond to a self-discharge rate of 1-2% per day. In a secondary battery, moreover, any loss due to self-discharge via reaction (1) may, in principle, be regained on charge.

Discharge capacities for cells of the configuration

Li / Celgard Separator / 5M Dissolved S, THF, 1M Li^+ (Li_2S_n) / Carbon Current Collector

exceed the requisite 1.5e$^-$/S at discharge rates of 0.5 mA/cm^2 and 1.0 mA/cm^2 at 25°C and 50°C [11-13]. The discharge curve, as shown in Fig. 1, is extremely flat; ~85% of it is over the range 2.0-2.1V. Some improvements in these rates have been noted with the use of appropriate heterogeneous and homogeneous catalysts [11,13,14], and work is still in progress in this area.

The purpose of this paper is to present results on the rechargeability of the Li/dissolved S cell, and to address the factors influencing the cycling

*Rechargeability data have never been provided for any of these cells.

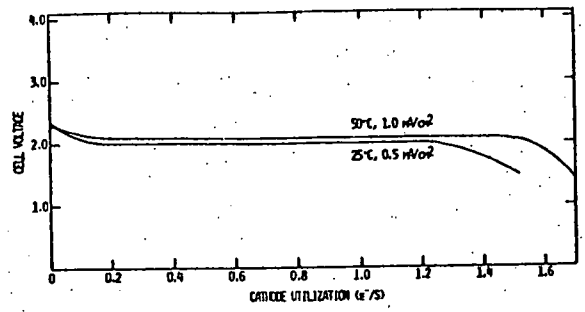

Fig. 1: Galvanostatic discharge curves for Li/$Li_2S_{12.2}$ (5.4M S), 1M $LiAsF_6$, THF/C cells at 25°C and 50°C.

efficiency and cycle life. A discussion of the rechargeability requires consideration of not only the cell as a whole, but also of the Li electrode. If a secondary Li battery is to succeed, conservation of the Li active mass during cycling is absolutely essential.

THE SULFUR ELECTRODE

The reversibility of the polysulfide electrode was first studied in dilute solutions using a 3-electrode coulometry cell. The cyclic voltammogram of 5X 10^{-3}M S_8 in THF is shown in Fig. 2. The reduction of S_8 occurs at E_{max} = 2.2V vs. Li^+/Li, and is of $2e^-$ stoichiometry. The reduction of S_n^{-2} occurs at E_{max} = 2.1V, and becomes kinetically limited with decreasing n, as is also shown in Fig. 2. Nevertheless, potentiostatic reduction of S_8 and S_n^{-2} at 2.0V on a C electrode can be carried out to very close to the Li_2S limit, albeit with increasing difficulty as the polysulfide order decreases.

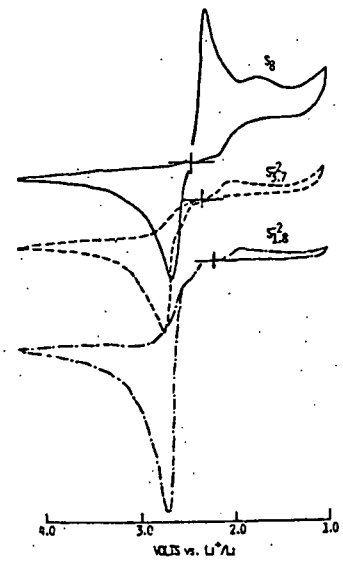

Fig. 2: Cyclic voltammograms of solutions of S8 and lower order polysulfides in THF, 1M $LiAsF_6$, on vitreous C. [S] = 0.04M. Sweep speed = 0.1V/sec, sweeping negative first.

The oxidation reaction occurs with an E_{max} = 2.7V, and its rate is probably diffusionally limited. Starting with Li_2S, potentiostatic oxidation of S^{-2} and S_n^{-2} leads to the production of high order soluble polysulfides, rather than (insoluble) S_8. This result is favorable for the development of the battery, as no precipitation is likely to take place during charge. The electrochemical production of polysulfide chains of n>50 has been observed.

The polysulfide electrode was investigated in a prototype cell configuration using a tightly packed array of electrodes separated by microporous polypropylene (Celgard 2400, Celanese Corp.). The Li electrodes were composed of 4.7 cm^2 squares of 0.015" Li foil pressed onto Ta or stainless steel Exmet supports. The current collectors were Teflon-bonded C [15] (Shawinigan, 50% compressed carbon black), also 4.7 cm^2, on similar supports. Typically, a cell was composed of 3 current collectors and 2 Li electrodes, in a configuration C/Li/C/Li/C. These were compressed into a rectangular glass vial. Exactly 2.5 ml of catholyte were pipetted into each cell.

The cells were mounted in a specially designed inert atmosphere holder, illustrated in Fig. 3. A glass dome was used to cover the cells, and an O-ring seal was made between the dome and the base. A vacuum tight Conax feedthrough was used for electrical contact through the base. The holder accepts two cells and a third container with electrolyte, to saturate the atmosphere under the dome with solvent vapor. The holders were determined to be leak free when used with THF at 50°C. Assembly was conducted inside an Ar filled dry box. After the dome was in place, however, the holder could be removed to the open atmosphere.

Open circuit potentials for these cells were typically 2.35 to 2.40V. On discharge, a rapid decrease in voltage occurs to 2.0-2.1V. The OCV is then 2.15V. Based on the studies of S_n^{-2} electrochemistry, it is most likely that the initial discharge corresponds to reduction of a small amount of S_8 suspended in solution. The majority of the discharge is ascribed to S_n^{-2} reduction, with all species apparently reducing at the same potential.

Recharge can be carried out smoothly at 2.3-2.4V, and at rates up to ~5 mA/cm^2 at 25°C before the charging curve becomes erratic. During charging, no precipitation was noted, as in the experiments on dilute solutions. However, a small amount of S_8 is produced on each charge, as subsequent discharges are of the same shape as that of the fresh cell.

Cell cycling efficiencies were determined for two types of cycling regimes. In the first case, a fresh cell was partially discharged, then charged again by the same amount. This symmetric charge-discharge process was continued for a number of cycles, after which the cell was discharged to a limit of 1.5V. The capacity realized in this final discharge was compared to that obtained in the discharge of a fresh cell. The total capacity

loss was divided by the number of cycles to obtain the average efficiency per cycle.

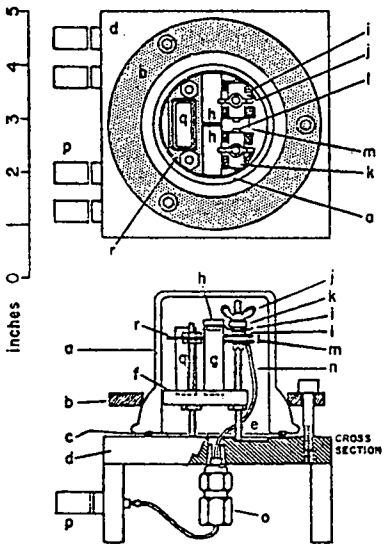

Fig. 3: Housing for studies of batteries containing volatile solvents. a) glass bell-jar made from 50 mm joint; b) aluminum hold-down ring; c) ethylene-propylene O-ring; d) aluminum base and legs; e) condensation trough; f) Teflon cell support; g) glass cell vessels (2); h) Teflon cell caps (2); i) Ta Exmet cell connections; j) wingnut; k) Teflon covered S.S. clamp bars (2); l) contact bolts with insulating collars (4); m) polypropylene-faced S.S. anvil; n) Teflon-covered nickel wire (one shown of four); o) Conax leakproof fitting; p) binding posts (4); q) glass evaporation reservoir; r) polypropylene support.

In the second cycling regime, the cell was first discharged to a limit of 1.5V, then charged to a predetermined capacity. The cell was then discharged to 1.5V, and cycling repeated in this manner. The efficiency could be computed directly for each cycle. When the efficiency was less than 100%, the cycles were, of course, asymmetric.

Starting with a fresh cell containing 5M S as Li_2S_8 in THF, 1M $LiAsF_6$, several cycling experiments have been carried out at low capacities, ranging from $0.04e^-/S$ to $0.1e^-/S$, at temperatures ranging from 25°C to 50°C. Over at least 100 cycles, efficiencies were always 95-100%. Under the harshest conditions, a cell was cycled 120 times to a depth of $0.1e^-/S$ at 1 mA/cm^2 and 50°C. The capacity remaining after 120 cycles was used to calculate an average cycling efficiency of 95%.

Shorter term experiments have been carried out on deeper cycles. A cell containing 4.82M S as Li_2S_8 in THF, 1M Li_2S_8 was cycled 10 times at $0.42e^-/S$ (0.5 mA/cm^2, 25°C). It was discharged completely following the 10th discharge, and the average efficiency was calculated to be 93.2%. All loss of efficiency can be attributed to self-discharge during cycling. Based on the time and capacity loss for each cycle, a self-discharge rate of 16 μA/cm^2 is obtained.

At 50°C and a current of 1 mA/cm^2, an identical cell cycled twelve times at an equivalent depth yielded an efficiency of 90.3% and a self-discharge rate of 46.8 μA/cm^2 (during cycling). The individual charge-discharge chronopotentiograms were smooth and reproducible, and are shown in Fig. 4.

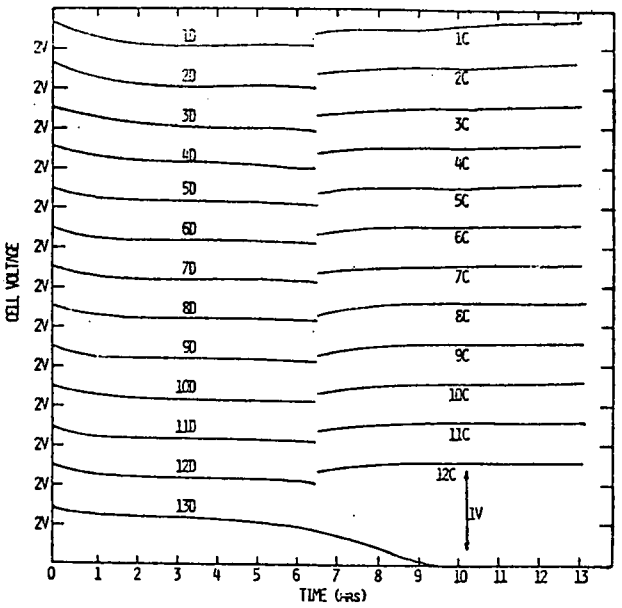

Fig. 4: Repeated cycling of Li/Li_2S_n cell containing 4.82M S, initially as Li_2S_8. Current density = 1.0 mA/cm^2; T = 50°C; cycle depth = $0.42e^-/S$. The cell was discharged completely at 13D to allow calculation of the average efficiency/cycle and the corresponding self-discharge rate.

In general, cycling efficiencies deteriorate more rapidly when cells are cycled to a 1.5V cutoff potential, as in the asymmetric mode described above. For example, the cell just described, following the polarization to 1.5V after 12.5 symmetrical cycles at 50°C, was charged at 0.42 e^-/S, then discharged to the same 1.5V cutoff voltage. The efficiency of this cycle as 95%, slightly better than the average of the previous 13 symmetrical cycles. Three more cycles of 95% were obtained before a sharp drop off in efficiency, to 30% by cycle 22.

One major difference between symmetric and asymmetric cycling modes is that, in the former case, some of the Li substrate is removed on each discharge, since the cycling efficiency is less than 100%. This probably has the effect of renewal of the substrate surface, leading to improved morphology of the Li deposited on the subsequent charge.

Without this surface renewal, as in the asymmetric cycles, the Li morphology deteriorates with every cycle, the self-discharge rate increases, and the efficiency drops off.

These experiments point out the importance of maintaining a low surface area, tightly bound Li deposit during charge in keeping the self-discharge reaction under control, and thus keeping the cycling efficiency high. Other factors which adversely affect the deposit morphology are high charging currents and impure electrolyte solutions. The tendency toward self-discharge and dendritic growth also increases with the depth of the deposit. Preliminary results suggest that, with the present solvent, electrolyte, and cell configurations, it is very difficult to obtain consistently high cycling efficiencies at greater than $1e^-/S$. In these cells, $1e^-/S$ for a 5M S solution corresponds to a Li deposit of 64 coul/cm^2.

THE LITHIUM ELECTRODE

Despite the intimate contact between the Li electrode and the highly oxidizing Li_2S_n catholyte, this battery is rechargeable. However, in any secondary battery, materials balance must be conserved during the cycling process. This is particularly a problem in secondary Li batteries, where the Li electrode is inefficient. In inert solvents, such as propylene carbonate [16-18], THF [19] or methyl acetate [20,21] containing Li salts as supporting electrolytes, Li may be electrodeposited onto inert substrates with close to 100% coulombic efficiency. However, not all of the deposit is retrievable during the stripping process. This is the result of insulation of Li granules from the substrate by Li-solution reaction products. Indeed, following stripping of the available electrodeposited Li, the electrochemically inaccessible material remains attached to the substrate. As cycling continues, the substrate becomes occluded with isolated Li and reaction products, and dendrite formation is aggravated. The net result is that some Li is lost from the system on each cycle, a fact which would result in early failure of a Li secondary battery or necessitate employing a huge excess of Li in preparing the cell [22].

As a result of these considerations, it is of obvious importance in terms of the practicality of the Li/Li_2S_n battery to differentiate between the negative electrode cycling efficiency and the cycling efficiency of the entire cell. The Li electrode efficiency will be either less than or equal to the cell efficiency. In the first case, the isolation of Li granules by reaction products would be indicated (as is observed for cycling Li in nonoxidizing environments), and there would be a loss of Li during each cycle. On the other hand, if the two efficiencies were equal, all of the Li electrodeposited during charge, and not available on discharge, would have been resolubilized via the self-discharge reaction.

To demonstrate the anode cycling efficiency under practical conditions, cells were designed with a limited amount of Li present initially on the anodes. This was accomplished by pressing 0.005" thick Li foil onto a Ta backing. Foil of this thickness is equivalent to ∿90 coul/cm^2 of Li.

In a typical experiment, two equivalent cells were constructed with these specially prepared anodes, each using 2.5 ml of 4.27M S as Li_2S_n in THF. The first cell was discharged totally at 1.0 mA/cm^2 and 50°C. The cell polarized to 1.5V with a capacity of $1.4e^-/S$. The cell was then overdischarged to strip the remaining Li from the anode. As shown in Fig. 5, this occurred at ∿ -0.5V cell polarization, a distinct end point being reached at 88 coul/cm^2 of Li substrate. The cell then polarized to ∿ -2.4V, when polysulfides started oxidizing on the exposed Ta support.

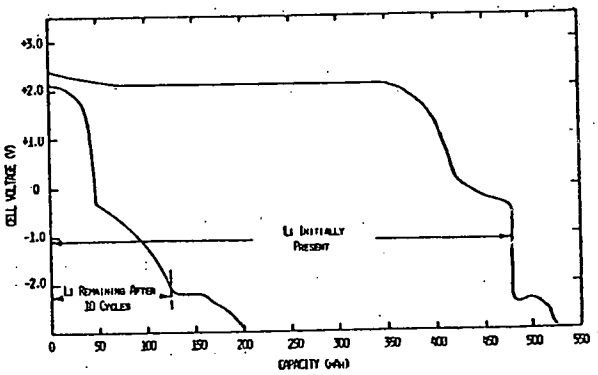

Fig. 5: Discharge before (a) and after (b) cycling of a Li limited cell. The cell was forced to discharge at reverse polarity in order to strip all the Li from the anode (∿90 C/cm^2 present initially). T = 50°C. Discharge current = 1.0 mA/cm^2.

The second cell was cycled 10 times at $0.51e^-/S$ and 1 mA/cm^2, also at 50°C, then discharged fully on the 11th cycle. From these data, an average efficiency of 83% and a self-discharge rate of 79 μA/cm^2 were calculated. This is by no means the best result that we have obtained for the self-discharge, and may reflect somehow the different cell construction. When this cell was overdischarged (Fig. 5), the amount of Li remaining on the substrate was used to calculate the average anode cycling efficiency. This too was 83%. Therefore, all of the anode inefficiency is realized as cell self-discharge

CONCLUSIONS

The Li/Li_2S_n cell is unusual in that it has a built-in self-discharge reaction which allows the materials balance in the cell to be maintained. In principle, if Li is used as the substrate for the negative electrode, it will never be usurped if the discharge is that fraction of the charge determined by the cell cycling efficiency. Hence, the problem of dendritic buildup of electrochem-

ically inaccessible Li, which is so characteristic of secondary Li systems, should be nonexistent in this case.

The principal difficulty with the rechargeability of the Li/Li_2S_n battery in its present form is the control of the self-discharge rate during extended cycling. For a few cycles of moderate depth, the self-discharge rate is reasonable, leading to charge-discharge efficiencies of 80-100%. However, deteriorating morphology on the Li electrode results in an increase in the self-discharge rate, particularly when the substrate surface is not renewed electrochemically previous to each charge.

It must be pointed out, however, that relative to the work that has yet been published on the Li electrode, the anodic efficiencies observed for this cell are quite impressive. This is particularly true considering the oxidizing nature of the electrolyte. In this cell, Li has been plated and stripped from the Li substrate at greater than 95% efficiency for over 100 cycles of ~7 coul/cm^2 (0.1e$^-$/S) at 50°C, and for at least 15 cycles at nearly the same efficiency for about 5 times that charge (0.4-0.5e$^-$/S). These efficiencies exceed those determined for Li cycled on Li in such "inert" media as propylene carbonate [22].

The effects of solvent, electrolyte preparation and additives, and cycling conditions are currently being explored in this laboratory to enhance the cycle life of this battery. A reasonable near-term goal is 250 deep (>1e$^-$/S) cycles, without the use of excessive Li. This achievement would provide the basis for a practical device of general utility.

ACKNOWLEDGEMENT

This work was supported by the U.S. Energy Research and Development Administration under Contract No. EY-76-C-02-2520.

REFERENCES

1. For a recent review, see Besenhard, J. and Eichinger, G., J. Electroanal. Chem. 68, 1 (1976); Eichinger, G. and Besenhard, J., ibid. 72, 1 (1976).

2. Maricle, D. and Mohns, J., Fr. Demandé 2,015,160 (1970).

3. Bro, P. et al., 9th Intl. Power Sources Symposium, Brighton, 1974, Paper 44.

4. Auborn, J. et al., J. Electrochem. Soc. 120, 1613 (1973).

5. Behl, W. et al., J. Electrochem. Soc. 120, 1619 (1973).

6. Driscoll, J. R. et al., Proc. 27th Power Sources Symposium, Atlantic City, N.J., June 1976.

7. Rao, M. L., U.S. Patent 3,413,154 (1968).

8. Coleman, J. R. and Bates, M. W., Power Sources 2, ed. D. N. Collins (1969).

9. Nole, D. and Moss, V., U.S. Patent 3,532,543 (1970).

10. Varta Batterie, Fr. Demandé 2,236,284 (1975).

11. Brummer, S. B. et al., Semiannual Progress Report, Contract EY-76-C-02-2520, Sept. 1976.

12. Rauh, R. D. et al., J. Inorg. Nuc. Chem. (1977), in press.

13. Rauh, R. D. et al., Symposium on Electrode Materials and Processes for Energy Conversion and Storage, The Electrochemical Society, 1977.

14. Abraham, K. M. et al., ibid.

15. Christopulos, J. A. and Gilman, S., Proc. 10th IECEC Conf., Newark, Delaware (1975), p. 437.

16. Selim, R. and Bro, P., J. Electrochem. Soc. 121, 1457 (1974).

17. Rauh, R. D. and Brummer, S. B., Electrochim. Acta 22, 75 (1977).

18. Koch, V. R. and Brummer, S. B., Electrochim. Acta, submitted for publication.

19. Brummer, S. B. et al., Semiannual Progress Report, Grant No. AER75-03779, February 1977.

20. Rauh, R. D. and Brummer, S. B., Electrochim. Acta 22, 85 (1977).

21. Dampier, F. W. and Brummer, S. B., Electrochim. Acta, in press.

22. Rauh, R. D. et al., "Efficiencies of Cycling Lithium on a Lithium Substrate in Propylene Carbonate," submitted to J. Electrochem. Soc.

☆U.S. GOVERNMENT PRINTING OFFICE: 1980-740-145/1034